# RHEOLOGICAL PROPERTIES AND REACTION KINETICS OF AMIDOAMINE OXIDE SURFACTANT-BASED ACIDS WITH CALCITE

A Dissertation

by

LINGLING LI

Submitted to the Office of Graduate Studies of
Texas A&M University
in partial fulfillment of the requirements for the degree of

DOCTOR OF PHILOSOPHY

May 2011

Major Subject: Petroleum Engineering

Rheological Properties and Reaction Kinetics of

Amidoamine Oxide Surfactant-based

Acids with Calcite

# RHEOLOGICAL PROPERTIES AND REACTION KINECTICS OF AMIDOAMINE OXIDE SURFACTANT-BASED ACIDS WITH CALCITE

A Dissertation

by

LINGLING LI

Submitted to the Office of Graduate Studies of
Texas A&M University
in partial fulfillment of the requirements for the degree of

DOCTOR OF PHILOSOPHY

Approved by:

| | |
|---|---|
| Chair of Committee, | Hisham A. Nasr-El-Din |
| Committee Members, | Stephen A. Holditch |
| | A. Daniel Hill |
| | Mahmoud El-Halwagi |
| Head of Department, | Stephen A. Holditch |

May 2011

Major Subject: Petroleum Engineering

# ABSTRACT

Rheological Properties and Reaction Kinetics of Amidoamine Oxide Surfactants-based Acids with Calcite.

(May 2011)

Lingling Li, B.E., University of Science & Technology of China;

M.S., Texas A & M University

Chair of Advisory Committee: Dr. Hisham A. Nasr-El-Din

A new type of viscoelastic amphoteric surfactants (amidoamine oxide) has been examined as a diverting agent during acidizing treatment. Rheological properties of viscoelastic surfactants are a function of surfactant concentration, acid additives, pH, temperature and shear rate. A HPHT rheometer was used to test the effect of common acid additives and organic acids/chelating agents on the apparent viscosity of amidoamine oxide-based acids. The compatibility and thermal stability of surfactants with corrosion inhibitor were also investigated. Rotating disk apparatus was used to examine the kinetic studies of surfactant-based acids with limestone.

The results show that the apparent viscosity of surfactant solutions prepared in deionized water, live acid, and spent acid was found to be a function of temperature. Apparent viscosity of live surfactant-based acids was also found to be a function of HCl concentration. Most of acid additives could adversely affect the rheological properties of spent acids. Compatibility tests should be done prior the field application. Cryo-TEM

studies show the changes of rod-like micelle structures with the addition of additives. The reaction between surfactant-based acid and limestone was found to be mass transfer limited at 170$^{o}$F.

# ACKNOWLEDGEMENTS

I would like to thank my research advisor, Dr. Hisham A. Nasr-El-Din, for his support and advice throughout this project. I am very thankful to him for all the help and for providing a conductive environment for carrying out independent research. Thanks to Dr. Stephen A. Holditch, A. Daniel Hill and Mahmoud El-Halwagi for serving on my graduate advisory committee. Thanks to Dr. Kay E. Cawiezel, James B. Crews and Jian Zhou for their technical support. Thanks to Dr. Christos Savva and Zhiping Luo for assistance on Cryo-Transmission Electron Microscopy.

Finally, thanks to my mother and father for their encouragement and to my husband for his support.

# NOMENCLATURE

| | |
|---|---|
| $A$ | surface area of the disk, $cm^2$ |
| $C_b$ | reactant concentration in the bulk solution, $gmol.cm^{-3}$ |
| $C_s$ | reactant concentration at the surface, $gmol.cm^{-3}$ |
| D | diffusivity, $g.cm^{-2}$ |
| K | power-law consistency index, $g.cm^{-1}.s^{(n-2)}$ |
| $K_m$ | reactant mass transfer coefficient, $cm.s^{-1}$ |
| n | power-law index |
| $r$ | radius of the disk |
| $r_1$ | radius of the water droplet |
| $r_2$ | radius of the water droplet |
| $Re$ | Reynold number |
| $Sc$ | Schmidt number |
| $Sh$ | Sherwood number |
| $\Delta P$ | pressure drop |
| $\sigma$ | surface tension, $dyn/cm^2$ |
| $\mu$ | fluid viscosity, cp |
| $\nu$ | kinematic viscosity |
| $\dot{\gamma}$ | shear rate, $s^{-1}$ |
| $\omega$ | disk rotating speed, $s^{-1}$ |
| $\rho$ | density, $g.cm^{-2}$ |

# TABLE OF CONTENTS

CHAPTER Page

# LIST OF FIGURES

FIGURE Page

FIGURE Page

FIGURE Page

FIGURE Page

FIGURE Page

FIGURE Page

# LIST OF TABLES

# CHAPTER I

# INTRODUCTION

## Definition of Surfactants and Their Properties

"Surfactants" is an abbreviation for surface active agent, which literally means active at a surface. The surface can be between solid and liquid, between air and liquid, or between a liquid and a different immiscible, liquid. Surfactants have some special characteristics and they are: Adsorption; Micelles; Solubility; Solubilisation; Microemulsions; Wetting; Foaming and defoaming; Macroemulsions; Dispersion and aggregation of solids; and Detergency.

### *Adsorption and Critical Micelle Concentration (CMC)*

A surfactant can adsorb on the surface because there are two groups in the molecule (**Fig. 1.1**): a hydrophobic (watering hating) group and a hydrophilic (water liking) group.

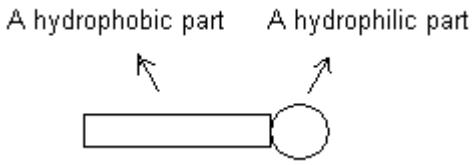


**Fig. 1.1—The basic structure of a surfactant.**

This dissertation follows the style of *SPE Production and Operations*.

There are two opposing forces of interaction between the surfactant molecules (Porter, 1994). One is the repulsive force between the polar groups in water. The larger this charge, the greater the repulsion and the less tendency to form micelles. Another force is between the hydrophobic groups if there is a bond attracting them together. The reason for this is complex and due to enthalpy and entropy changes when the alkyl group is transferred from a hydrocarbon environment to solution in water.

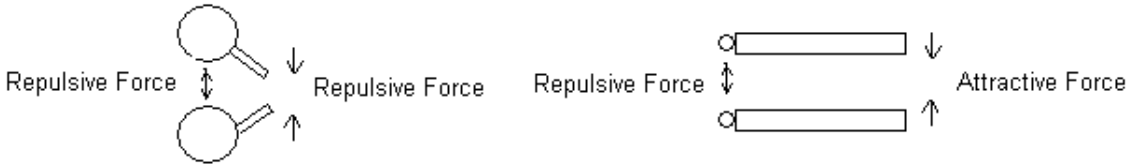


**Fig. 1.2—Forces between surfactants.**

When the molecules are very far apart, both of these two forces are very weak. The two interactions will increase if the concentration increases. The molecules probably can not aggregate if the repulsive force is much greater than the attractive force. The surfactant molecules will remain monodisperse in solution at high concentration. This is the situation when the surfactant is very soluble due to the hydrophobic effect is very weak. On the other hand, the molecules will aggregate together if the attractive force is much stronger. This is the situation when the molecule is partially soluble because of the large size of hydrophobic group.

The relative strength of repulsive and attractive forces determines Critical Micelle Concentration (CMC, will be defined in later). In comparison two surfactants, the one with larger hydrophobic effect will have a lower CMC than the other.

The adsorption of a surfactant from the solution on to a surface depends on the concentration (**Fig. 1.3**) (Porter 1994).

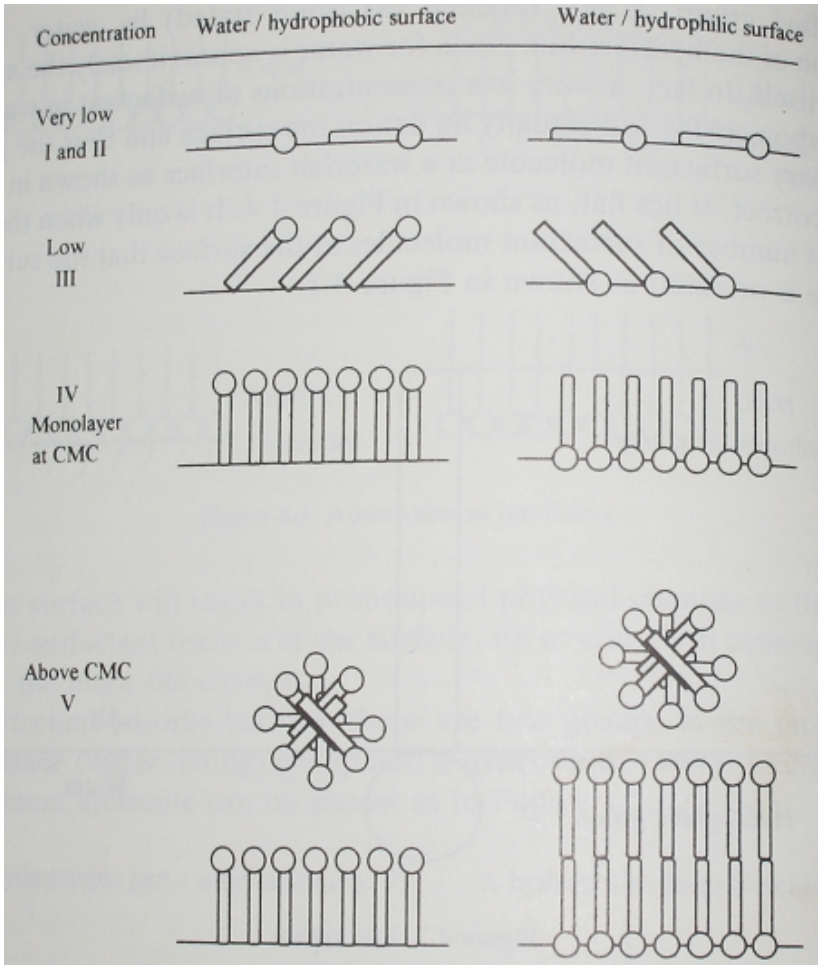


**Fig. 1.3—Adsorption of surfactants. (Porter, 1994)**

At very low concentrations (I and II), there is no orientation and surfactant molecules lie on the surface. At stage III, the concentration increases and the number of molecules increases, there is no enough room for all the molecules to lie on the surface, so they are orientated in a way. At concentration IV, the number of molecules is large enough to

form a monolayer, and this particular concentration is called Critical Micelle Concentration (CMC). Once the concentration is above CMC (V), more than one layer of surfactant molecules can form ordered structures on the hydrophilic surfaces.

***The Shape of Micelles in Solutions***

The actual structure and shape of a micelle depends on the temperature, the type of surfactant and its concentration, other ions in solution and other water-soluble organic compounds. Micelles can form spherical, rod-like or lamellar shapes (**Fig. 1.4**) (Porter 1994). The number of surfactant molecules in a micelle is known as the aggregation number.

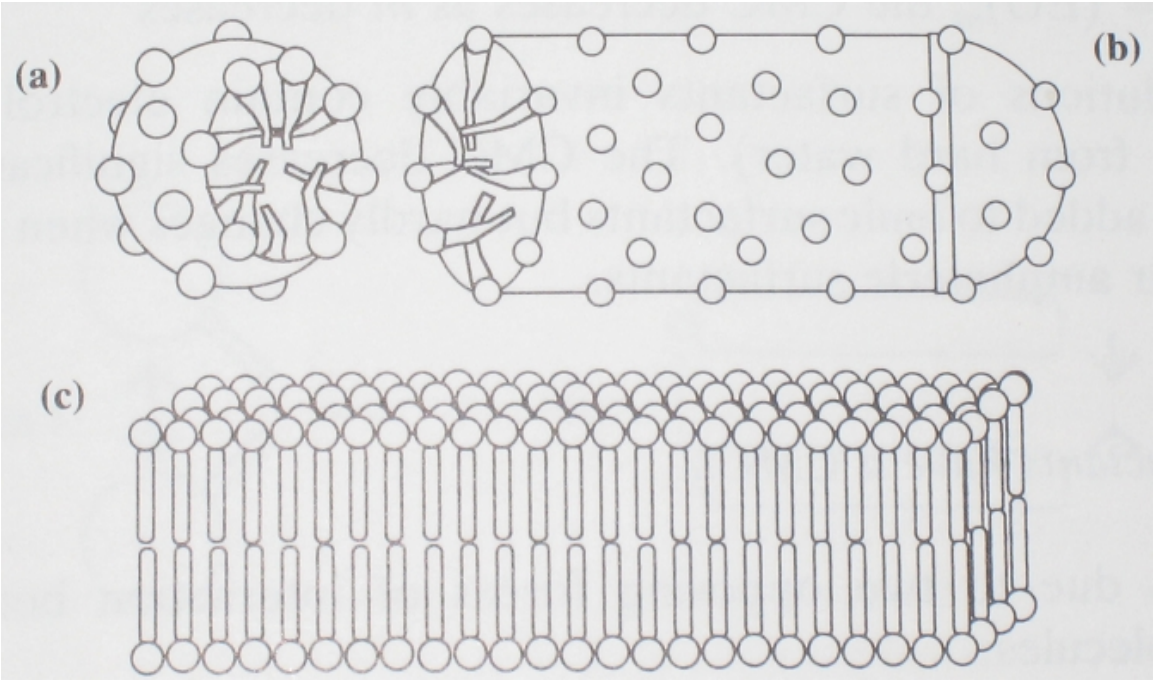


**Fig. 1.4—Shape of micelles: (a) spherical; (b) rod-shaped or cylindrical; (c) lamellar. (Porter 1994)**

**Table 1.1** shows aggregation number as a function of chain length and temperature for alkyl dimethyl betaines (Porter 1994).

**TABLE1.1—AGGREGATION NUMBERS FOR ALKYL DIMETHYL BETAINES**

| R | Temp ($^{o}$C) | Micellar Mol Wt (x $10^{-3}$) | Weight aggregation numbers |
|---|---|---|---|
| $C_{10}H_{21}$ | 20 | 8.18 | 33.7 |
| | 25 | 8.23 | 34 |
| | 31 | 8.47 | 34.9 |
| | 37 | 8.6 | 35.4 |
| | 43 | 8.07 | 33.2 |
| | 50 | 7.82 | 32.2 |
| | 58 | 7.76 | 31.9 |
| | 65 | 7.66 | 31.5 |
| $C_{11}H_{23}$ | 25 | 14.9 | 58 |
| | 35 | 17.5 | 68.1 |
| | 45 | 17.6 | 68.5 |
| | 55 | 17.7 | 68.9 |
| | 65 | 16.2 | 63 |
| $C_{13}H_{27}$ | 25 | 26.5 | 87.3 |
| $C_{15}H_{31}$ | 25 | 43.1 | 130 |

The size of cylindrical micelles depends on the concentration, length of hydrophobic group, temperature and the ionic strength of the solution. The micelle size will increase if any changes can reduce the effective size of the hydrophilic head group. Cylindrical micelles can be formed in a number of ways:

1. The counter ion: the addition of counter ions can decrease repulsion between hydrophilic head groups by reducing the charge density. Therefore, the

molecules can pack together more closely and it can cause a sphere-to-rod transition.

2. Addition of cosurfactant with a compact group. Mixed micelles can be generated if the head group of the cosurfactant has similar properties as that of surfactant but smaller in size.
3. Change in the nature of the head groups. Polyoxyethylene hydrophilic group is reduced in size if temperature increases.
4. Change in pH of amphoteric surfactants. The effective size of head will change if pH changes alter the degree of protonation.

***Viscosity***

The surfactant solutions have the viscosity behavior. It is a function of surfactant concentration, temperature, shear rate and salinity etc. Viscosity/concentration data for an ether sulphate is shown in **Fig. 1.5** (Porter 1994). The viscosity at low concentrations is low because of spherical micelles. The viscosity increases when the spherical micelles change to rod-like micelles, and the viscosity increases even higher when the rod-like micelles form the hexagonal packing. However, when the concentration reaches the lamellar stage, the viscosity drops down.

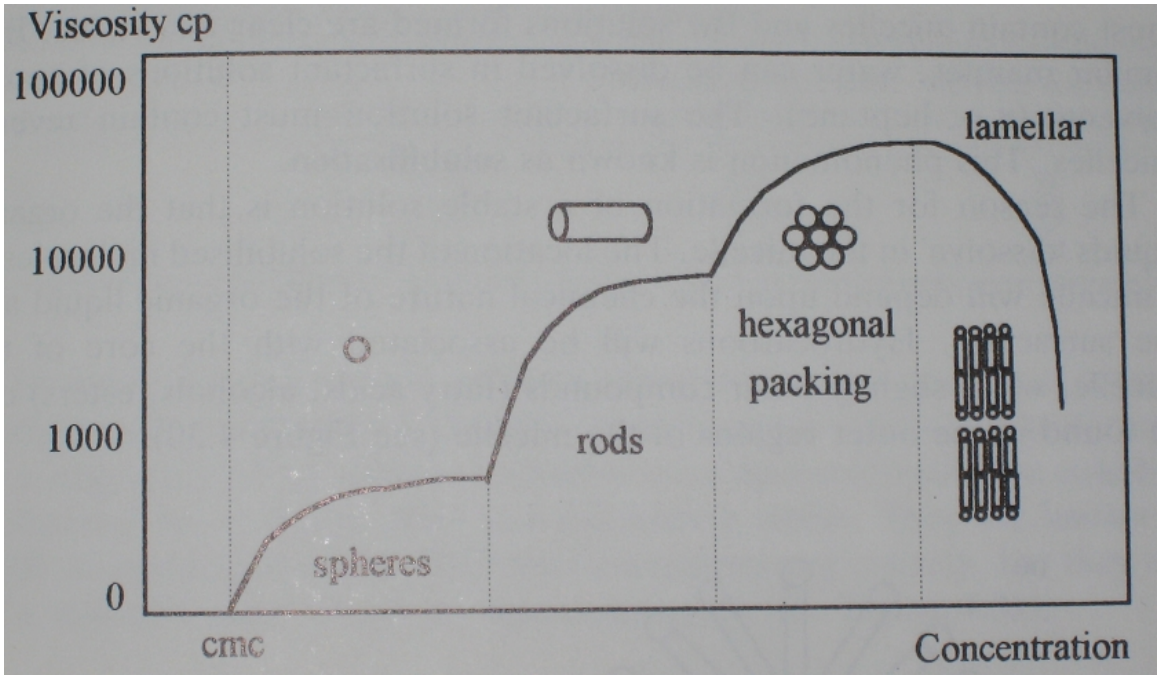


**Fig. 1.5—Viscosity and concentration for an ether sulphate. (Porter 1994)**

**Surfactant Classification**

Based on the chemical structures of the hydrophilic group, surfactants can be classified by:

- Anionic-carrying a negative charge
- Nonionic-carrying no charge
- Cationic-carrying a positive charge
- Amphoteric-carrying a positive or a negative charge or both

***Anionics***

The main types of anionics commercially available are:

1. Carboxylates soaps; ethoxy carboxylates; ester carboxylates; amide carboxylates

Soaps are prepared by saponification of triglycerides from vegetal or animal source. For instance, sodium hydroxide reacts with a triglyceride containing 3 stearic acid, and produces 3 moles of sodium stearate and 1 mol of glycerol.

$$3NaOH + (C_{17}H_{35}COO)_3C_3H_5 \rightarrow 3C_{17}H_{35}COONa + CH_2OH - CHOH - CH_2OH$$

2. Sulfates

Alkyl sulfate (e.g. sodium lauryl sulfate) is the foaming agent found in shampoos, tooth paste and some detergents

$$R - O - SO_3^-H^+ + NaOH \rightarrow R - O - SO_3^-Na^+$$

Sodium laureth sulfate is alkyl ether sulfate. The presence of the EO (ethylene oxide) group confers some nonionic character to the surfactant and a better tolerance to divalent cations.

$$C_{12}H_{25} - (O - CH_2 - CH_2)_3 - O - SO_3^-Na^+$$

Sulfated alkanolamides can be obtained by sulfating alkanol amides, particularly in C12-C14 (cocoamide). These surfactants have a large hydrophilic group and do not irritate the skin. In general, only 80-90% of the alkylamide is sulfated, so the remaining unsulfated alkyl-amide can play a role in foam booster (Salager 2002).

$$C_{11}H_{23} - CONH - CH_2CH_2OH + SO_3^- \rightarrow C_{11}H_{23} - CONH - CH_2CH_2O - SO_3^-H^+$$
$$+ NH_2CH_2CH_2OH \rightarrow C_{11}H_{23} - CONH - CH_2CH_2O - SO_3^-NH_3^+ - CH_2CH_2OH$$

3. Phosphates (ethoxylates, alcohols, amides)

Three acids containing phosphorus are listed below in **Fig 1.6**. The mono and diesters of fatty alcohols (R-OH) have a good tolerance to electrolytes and they are used in agrochemical emulsions, particularly when the aqueous phase contains fertilizers.

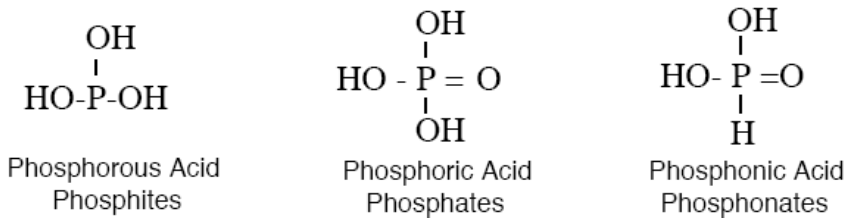


**Fig. 1.6—Acids containing phosphorus.**

4. Sulfonates

Dodecyl benzene sulfonates are today domestic detergent formula, either in powdered or liquid forms; contain a high proportion of linear alkylbenzene sulfonates (LAS) (Salager 2002). They have an alkyl chain in the C10-C16 range with a benzene ring which is attached to any position of the linear chain, for instance (**Fig. 1.7**):

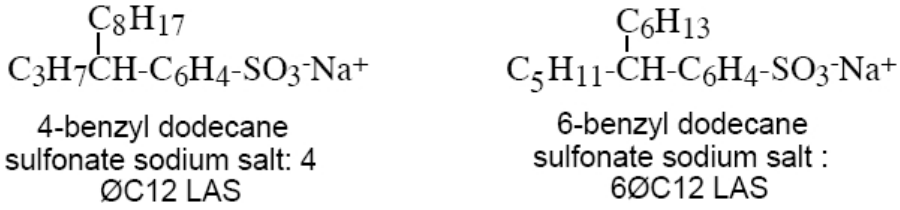


**Fig. 1.7—Structures of two dodecyl benzene sulfonates (Salager 2002).**

Alpha olefin sulfonates displays a better hard water tolerance than LAS, but they are not good detergents (**Fig. 1.8**).

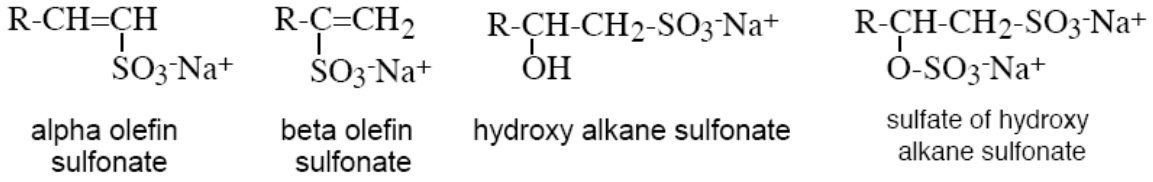


**Fig. 1.8—Structures of alpha olefin sulfonates (Salager 2002).**

Sulfo-carboxylic compounds: sulfosuccinates (**Fig. 1.9**) and sulfosuccinamates are well known and used in many applications (**Fig. 1.10**).

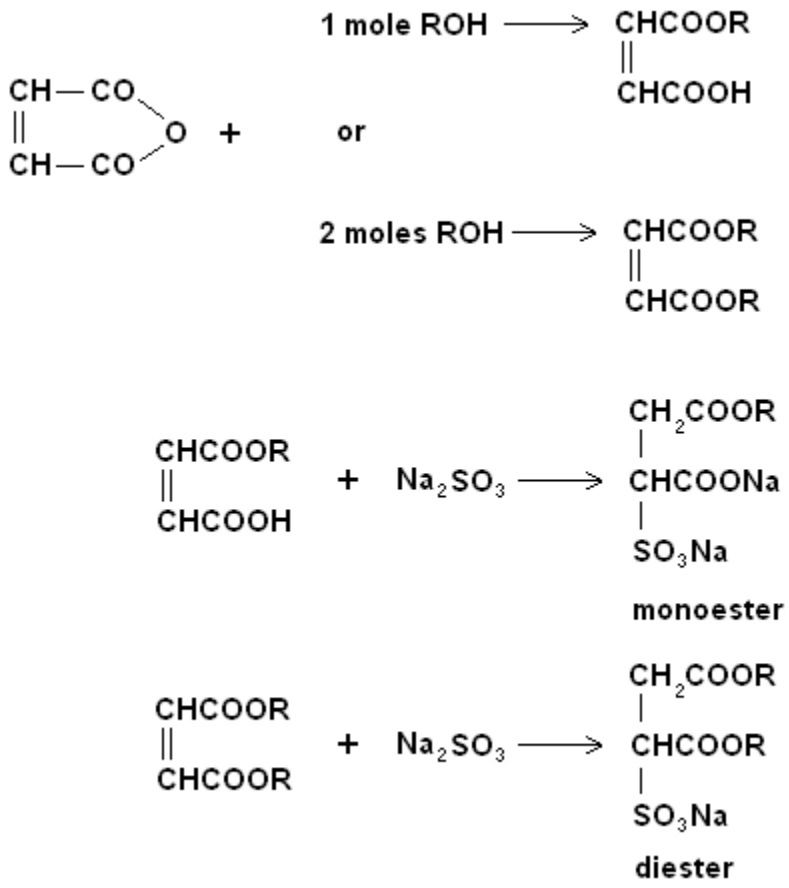


**Fig. 1.9—Syntheses of sulfosuccinates.**

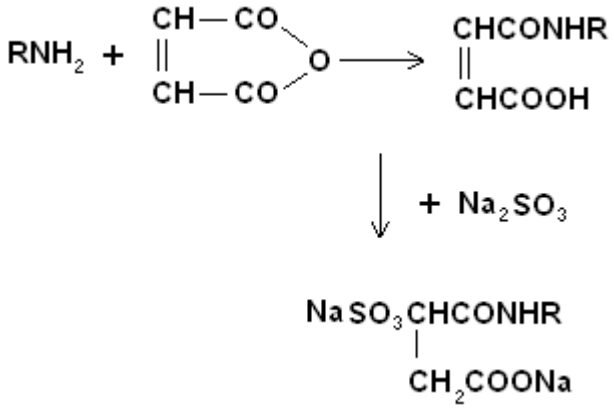


**Fig. 1.10—Synthesis of sulfosuccinamate.**

***Nonionics***

Nonionic surfactants do not produce ions in aqueous solutions; therefore, they are compatible with other types and are excellent candidates to enter complex mixtures. They are much less sensitive to electrolytes and are good detergents, wetting agents and emulsifiers.

1. Ethoxylated alcohols and alkylphenols

The most used Ethoxylated linear alcohol is actually a C12-C16 mixture. The ethoxylation degree ranges from EON = 6-10 for detergents, and EON>10 for lime soap dispersants, wetting agents and emulsifiers.

For common commercial available ethoxylated alkyl-phenols, products are the octyl, nonyl and dodecyl-phenol with a degree of ethoxylation from 4 to 40. Octyl and nonyl-phenols with EON = 8-12 are used in detergents. The products with EON<5 are antifoaming agents or detergents in non-aqueous media. For EON = 12~20, they are

wetting agents and O/W emulsifiers. With EON > 20, they have detergents properties at high temperature and high salinity (Salager 2002).

Ethoxylated thiols are also used in industry as excellent detergents and wetting agents and they have the alcohol structure in which the O atom is replace by S atom.

2. Fatty acid esters

Polyethoxy-esters are produced by the esterification of the acid by the polyethylene glycol (**Fig. 1.11**).

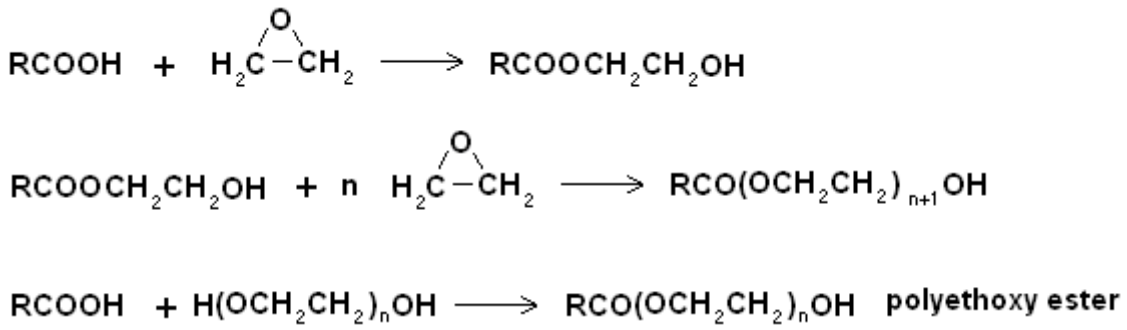


**Fig. 1.11—Esterification.**

Glycerol estsers are used in the conditioning of foodstuffs, bread, dairy emulsions and foams such as beverages, ice cream, etc. They are used in pharmaceuticals as emulsifiers, dispersants and solubilizing agents.

Esters of hexitols and cyclic anhydrohexitols can be easily adjusted with hydrophilicity. The commercial products can be used as emulsifying agents employed in food conditioning and cosmetics.

Hexitol are hexa-hydroxy-hexanes. Two hydroxyl groups can merge to produce an ether link and generate a 5 or 6 atom cycle called hydrosorbitol or sorbitan (**Fig. 1.12**)

.

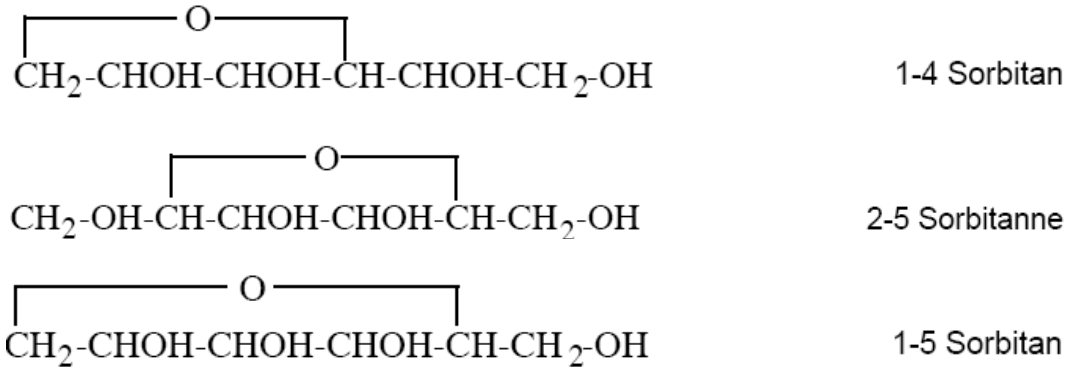


**Fig. 1.12—Chemical structures of sorbitan (Salager 2002).**

The OH groups can react with either fatty acid or a polyethylene oxide condensate. The following structure (**Fig. 1.13**) shows TWEEN 20, a polyoxyethylene derivative of sorbitan monolaurate. It should be noted that the hydrophilic part of TWEEN 20 is much bulkier than the hydrophobic part and hydrophile-lipophile balance (HLB) is 16.7, which indicating that TWEEN 20 will travel into the water phase (Kim and Hsieh 2001).

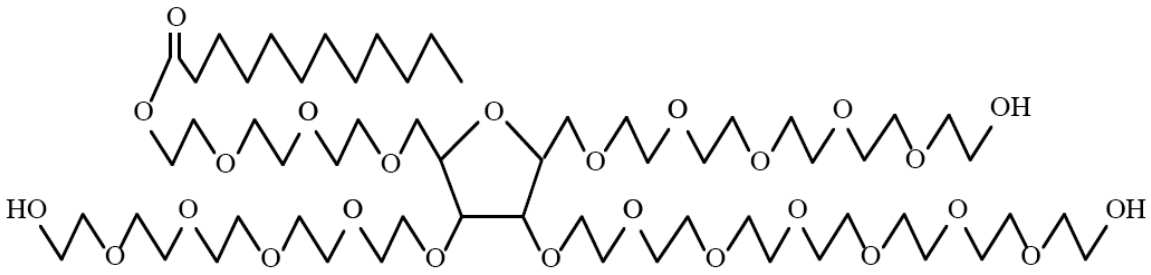


**Fig. 1.13—Chemical structure of TWEEN 20.**

3. Nitrogenated nonionic surfactants

Imidazoles (**Fig. 1.14**) are ethoxylated to produce fabric softener for machine washing, and also provide an anticorrosion protection for the hardware.

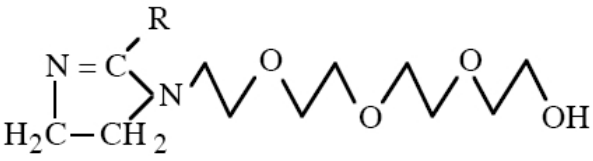

**Fig. 1.14—Structure of imidazoles.**

**Fig. 1.15** shows the structures of ethoxylated alkyl-amides are good foamers. Ethoxylated and acylated urea are also fabric softening substances.

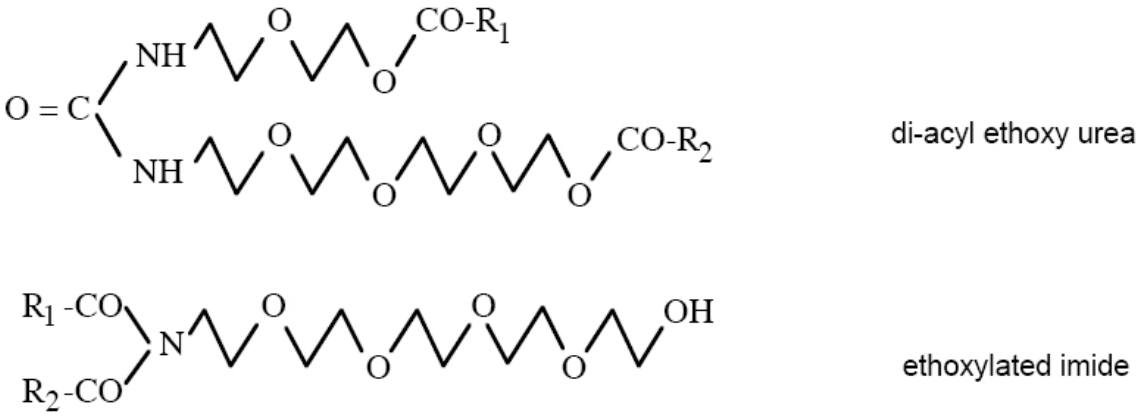


**Fig. 1.15—Structures of ethoxylated alkyl-amides.**

***Cationics***

Cationic surfactants are not good detergents or foaming agents. They usually can not be mixed with anionic surfactants. The positive charge makes them to be floatation collectors, hydrophobating agents, corrosion inhibitors and dispersant.

1. Linear alkyl-amines and alkyl-ammoniums

Most used cationic surfactants are fatty amines, their salts and quaternary derivatives (**Fig. 16**). Actually fatty amines are not cationic surfactants, but generally classified with cationics because they are mostly used at acidic condition and their salts are cationic.

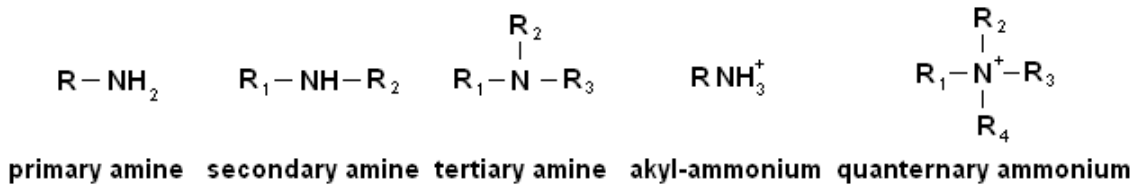


**Fig. 1.16—Structures of fatty amines, their salts and quaternary ammonium.**

2. Nitrogenated surfactants with a second hydrophile

Amide-, ester- and ether-amines are listed below:

$RCO - (NHCH_2CH_2)_2 - NH - COR$ $\qquad$ $RCO - O - CH_2CH_2 - N(CH_3)_2$

$R - O - CH_2CH_2CH_2 - NH_2$

Ethoxy-amines are used in textile industry as untangling and softening agents, as well as corrosion inhibitor, $H - (OCH_2CH_2)_n - N^+R(CH_3)_2Cl^-$.

***Amphoterics***

An amphoteric has at least one anionic group and at least one cationic group. The value of pH determines which group would dominate: anionic at alkaline pH and cationic at low pH. The pH where these ionic groups neutralize each other is called the isoelectric point.

1. Amino acids

For instance, amino propionic acid, their isoelectric point is around pH = 4. The structures at different pH are shown in **Fig 1.17**. They adsorb on skin, hair and textile fibers. They are used as antistatic and lubricants for hair and fabric. The dodecyl amino propionic acid is used as wetting agent and bactericide in cosmetics.

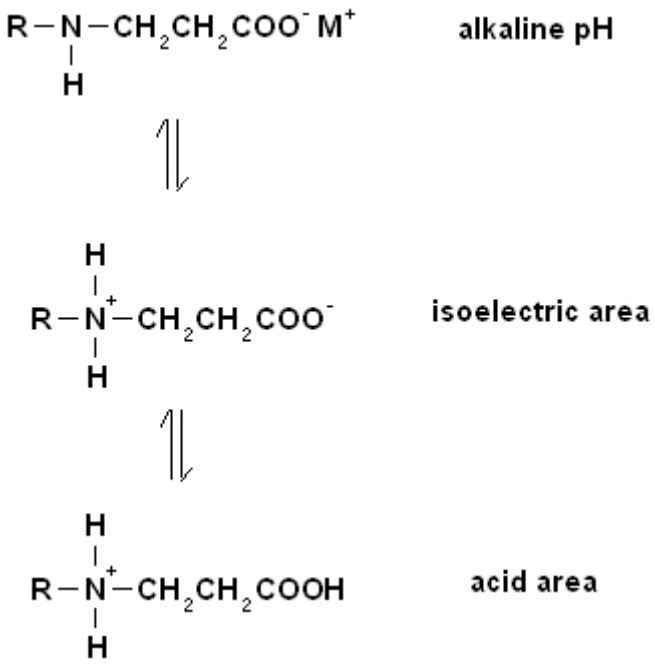


**Fig. 1.17—Structures of amino acids at different pHs.**

2. Betaine

Trimethylammonium acetate is a natural product and named “beta-in” by Scheibler (Lomax 1996). The structure is shown in **Fig 1.18**.

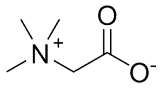

**Fig. 1.18—Basic structure of betaine.**

The simplest surface-active betaine is the alkylbetaine, and the one derived from coconut is the most commonly used.

Another type of betaine surfactant is alkylamidobetaines. The synthetic reaction is shown below (**Fig. 1.19**).

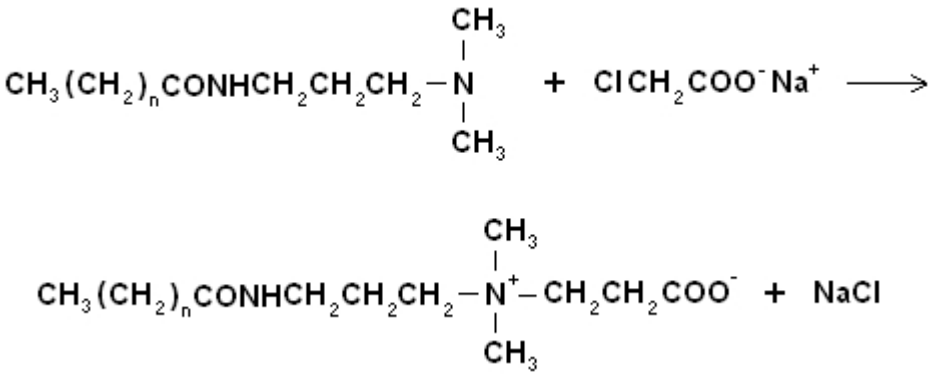

**Fig. 1.19—Synthesis of alkylamidobetaines.**

Sulfobetaines (**Fig. 1.20**) are similar to betaines but having the alkylsulfonate group rather than carboxyalkyl group.

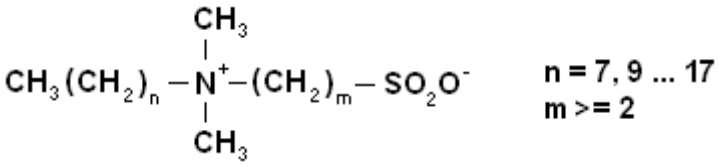

**Fig. 1.20—Structure of sulfobetaines.**

Sulfitobetaines (**Fig. 1.21a**) and sulfatobetaines (**Fig. 1.21b**) are other types of modified betaines.

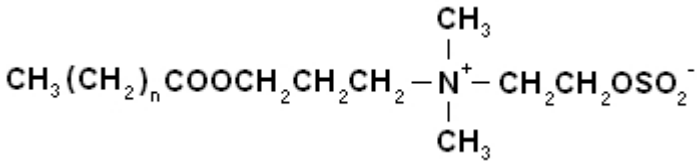

(a)

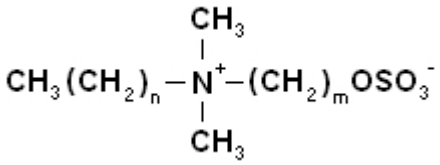

(b)

**Fig. 1.21—Structures of sulfitobetaine (a) and sulfatobetaine (b).**

Phosphinatebetaines and phosphonatebetaines (**Fig. 1.22**) are similar to alkylbetaines and sulfobetaines where carboxyl or sulfonic group has been replaced by phosphinate or phosphonate group.

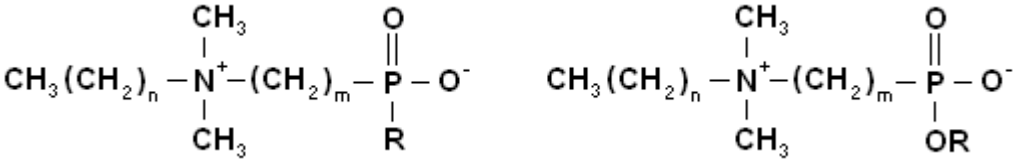

**Fig. 1.22—Structures of phosphinatebetaine and phosphonatebetaine.**

Phosphitobetaines and phosphatobetaines are just like sulfite and sulfatobetaines (S-O-C linkage). Phosphito and phosphatobetaines have P-O-C bonds (**Fig. 1.23).**

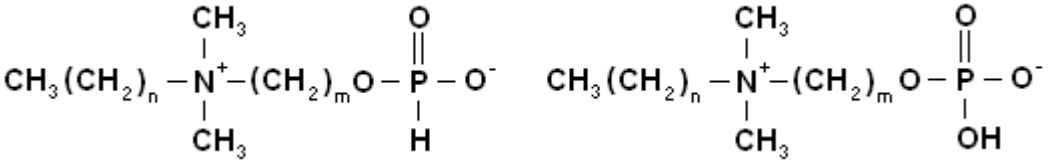

**Fig. 1.23—Structures of phosphitobetaine and phosphatobetaine.**

Sulfonium and phosphonium betaines are shown in the following figure (**Fig. 1.24**). The S and P atoms replace the N atom in the basic betaine structure.

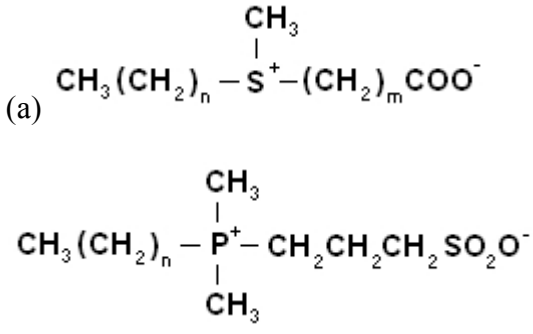

**Fig. 1.24—Structures of sulfonium and phosphonium betaines.**

3. Imidazoline derived amphoterics

The reactions between imidazoline and chloroacetic acid are shown in **Fig 1.25** and monocarboxylated or dicarboxylated structures are generated by the hydrolysis of the imidazoline ring and then reaction of the secondary amine with chloroaectic acid (Lomax 1996).

(a)

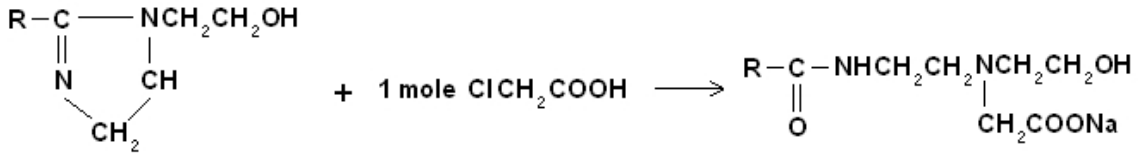


(b)

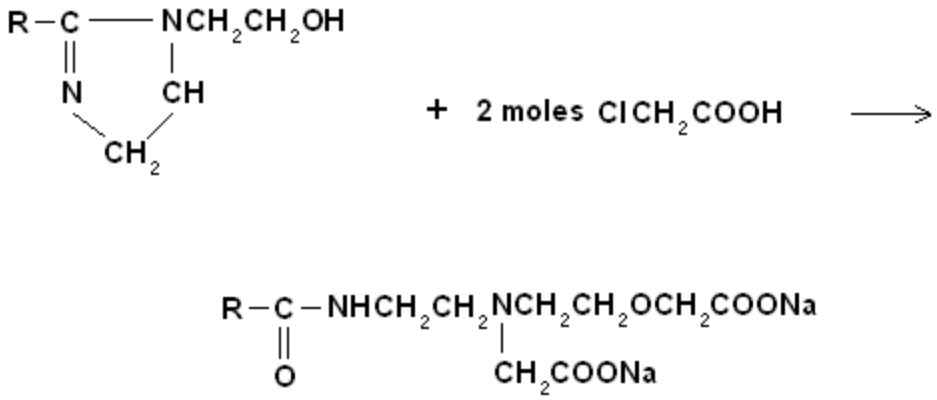


and

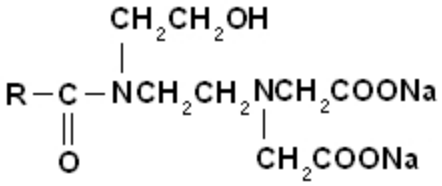


and

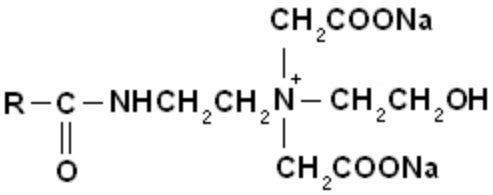


**Fig. 1.25—Syntheses of monocarboxylated (a) and dicarboxylated (b) imdazoline derived amphoteric surfactants.**

4. Amine oxide (will be described later in this chapter )

**Surfactant Use in Acid Stimulation**

Surfactants are used in acidizing treatments to do one or more following function: water-wet the formation, break emulsions or sludges, reduce surface or interfacial tension, remove fine particles, form foams for acid diversion and prepare emulsified acids for deep acid penetration.

***Surfactants as Anti-sludge Agents***

For oil producing wells, one common problem is the formation of acid-in-oil emulsions and precipitation of asphaltene, which induce sludge formation. These viscous emulsions and sludges can cause the formation damage and result in severe operational problem in surface facilities following acid stimulation. One reason that causes acid sludge formation is the precipitation of asphaltene and heavy hydrocarbons when oil contacts strong acids. Asphaltenes are colloidal particles and dispersed in crude oil. They are composed of condensed aromatic ring structures containing many heteroatoms, such as oxygen, sulfur and nitrogen (Houchin and Hudson 1986). Natural resins adsorbed on the surface of the asphaltene particle (Lichaa and Herrera 1975).

Asphaltene particles are negatively charged (Moore et al. 1965). Therefore, during acidizing treatments, a large number of $H^+$ can make larger aggregates of asphaltenes by neutralization (Jacobs and Thorne 1986). These aggregates can form very rigid emulsions and reduce well productivity by depositing at the pore throat. Besides, the

problem can be even more severe if sand, silt or metal oxides are present to stabilize acid-in-oil emulsions (Moore et al. 1965). Vison (1996) noted that iron contamination, especially ferric iron, plays a very important role in the formation of sludge. The flocculation of asphaltene particles occurs due to the coordination of iron with porphyrin, pyrroles, pyridines or possibly phenolic hydroxyl groups present in the crude oil. Jacobs and Thorne (1986) reported that iron can also catalyze polymerization of heavy hydrocarbons at high temperatures.

Anti-sludge agents, surfactants and mutual solvents are usually added to the injected acid to minimize the impact of acid-oil sludge (Dunlap and Houchin 1990). These agents disperse the asphaltene and prevent its precipitation. Another method to reduce sludge formation is to minimize acid contact with the crude oil. One way is to use solvent preflush (xylene or toluene) that forms a barrier between crude oil and the acid (Dunlap and Houchin 1990). A second way is to use acid emulsified in solvent (Figueroa-Ortiz 1996). The solvent in this emulsion will separate acid and oil.

### *Surfactants Used to Make Emulsified Acid*

Hydrochloric acid is commonly used to stimulate carbonate reservoirs. The reaction rate between HCl solution and carbonates are very fast, especially at high temperatures (Nierode and Williams 1971; Lund et al. 1975). Therefore, acid is consumed on the formation surface (Hoefner et al. 1987) and can not penetrate deeply to the damaged zone. Acid-in-diesel emulsions can solve this problem (Al-Anazi et al. 1998; Nasr-El-Din et al. 1999; Crowe and Miller 1974; and Bergstrom and Miller 1975). This emulsion

contains diesel, HCl acid and an emulsifier. Diesel is a barrier between the acid and the rock to slow down the reaction rate (Peter and Saxon 1989; Daccord et al. 1987; Williams and Nierode 1972). Typically the acid to diesel volume ratio is 70:30 (Al-Anazi et al. 1998). Surfactants are used to form emulsified acid, where acid is the dispersed or internal phase. The acid in this form can penetrate deeper in the formation due to less acid contact with the rock. It also reduces acid contact with the crude oil, and this will reduce sludge formation. Besides, the acid does not come in contact with the well tubulars which can minimize the corrosion and reduce the iron concentration in the acid.

Care should be taken during the preflush and postflush (Al-Anazi et al. 1998). The presence of demulsifier and mutual solvent may break the emulsified acid.

***Surfactants to Reduce Surface Tension***

For gas wells in low permeability reservoirs, accumulation of the aqueous phase near the wellbore formation rock, known as water blockage and shown in **Fig. 1.26**, will reduce the relative permeability to gas and gas production (Bennion et al. 1996). Therefore, low surface tension is required to reduce capillary force that traps the aqueous phase in the pore throat.

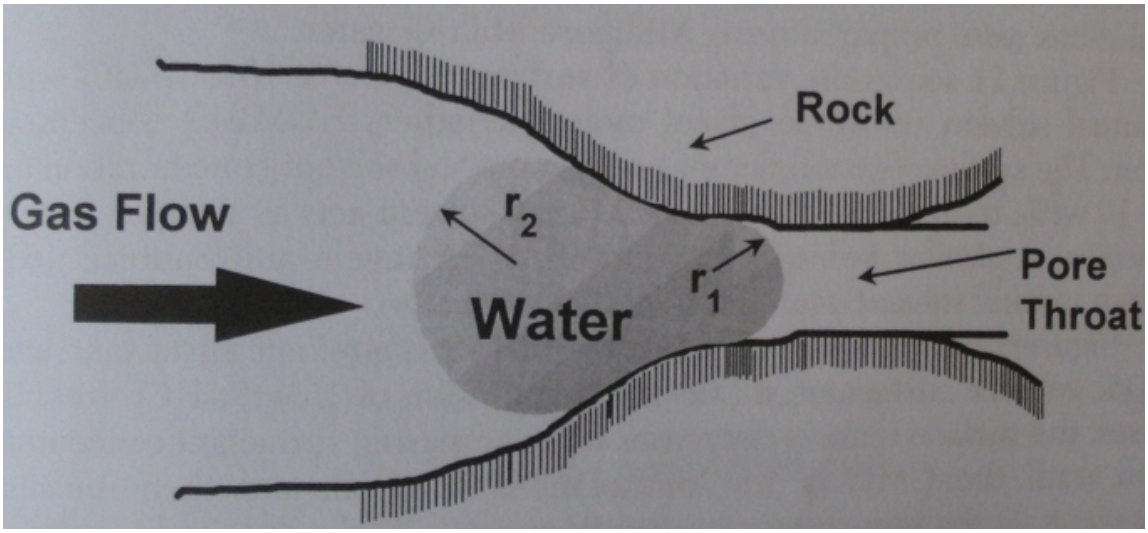


**Fig. 1.26—Water blockage in gas reservoirs (Schramm, 2000).**

The pressure drop required to mobilize a drop of trapped spent acid can be expressed as

$$\Delta p = 2\sigma\left(\frac{1}{r_1} - \frac{1}{r_2}\right) \quad \text{.....(Eq. 1.1)}$$

where $\sigma$ is the surface tension, $r_1$ and $r_2$ are the radius of the water droplet. To reduce the capillary force, one way is to lower surface tension and it can be achieved by the addition of surfactants.

Dabbousi et al. reported that surface tension is a function of acid type, concentration, ionic strength and additive type and concentration (1999). Addition of surfactants to a strong acid reduces its surface tension until critical micelle concentration CMC, after that, the surface tension does change much if increasing surfactant concentration (**Fig. 1.27**).

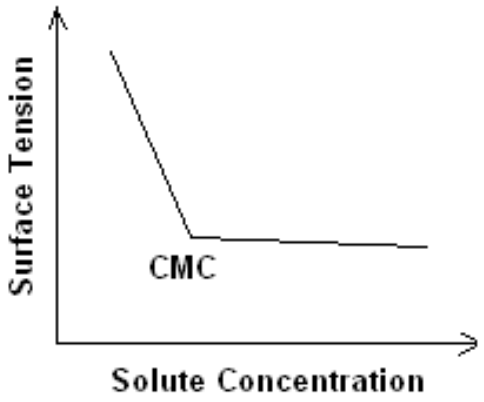


**Fig. 1.27—Surface tension changes with surfactant concentration.**

***Surfactants to Divert Acid***

Most of reservoirs are heterogeneous and permeability varies from one layer to another. During acidizing treatment, the acid will flow into the zones with high permeability, because they are less resistant. Only a limited amount of the acid flows into the low permeable zones or damaged zones. This uneven distribution of the injected acid could cause a major economic loss. The method that can effectively solve this problem is to use acid diversion technique. There are mechanical and chemical means for acid diversion. Mechanical methods include ball sealers, and packers, but they have limited use in openhole, gravel packed and slotted liner completions (Thomas et al. 1998). Chemical means can be used in cased and openhole wells. An effective method is to viscosify the acid. Polymer-based acids and surfactant-based acids are most commonly used today. The goal of this diversion is to reduce acid flow into the zones with high permeabilities and force acid to stimulate the damaged zones.

*Polymer-based Acid*

Crosslinked-acid systems were introduced because they have much higher viscosity than uncrosslinked acids. There are two types of crosslinked acids. The first type of acid is crosslinked on the surface and remains crosslinked in the formation (Johnson et al. 1988). The second type of acid is uncrosslinked when it reaches the formation, and the crosslinking reaction occurs in the formation (Yeager and Shuchart 1997; Saxon et al. 2000). The second type of crosslinked acids is called in-situ gel. It includes HCl, a polymer, a crossliker, a buffer, a breaker and other acid additives. The most commonly used polymer is partially hydrolyzed polyacrylamide (**Fig. 1.28**).

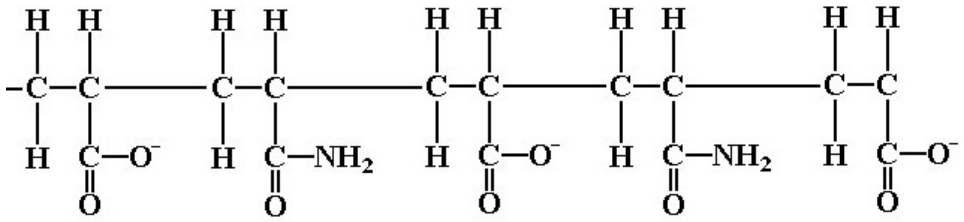

**Fig. 1.28—Structures of partially hydrolyzed polyacrylamide.**

The in-situ-gelled acids use the pH value to control the crosslinking reaction. The cross-linker may be iron (III), zirconium (IV), or other multivalent cations. When hydrochloric acid is injected into the formation, it has a pH of nearly zero. The pH value of the acid increases while the acid reacts with the carbonate reservoir. Polymer will not start reacting with the cross-linker to form a viscous gel unless the pH value approximately reaches 2. When pH is greater than 4, the breaker starts dissociating the polymer and the crosslinker to decrease the viscosity of the acid and prevent the

formation damage. However, there are several concerns related to this system. One noted concern is the precipitation of the crosslinker [Fe (III)] (**Fig. 1.29**) in the formation (Lynn and Nasr-El-Din 2001; Nasr-El-Din et al. 2002). Taylor and Nasr-El-Din (2002; 2003) noted permeability loss after injection of in-situ-gelled acids, which was explained in terms of polymer retention in the core and on the injection face of the core. Poor field data were reported when large volumes of this acid were used to acidize sea water injectors (Mohamed et al. 1999).

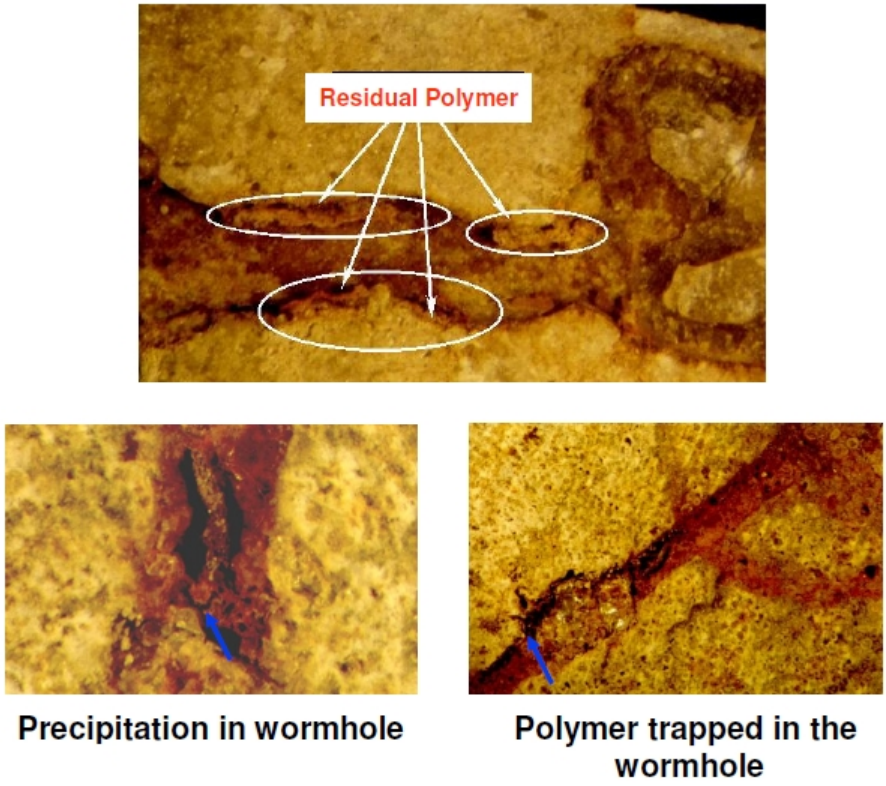


**Fig. 1.29—Residual polymer and Fe precipitation were observed in the core (Lynn and Nasr-El-Din 2001).**

**Fig. 1.30** (Nasr-El-Din et al. 2002) show that the inlet and outlet of the core after the injection of polymer-based acid. Significant amount of polymer was observed on the injection face of the core due to its large size and number.

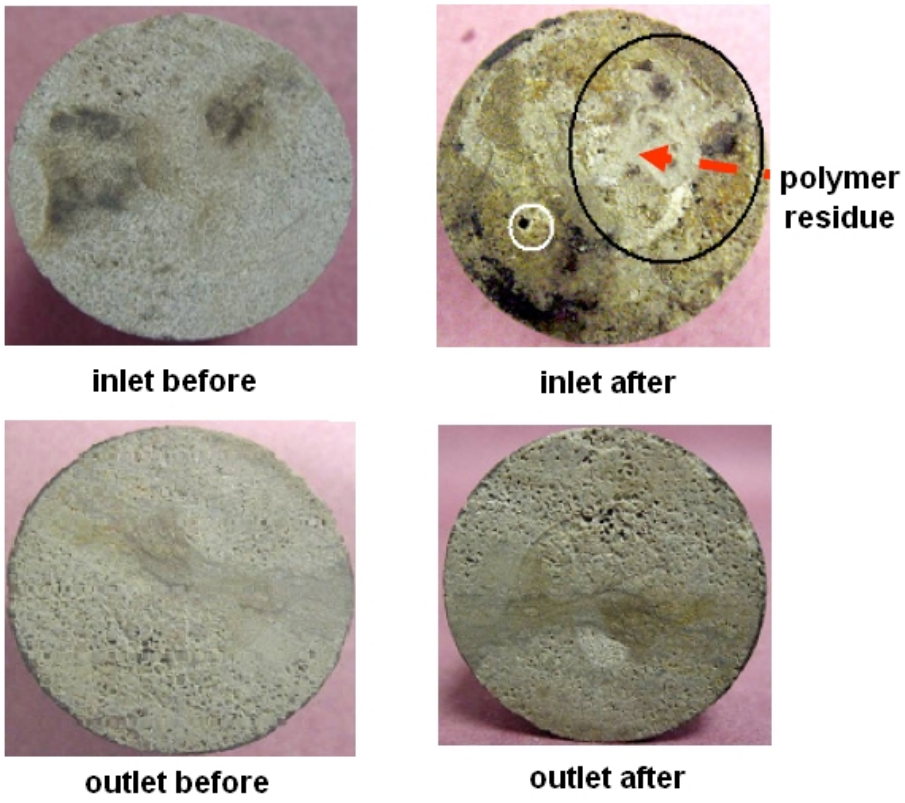


**Fig. 1.30—Surface of cores before and after polymer injection. (Nasr-El-Din et al. 2002)**

*Surfactant-based Acid*

Surfactant-based acids were introduced over the last few years to overcome these potential disadvantages (Chang et al. 2001; 2002; Qu et al. 2002; Nasr-El-Din et al. 2003b; Fu and Chang 2005). Unlike conventional crosslinked acids, surfactant-based acid fluids do not require a metallic crosslinker, and they can significantly reduce

frictional pressure loss when pumped through coiled tubing. These systems were used successfully in both matrix stimulation (Taylor et al 2003; Al-Mutawa et al. 2005; Nasr-El-Din et al. 2006a; Lungwitz et al. 2007) and acid fracturing (Al-Muhareb et al. 2003; Nasr-El-Din et al. 2003a). Huang and Crews (2008) reported a newly developed organic-acid-based surfactant system that is also self-diverting and may not require corrosion inhibitor, even at high temperatures. Field application using surfactant-based acids was very positive (Samuel et al. 2003; Nasr-El-Din and Samuel 2007).

After the acid reacts with the carbonate rock, pH increases and concentrations of divalent cations [Ca (II) and Mg (II)] increase in the spent acid. Both factors cause the surfactant molecules to form long rod-like micelles that will increase the apparent viscosity of the solution significantly (**Fig. 1.31**). Converting rod-like micelles to spherical micelles is necessary to break the gelled spent acid. This can be achieved in water injectors by reducing the concentration of salts and/or surfactant by the injection water. Hydrocarbon phase can be used to break the surfactant gel in oil and gas wells. External (mutual solvent) and internal breakers have also been used to break the rod-like micelle successfully (Nelson et al. 2005; Crews 2005; Crews and Huang 2007).

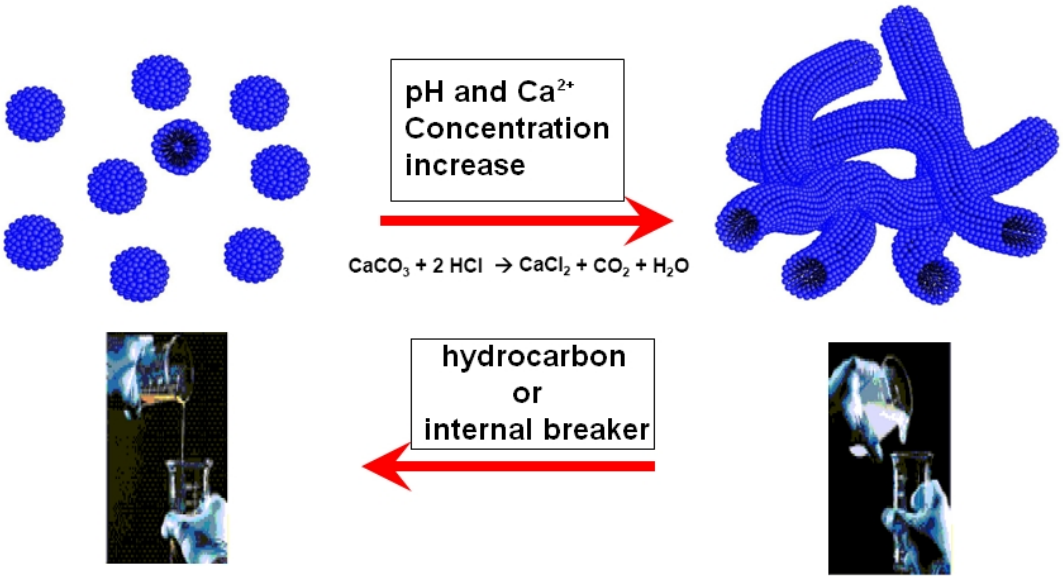


**Fig. 1.31—Mechanism of viscosity build up and break down (Yu et al., 2009; Nasr-El-Din et al., 2008a).**

### Amine Oxide

Amine oxides are prepared by reacting a peroxide or a peracid with a tertiary amine. The polar N→O bond in amine oxides shows the nitrogen atom provides two electrons so that there is a strong electronic density on the oxygen atom. Amine oxides can be protonated and become positively charged in acidic solution, and remain nonionic in neutral and alkaline conditions. They are good foam boosters at neutral and alkaline pH.

$$O \leftarrow NR(CH_3)_2 + H^+ \rightarrow HO\text{-}N^+R(CH_3)_2$$

In the oilfield, amine oxides can be used as diverting agents. The gelled or thickened foam or fluid may be generated by mixing amine oxide gelling agent and acid or foam, water and/or brine. The basic structure of amidoamine oxide is shown in **Fig. 1.32.** At low pH, the surfactant is protonated, and the net charge of the molecule is positive. The surfactant carries both negative and positive charges at pH values greater than 4.

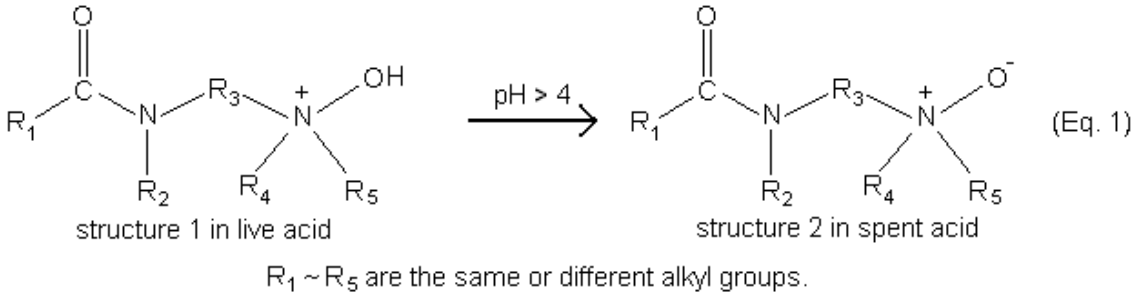


**Fig. 1.32—Basic structure of amidoamine oxide surfactant.**

The properties of this surfactant were discussed by Cawiezel and Dawson (2007). Field application of this type of viscoelastic-surfactant-based acid as a diversion fluid during matrix stimulation was discussed by Nasr-El-Din et al. (2006b-d).

As the acid spends, the acidizing fluid thickens. The fluid viscosity declines when the acid is further consumed, finally returning to a low viscosity state, which allows for the easy cleanup. The process allows for selective acidizing of damaged zone of the formation.

Parallel core diversion tests were conducted and the fluid system contained 28% HCl, 4% amine oxide surfactant and 10 gpt corrosion inhibitor. The experiment was done at 150 $^{o}$F. The results show that the amine oxide gelled acid solution produced wormholes that channeled all the way through the core. The cores had initial permeability of 38 and 68 md, respectively. After the acid injection, the low permeability core had a higher regained permeability (3007 md) than the high permeability core (2644 md), indicating the excellent stimulation and diverting ability (**Fig. 1.33**).

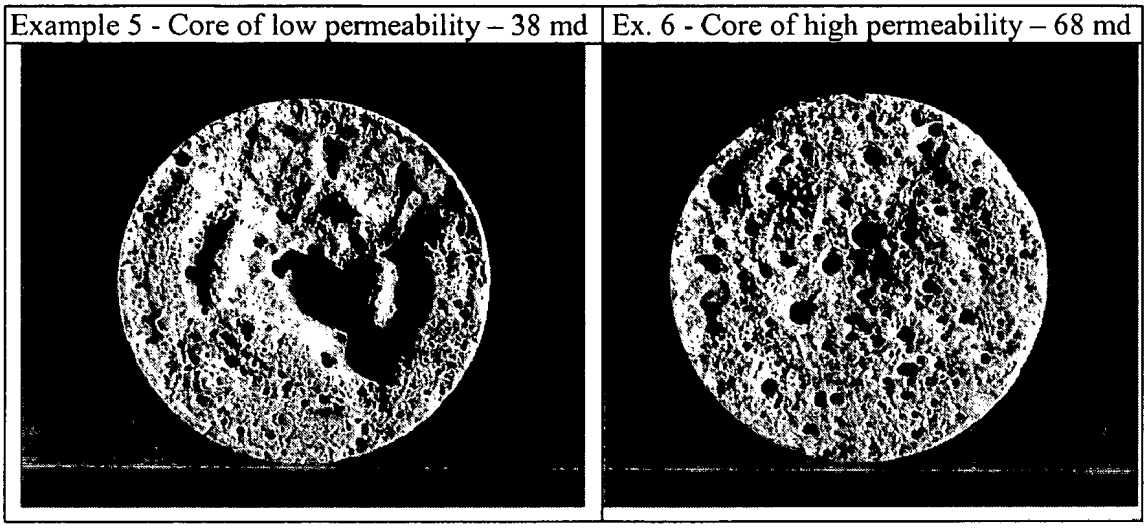


**Fig. 1.33—Results after parallel core flooding tests. (Cawiezel and Dawson, 2007)**

Amidoamine oxide was selected in this study, not only because the positive results were obtained in the carbonate reservoirs (Nasr-El-Din et al. 2006b-d), but also because it is compatible with divalent cations and its gel can be removed from the formation with internal breakers (Crews 2005).

Rheological properties and kinetic studies of amidoamine oxide-based acids have been examined and the results will be described in Chapters II-V.

# CHAPTER II

# RHEOLOGICAL PROPERTIES OF AN AMIDOAMINE OXIDE SURFACTANT*

## Objective

Surfactant-based acid systems were developed over the last few years for diversion to overcome the severe problems caused by polymer residue and crosslinker precipitate after polymer-based system treatments during matrix and fracture acidizing. The physical properties of viscoelastic surfactants are a complex function of surfactant type, concentration, additives, salinity, pH, temperature, and shear rate. These properties are more complicated for amphoteric surfactants, since the rheological properties, surface tension and adsorption depend on pH in the solution. Nasr-El-Din et al. (2008a) reported rheological properties of a carboxybetaine surfactant. A new class of viscoelastic surfactants, amidoamine oxide (Surfactant-A) was examined in this chapter. It carries a positive charge in live HCl acids. The objective of this study is to determine the effects of common acid additives and Fe (III) contamination on the apparent viscosity of live and spent acids that are prepared with the new viscoelastic surfactant.

---

## Experimental Studies

### *Materials*

The viscoelastic surfactant-A used was a mixture of an amphoteric surfactant and solvent. Hydrochloric acid (ACS reagent grade, 36.8 wt%) and deionized water (resistivity = 18.2 $M\Omega \cdot cm$) were used to prepare the acid solutions. Acid concentration was determined by titration using 1N sodium hydroxide solution. Acid additives examined included: Corrosion Inhibitors A and B, a demulsifier, a hydrogen sulfide scavenger, a mutual solvent, iron-control agents (citric acid, lactic acid, and tetrasodium EDTA), and methanol. **Table 2.1** summarizes the main components of these additives. Calcium chloride dihydrate was purchased from VWR. Anhydrous ferric chloride, citric acid, and lactic acid were obtained from Sigma-Aldrich. Tetrasodium EDTA, calcium carbonate, and methanol were obtained from Fisher Scientific, EM Science, and EMD Chemicals, respectively.

**TABLE 2.1--COMPOSITION OF ACID ADDITIVES EXAMINED**

| Additive | Main Components | Concentration (wt%) |
|---|---|---|
| Viscoelastic Surfactant-A | amides, tallow, n-[3-dimethylamino)propyl], n-oxides | 50-65 |
| | 1,2-propanediol | 25-40 |
| Corrosion inhibitor-B | methanol | 10-30 |
| | isopropanol | 10-30 |
| | substituted alcohol | 1-5 |
| | haloalkyl heteropolycycle salt | 10-30 |
| | propargyl alcohol | 1-5 |
| | formamide | 10-30 |

| TABLE 2.1—CONTINUED. | | |
|---|---|---|
| | ethoxylated 4-nonylphenol | 5-10 |
| | heavy aromatic naphtha | 1-5 |
| | pine oil | 1-5 |
| | naphthalene | 0.1-1 |
| Corrosion inhibitor-A | isopropanol | 10-30 |
| | dimethylformamide | 10-30 |
| | propargyl alcohol | 5-10 |
| | substituted alcohol | 1-5 |
| | haloalkyl heteropolycycle salt | 10-30 |
| | quaternary ammonium compound | 10-30 |
| | oxyalkylated alcohol | 10-30 |
| Non-emulsifying agent | aromatic hydrocarbon solvent | < 35 |
| | xylene | < 5 |
| | isopropyl alcohol | < 65 |
| | naphthalene | < 5 |
| Mutual solvent | ethylene glycol monobutyl ether | > 99 |
| $H_2S$ scavenger | aldehydes | Not available |
| Iron control agent | citric acid | > 99 |
| Iron control agent | lactic acid | > 99 |
| Iron control agent | EDTA tetrasodium salt | > 99 |
| Methanol | | > 99 |

***Fluid Systems***

Most of the experiments in this paper were performed using 20 wt% HCl, 4 wt% viscoelastic surfactant-A, and 1 wt% Corrosion Inhibitor A. The 4 wt% surfactant was selected because this is the typical use concentration for this surfactant. The effects of changing concentrations of surfactant on the viscosity of live acid are reported in Chatriwala et al. (2005). The effects of changing the concentration of surfactant on the viscosity of spent acids were reported in Nasr-El-Din et al. (2006c). Acid solutions with various additives were prepared such that the final acid concentration was 20 wt%.

*Live Surfactant-based Acid*

The live-acid solution (200 g) was prepared by mixing 4 wt% viscoelastic surfactant-A with concentrated hydrochloric acid, followed by diluting with deionized water, and then the resulting solution was mixed with 1 wt% corrosion inhibitor. Every effort was made not to contaminate the acid with iron. Therefore, the system was mixed by overhead stirrer assembled with polished (glass) stirring shaft and Teflon agitator for 30 min at 300 rev/min.

*Spent Surfactant-based Acid*

Calcium carbonate was added carefully to neutralize 20 wt% HCl until pH was 4 to 5. Corrosion inhibitor and other additives were then added to the spent acid. A blender was used to mix these solutions. The viscoelastic surfactant-A was added quickly as the last additive to the spent-acid mixture. The whole mixture was blended well at a high shear rate (approximately 4,000 rev/min) for 1 to 2 minutes.

*Removal of Air Bubbles*

A considerable number of air bubbles remained in the viscous live and spent acids after mixing. These bubbles were removed by centrifuging the acid samples for 30 minutes at 2,500 rev/min.

### *Equipment*

A Grace Instrument M5600 HPHT Rheometer was used to measure the apparent viscosity of live and spent acids under different conditions. The wetted material was Hastelloy C-276, an acid-resistant alloy. The rheometer can measure viscosity at various temperatures up to 500$^{o}$F, over shear rates of 0.00004 to 1,870 sec$^{-1}$. A B5 bob was used in this work, which required a sample volume of 52 cm$^{3}$. A pressure of 300 psi was applied to minimize evaporation of the sample, especially at high temperatures. An Orion 950 analytical titrator was used to measure HCl concentration. The centrifuge used to remove air bubbles was Z 206 A, obtained from Labnet International.

## Results and Discussions

The surfactant solutions were prepared in water, live acid, or spent acid. For water solutions, deionized water was mixed with 4 wt% surfactant to form a viscous gel. In live-acid solutions, the viscoelastic solutions were mixed with 20 wt% HCl, and various additives were mixed so that the final acid concentration was 20 wt% and the surfactant concentration was 4 wt%. To prepare spent-acid solutions, the live acid was neutralized using calcium carbonate to a pH value of nearly 4-5. A pH value of 5 was selected to simulate pH values of spent acid following acid treatments in carbonate reservoirs. The presence of $CO_2$ in spent acids buffers the pH at 4 to 5 (Nasr-El-Din et al. 2009).

### *Apparent Viscosity of Amidoamine Oxide in Water*

*Effect of Shear Rate*

**Fig. 2.1** shows the apparent viscosity as a function of shear rate for a surfactant solution that contained 4 wt% viscoelastic surfactant-A. The results of two shear sweeps (ascending and descending) indicate that the apparent viscosity was almost independent of the shear-rate history at room temperature.

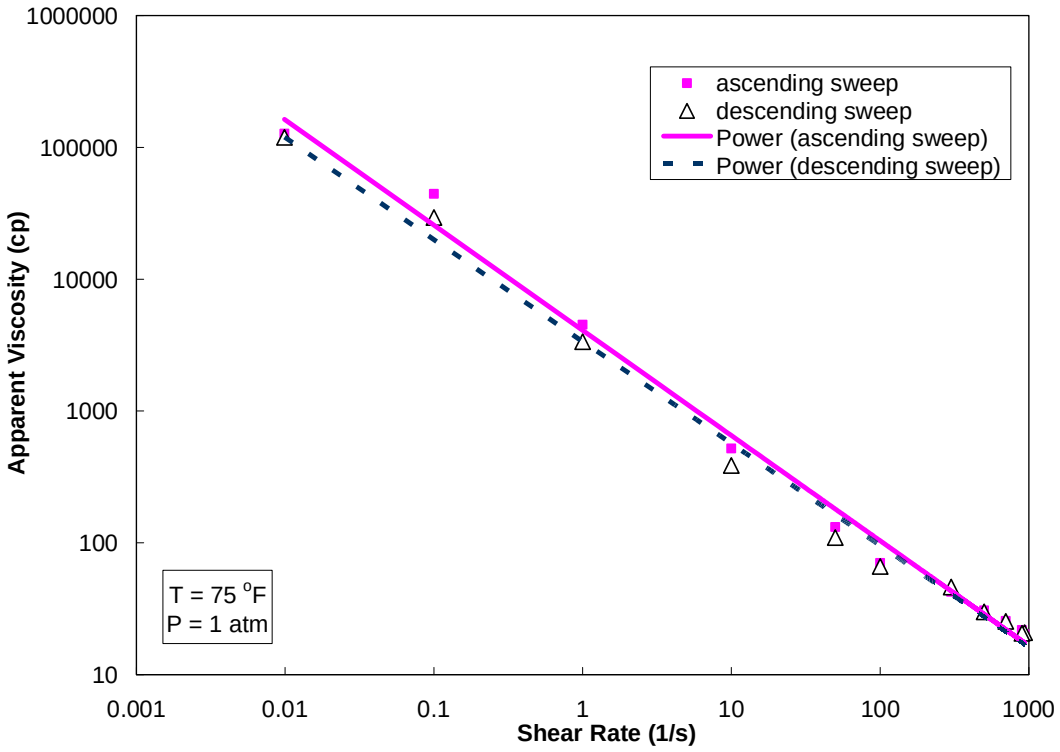


**Fig. 2.1—Shear history dependence of the apparent viscosity of a 4 wt% surfactant-A solution in water at 75°F.**

*Effect of Temperature*

**Fig. 2.2** shows the apparent viscosity as a function of temperature for the solution containing 4 wt% viscoelastic surfactant-A at a shear rate of 10 $sec^{-1}$ and at 300 psi. The apparent viscosity increased and reached a maximum at 135°F. The maximum value obtained was approximately twice that obtained at room temperature. After that, the apparent viscosity rapidly decreased as temperature was increased to 195°F. At that temperature, the solution had an apparent viscosity similar to water. It is important to note that the increase in viscosity with temperature was noted with different solutions of viscoelastic surfactants (Nasr-El-Din et al. 2008a), and most likely occurs because of the changes in the shape of micelles with temperature.

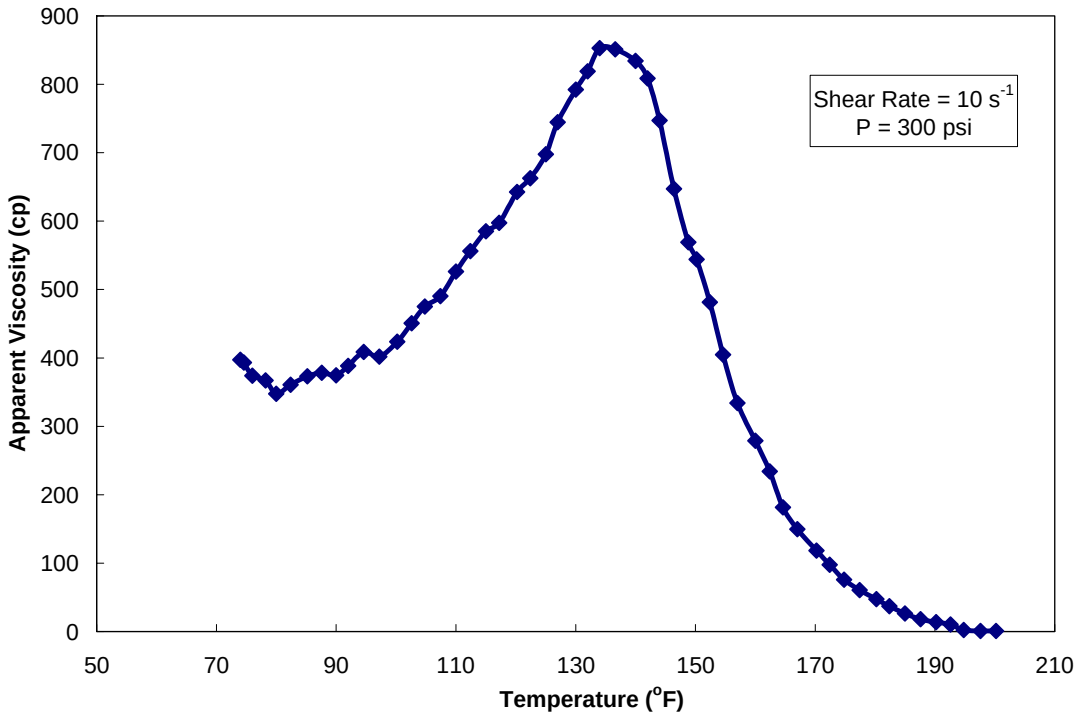


**Fig. 2.2—Effect of temperature on the apparent viscosity of a 4 wt% surfactant-A solution in de-ionized water at 10 $s^{-1}$.**

### *Apparent Viscosity of Live Acids*

*Effect of Temperature and Corrosion Inhibitors*

**Fig. 2.3** shows the apparent viscosity as a function of temperature for live acids containing 4 wt% surfactant-A, 20 wt% HCl, and 1 wt% corrosion inhibitor (A or B) at a shear rate of 10 $sec^{-1}$ and at 300 psi. The apparent viscosity of live acid was much lower than that noted when the surfactant was dissolved in deionized water. Another very important observation is that the viscosity depends on the type of corrosion inhibitor used. Corrosion inhibitors used with HCl always contain short-chain alcohols (e.g., isopropanol). These alcohols can impact the viscosity of surfactant solutions adversely. Therefore, it is very important to select a corrosion inhibitor that will have minimum impact on the apparent viscosity of surfactant-based acids.

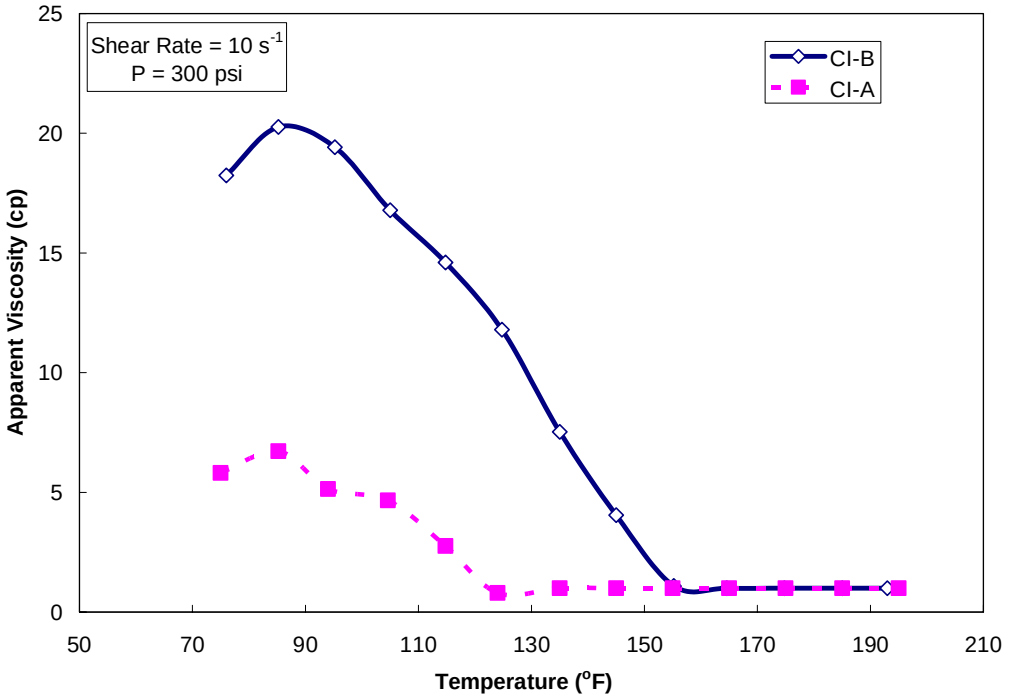


**Fig. 2.3—Effect of corrosion inhibitors on the apparent viscosity of live acids containing 4 wt% surfactant-A and 20 wt% HCl.**

*Effect of Salinity*

Salts are sometimes added to live acids to increase their density. It is of interest to examine how these salts affect the apparent vicosity of surfactant-based acids. **Fig. 2.4** shows the influence of calcium chloride on the apparent viscosity of live acids containing 4 wt% surfactant-A, 20 wt% HCl, and 1 wt% Corrosion Inhibitor A at a shear rate of 10 $sec^{-1}$ and at 300 psi. The live-acid solution that contained 10 wt% calcium chloride gave higher apparent viscosity than the one with 5 wt% calcium chloride, and the latter solution was more viscous than the solution without salts.

The net charge of amidoamine oxide in live acids is positive (Structure 1, Fig. 1.32). Therefore, there is no electrostatic interaction between the positive calcium ions and the surfactant molecules. However, a complexing reaction between $CaCl_3^-$ and cationic surfactants may exist (Kim et al. 1996). This may explain the increase in viscosity.

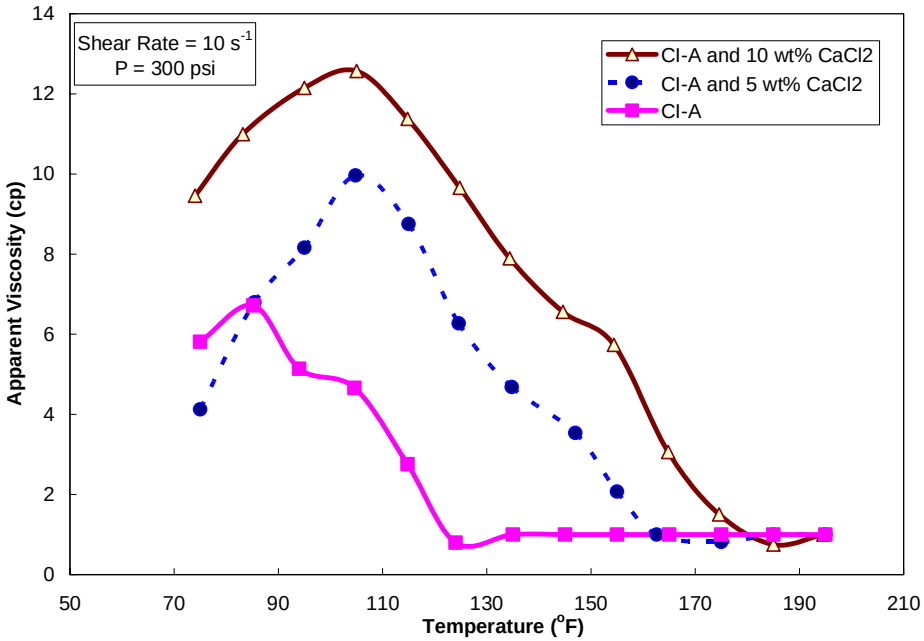


**Fig. 2.4—Effect of calcium chloride on the apparent viscosity of live acids containing 4 wt% surfactant-A, 20 wt% HCl and 1 wt% CI-A.**

*Effect of Fe(III)*

**Fig. 2.5** shows the effect of Fe(III) concentration on live-acid solutions with 4 wt% surfactant-A and 20 wt% HCl. A yellowish clear gel was noted at 0.3 wt% $FeCl_3$. Phase separation was noted when 0.5 wt% $FeCl_3$ was added to live acid and both of the phases were yellow. A thin, light, reddish layer was separated in the system at 1 wt% $FeCl_3$. There was a precipitate at $FeCl_3$ concentration of 3 wt%. These results were similar to those obtained with a betaine-based system (Al-Nakhli et al. 2008) and highlighted the detrimental effects of ferric ion on these acid systems.

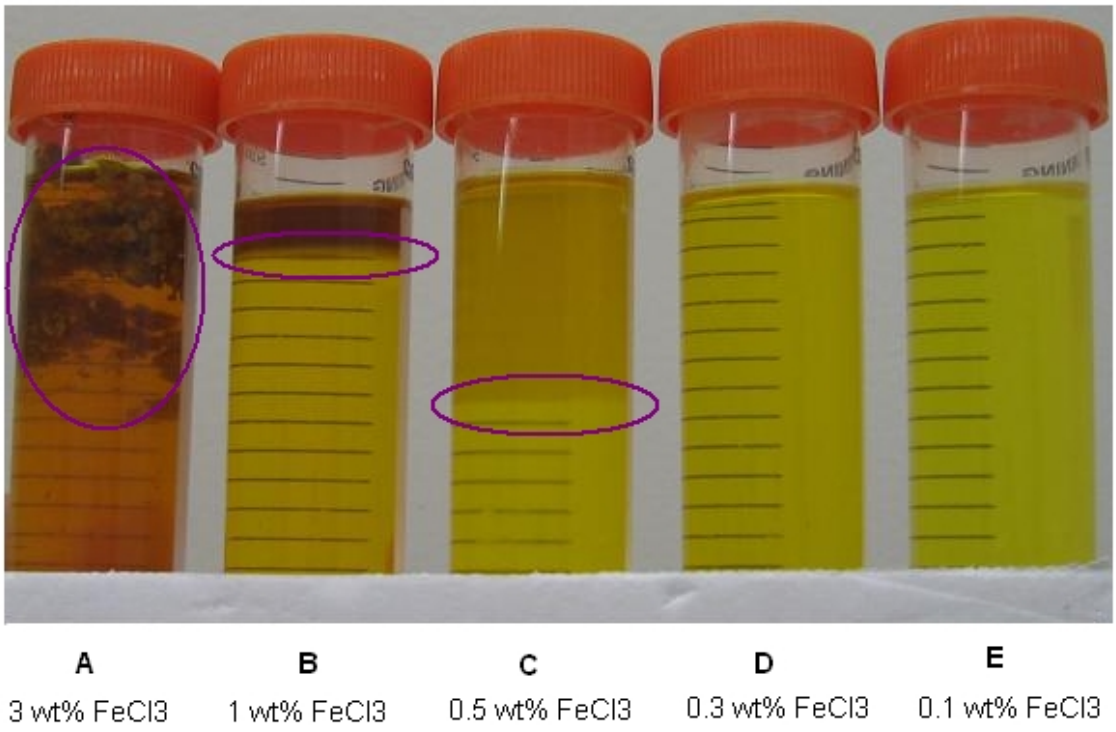


**Fig. 2.5—Effect of Fe (III) concentration on the viscoelastic surfactant-based live acids containing 4 wt% surfactant-A and 20 wt% HCl. Tubes E and D were homogeneous solutions. B and C showed two phases. Tube A contained some brown precipitate.**

The apparent viscosity of live-acid systems was measured at low concentrations of $FeCl_3$. **Fig. 2.6** shows that a system with a low concentration of $FeCl_3$ was more viscous than the system without $FeCl_3$ at temperatures below 100°F, especially at 0.3 wt% $FeCl_3$. Low concentrations of Fe (III) may complex with surfactant by forming ligands with –N and/or –OH groups of the surfactant (Laulhere and Briat 1993). This interaction can cause an increase in the apparent viscosity of live acid. Concentrated Fe (III) can form $FeCl_4^-$ in strong acid solutions, which continue with viscoelastic surfactants and form a precipitate in live acids (Al-Nakhli et al. 2008). Therefore, to prevent the contamination of acids with Fe(III), it is necessary to use clean tanks in preparing the acid in the field and necessary to pickle well tubulars before acid injection.

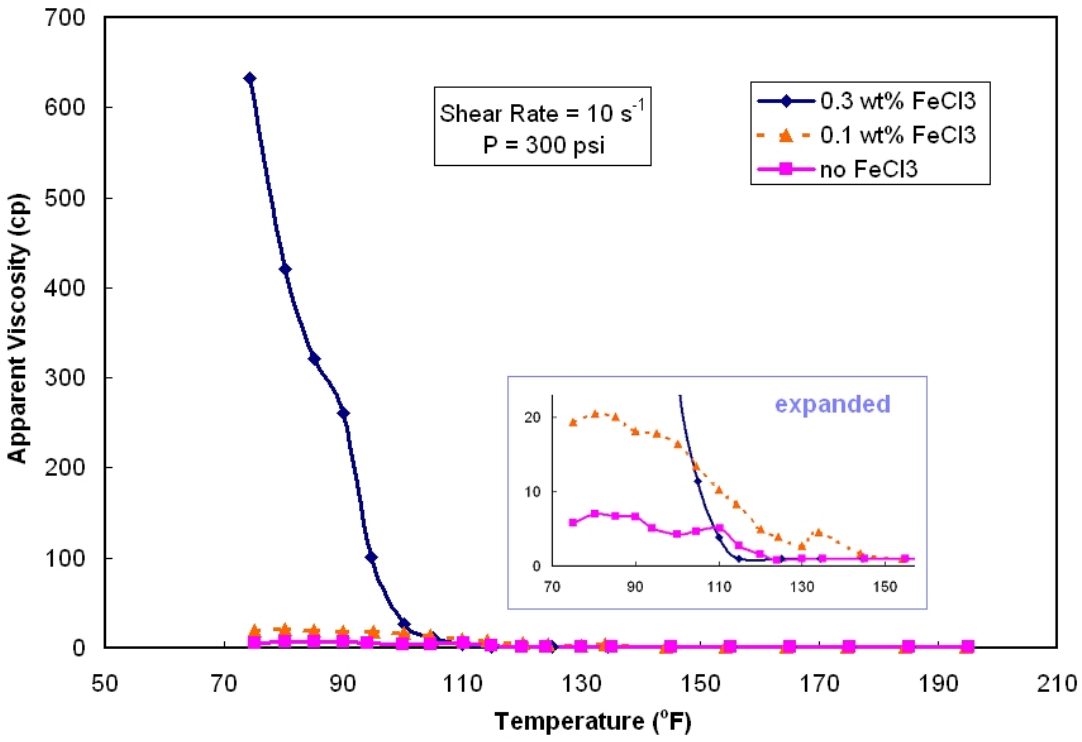


**Fig. 2.6—Effect of Fe (III) on the apparent viscosity of live acids containing 4 wt% surfactant-A, 20 wt% HCl and 1 wt% CI-A.**

*Effect of HCl Concentration*

Various concentrations of HCl can result in significantly different apparent viscosities of carboxybetaine surfactants in live HCl acid solutions (Nasr-El-Din et al. 2008a). The carboxybetaine system showed increased apparent viscosity when the concentration of HCl decreased from 28 to 16 wt%, then the apparent viscosity was constant at acid concentrations of 12 to 16 wt%; after that, the apparent viscosity increased again when lowering concentrations of HCl to 3 wt%. Compared to the carboxybetaine system, the amidoamine oxide surfactant-A exhibited a significantly different behavior. **Fig. 2.7** shows that solutions with high HCl concentrations (18 to 28 wt%) were slightly viscous. Much higher viscosity can be obtained for solutions with moderate HCl concentrations (8 to 15 wt%). It can be seen that the acid that contained 12-wt% HCl gave the highest apparent viscosity. However, phase separation was observed when HCl concentrations were reduced to 4 to 7 wt%. Homogeneous and viscous solutions were obtained at low HCl concentrations (1 to 3 wt%), whereas the viscosity decreased rapidly when HCl was less than 1 wt%. It is interesting to note that the current surfactant and betaine-type surfactants are both amphoteric, but have different viscosity behavior.

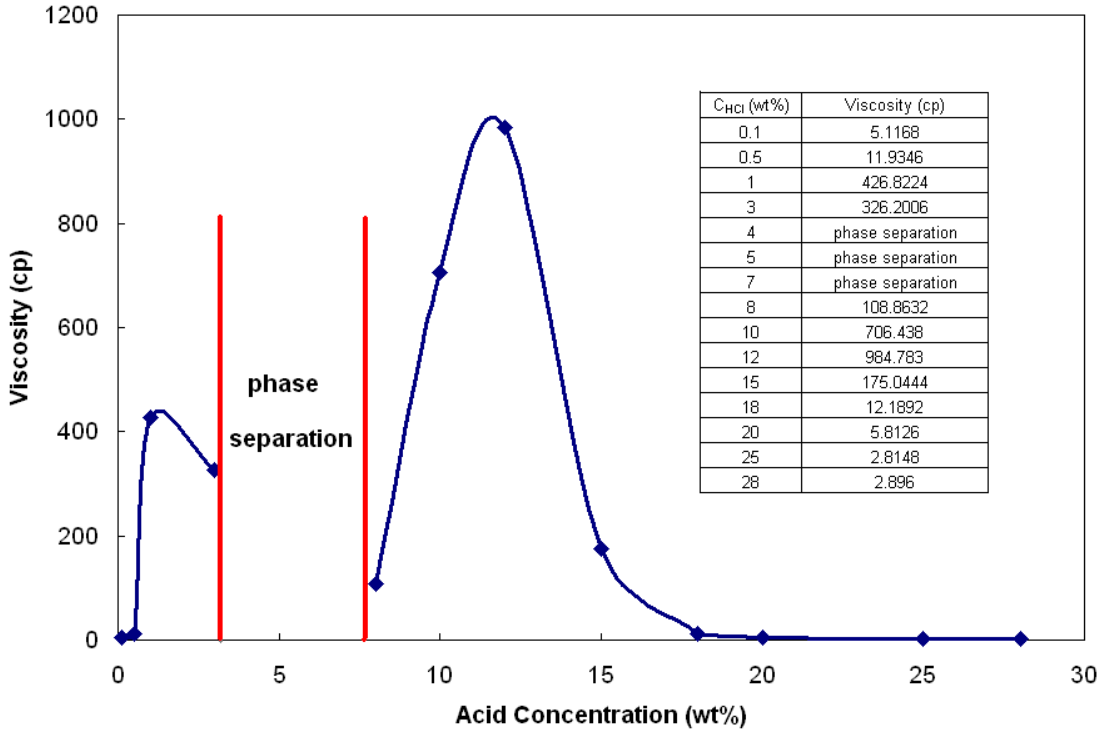


| $C_{HCl}$ (wt%) | Viscosity (cp) |
|---|---|
| 0.1 | 5.1168 |
| 0.5 | 11.9346 |
| 1 | 426.8224 |
| 3 | 326.2006 |
| 4 | phase separation |
| 5 | phase separation |
| 7 | phase separation |
| 8 | 108.8632 |
| 10 | 706.438 |
| 12 | 984.783 |
| 15 | 175.0444 |
| 18 | 12.1892 |
| 20 | 5.8126 |
| 25 | 2.8148 |
| 28 | 2.896 |

**Fig. 2.7—Effect of HCl concentration on the apparent viscosity of live acids containing 4 wt% surfactant A and 1 wt% Cl-A.**

### *Apparent Viscosity of Spent Acids*

*Effect of Mutual Solvent*

Mutual solvent, ethyleneglycol monobutyl ether, can break rod-shaped micelles (Fu and Chang 2005). **Fig. 2.8** shows that the apparent viscosity of the spent acid decreased significantly with the addition of mutual solvent. The system with 10 wt% mutual solvent was less viscous than the system with 5 wt% mutual solvent.

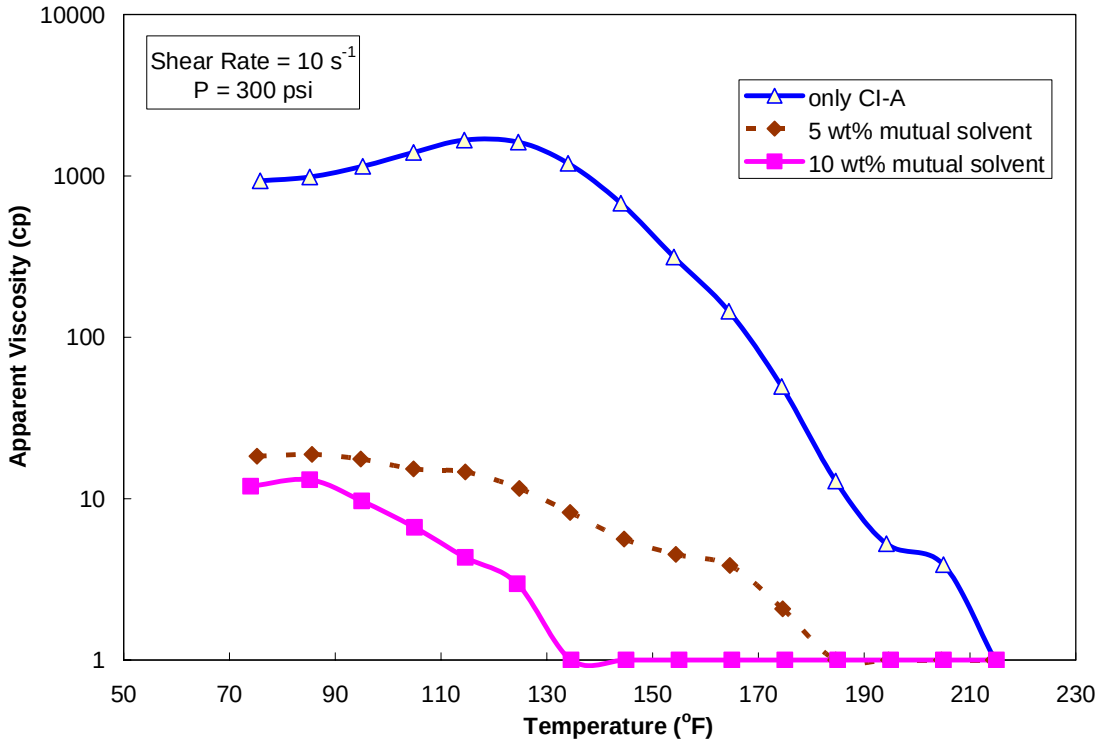


**Fig. 2.8—Effect of mutual solvent on the apparent viscosity of spent acids (pH = 4 ~ 5). All solutions contained CI-A.**

Phase separation occurred when 15 wt% mutual solvent was added to the spent acid **(Fig. 2.9).** It is interesting to note that no phase separation was noted when mutual solvent was added to live acids.

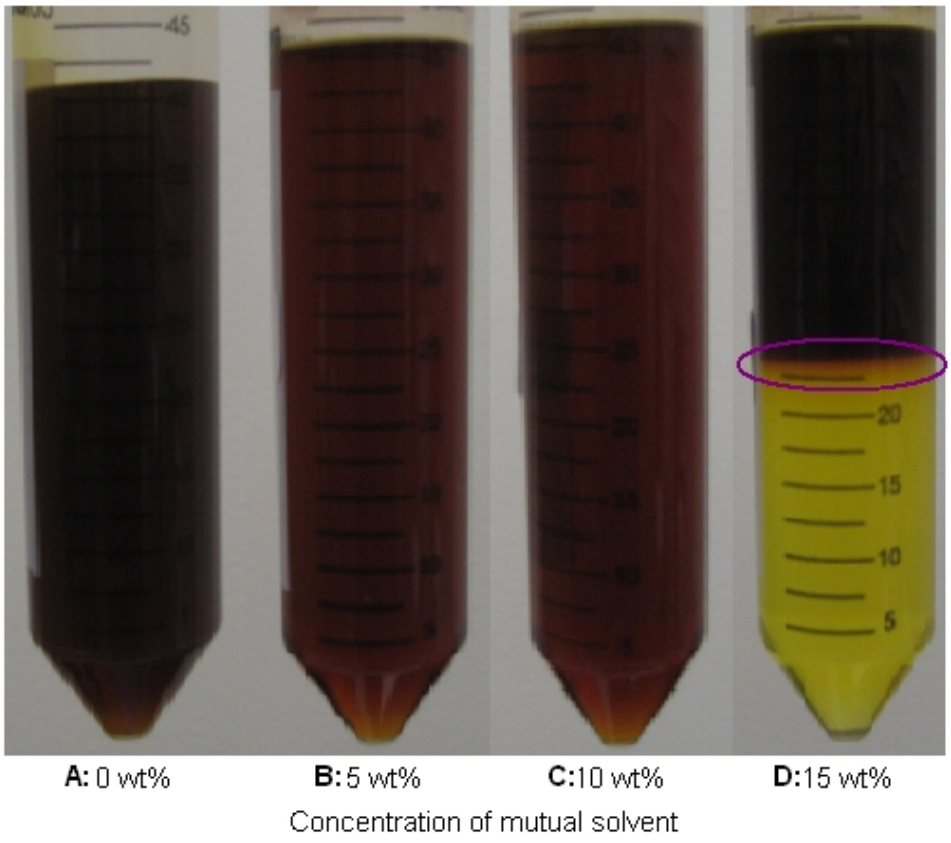


**Fig. 2.9—Effect of mutual solvent concentration on spent acids (pH = 5). Tube D had two phases.**

*Effect of Fe(III), $H_2S$ Scavenger, and Demulsifier*

On the basis of the results of the live-acid system, only 0.1- and 0.3 wt% $FeCl_3$ were tested to examine the effect of Fe (III) on the apparent viscosity of spent acids. However, the results obtained showed that the spent-acid system with 0.3 wt% $FeCl_3$ gave two immiscible phases **(Fig. 2.10)** even though the related live-acid system was homogeneous. A reddish precipitate was noted at the bottom of the tube. Ferric ion precipitates at pH 1 to 2 (Taylor et al. 1999). **Fig. 2.11** shows that solutions that contained 0.1 wt% $FeCl_3$ and 0.5 wt% $H_2S$ scavenger behaved almost in the same

manner. First, their apparent viscosity increased when the system was heated to 105°F, and then decreased from 1,400 to 10 cp within a 40°F temperature span. At pH 5, the viscoelastic surfactant-A had Structure 2 in Fig. 1.32. The amine oxide group $N^{+}$-$O^{-}$ can attack the carbonyl group in $H_2S$ scavenger (aldehydes) and change the rod-shaped micelles shaped into spherical ones, which might result in low apparent viscosity.

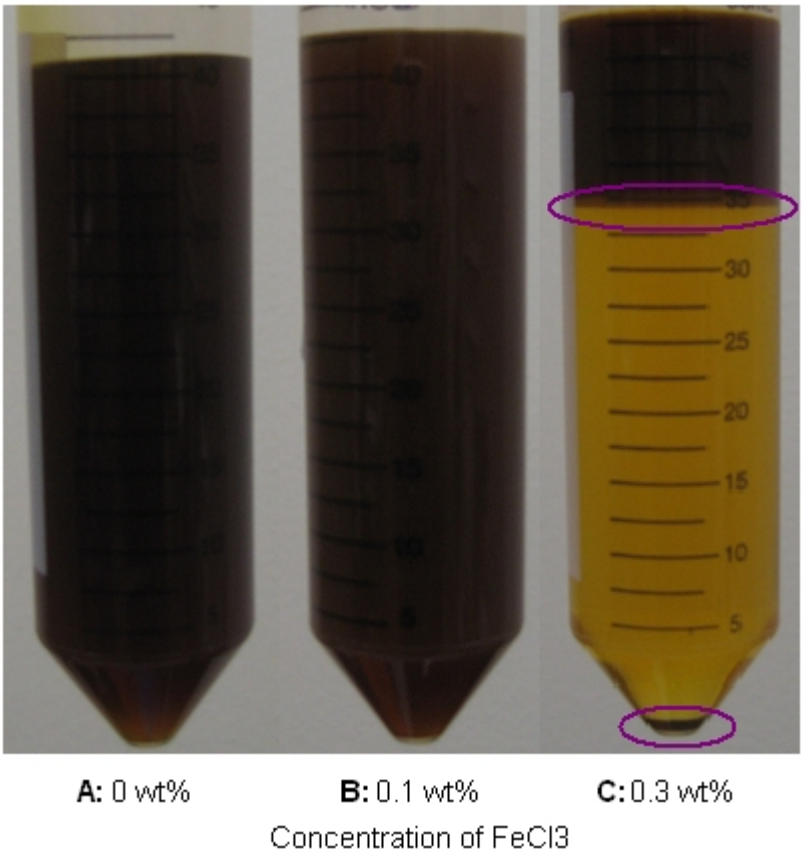


**Fig. 2.10—Effect of Fe (III) concentration on spent acids (pH = 4 ~ 5). C showed two immiscible liquids and precipitate of iron at the bottom**

Fig. 2.11 also shows that the demulsifier decreased the apparent viscosity of spent acid at all temperatures from 70 to 215°F. It can be seen from Table 2.1 that the main

components of demulsifer, hydrocarbons and alcohol, can break the rod-shaped micelles and decrease the apparent viscosity.

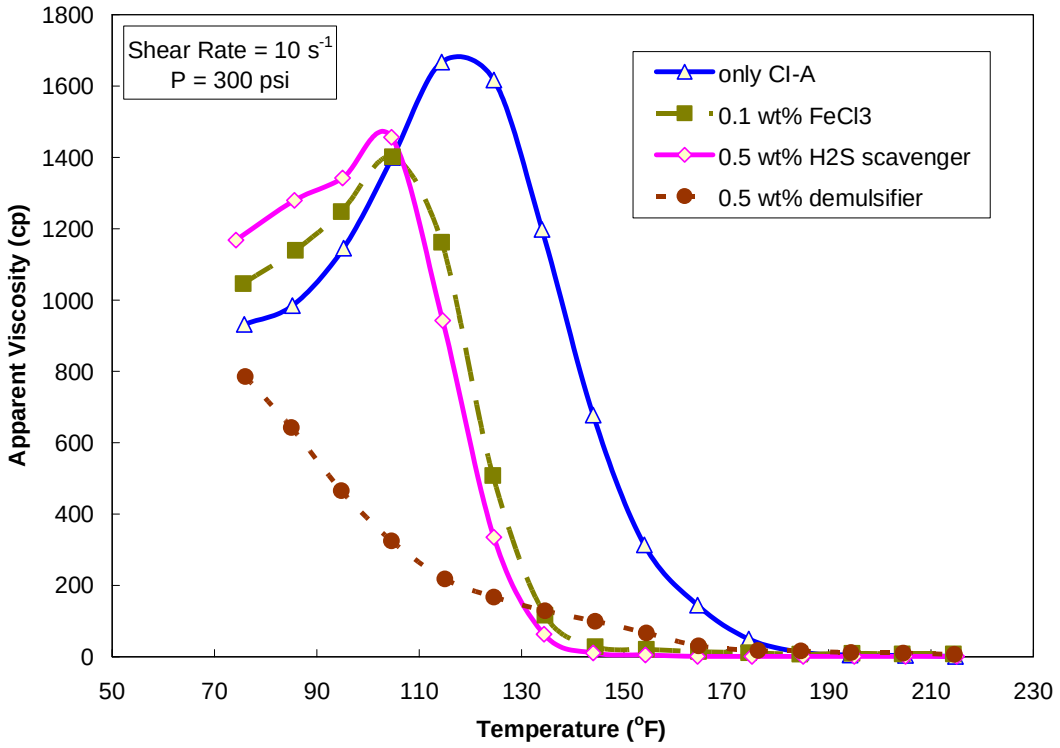


**Fig. 2.11—Effect of some acid additives on the apparent viscosity of spent acids (pH = 4 ~ 5). All solutions contained CI-A.**

*Effect of Iron-control Agents*

Citric acid, lactic acid, and tetrasodium EDTA were examined. **Fig. 2.12** shows that the system with 0.5 wt% citric acid was homogeneous. However, there were two phases and a white precipitate (calcium citrate) at the bottom of the test tube when the concentration of citric acid was increased to 1 wt%.

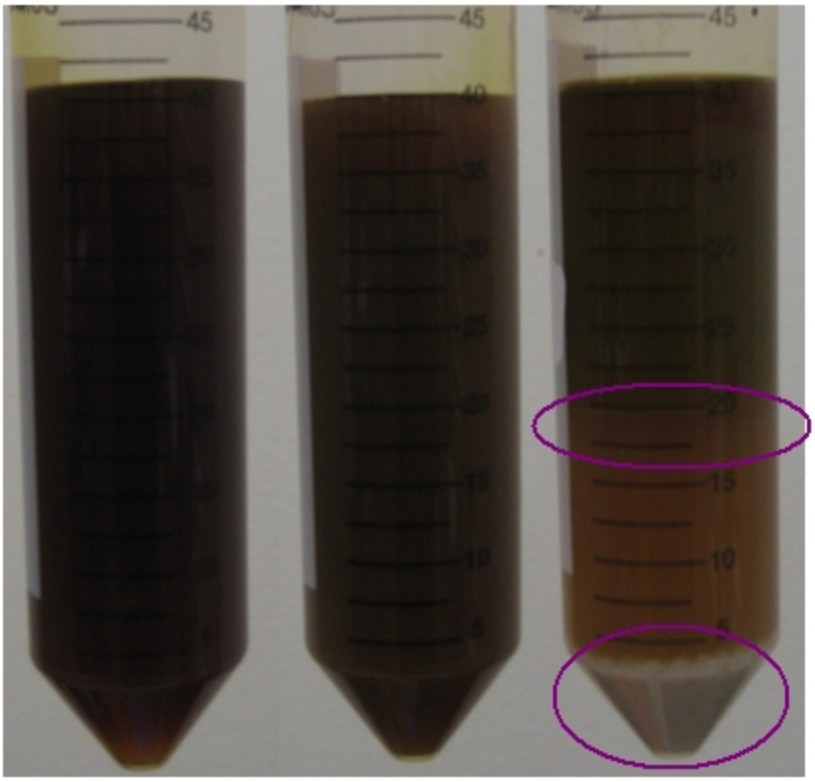


**Fig. 2.12—Effect of citric acid concentration on spent acids (pH = 4 ~ 5). C showed two immiscible liquids and a white precipitate of calcium citrate at the bottom.**

It can be seen from **Figs. 2.13 through 2.15** that the addition of iron-control agents to the spent acid reduced its apparent viscosity. The apparent viscosity of surfactant-based acids decreased significantly as the concentration of lactic acid was increased. The apparent viscosity of spent acid that contained 1 wt% tetrasodium EDTA was similar to that obtained with 0.5 wt% tetrasodium EDTA. It should be mentioned that there were white undissolved solids in live acid with 1 wt% tetrasodium EDTA salt because of the limited solubility of EDTA in 20 wt% HCl (Hall and Dill 1988).

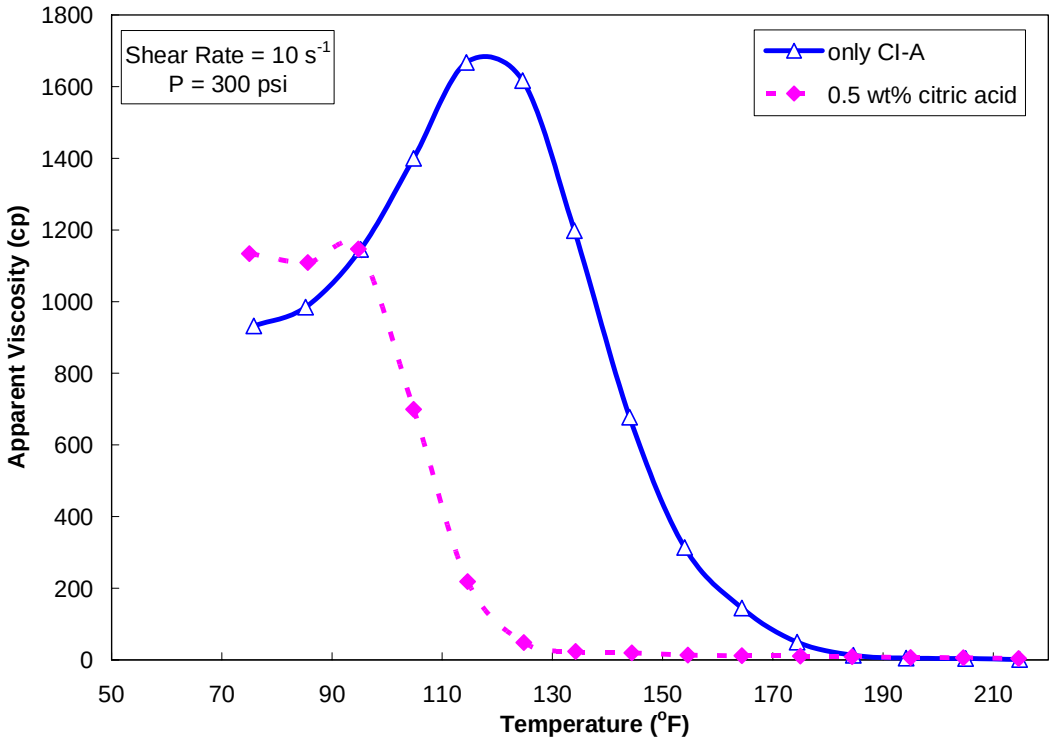


**Fig. 2.13—Effect of citric acid on the apparent viscosity of spent acids (pH = 4 ~ 5). All solutions contained CI-A.**

Nine water molecules surround one calcium ion in aqueous solutions, which means that nine chelating functional groups are needed to replace water and form a complex (Bakken and Schöffel 1996). In the spent acids, $Ca^{2+}$ was already chelated by the iron-control agent. Thus, less $Ca^{2+}$ was available to form rod-shaped micelles.

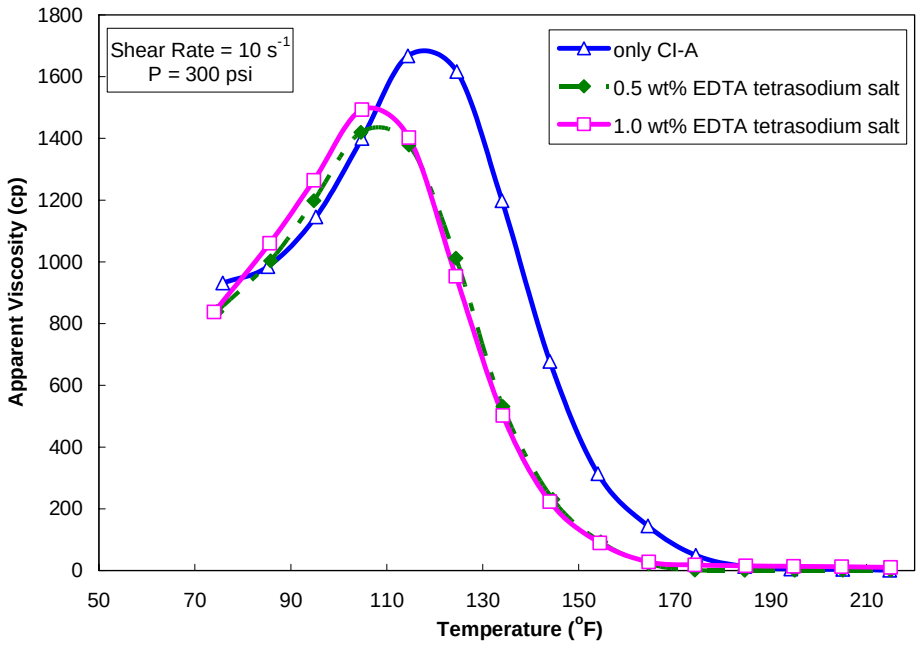


**Fig. 2.14—Effect of EDTA on the apparent viscosity of spent acids (pH = 4 ~ 5). All solutions contained CI-A.**

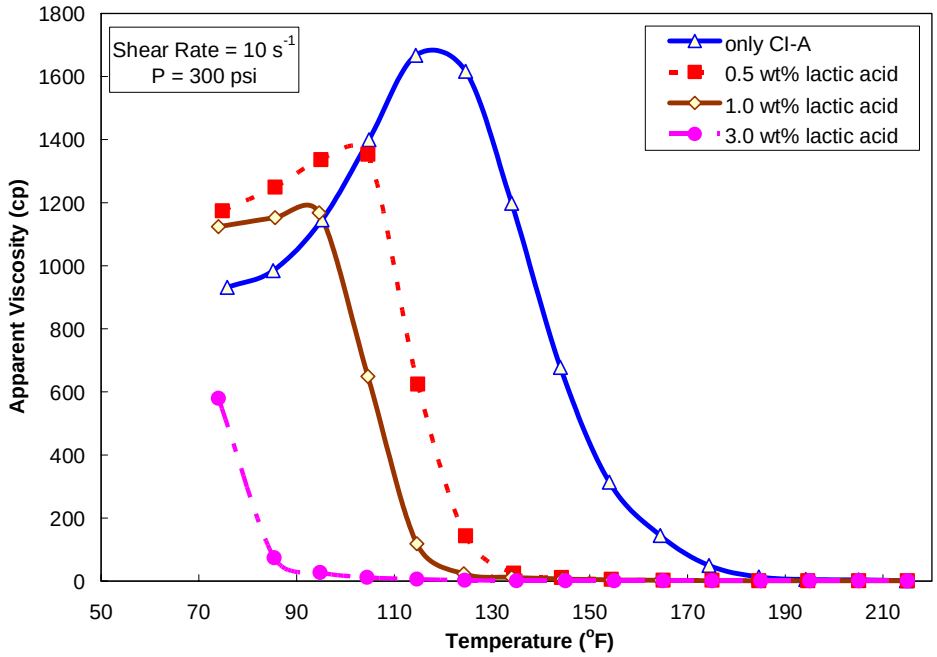


**Fig. 2.15—Effect of lactic acid on the apparent viscosity of spent acids (pH = 4 ~ 5). All solutions contained CI-A.**

*Effect of Methanol*

The apparent viscosity was measured at various methanol concentrations from 1 to 15 wt%. The addition of methanol to the spent acid decreased its apparent viscosity. **Fig. 2.16** shows that up to 1 wt% methanol can be used with this spent-acid system at temperatures below 175°F. Higher concentrations of methanol (15 wt%) resulted in higher apparent viscosity than lower concentrations (5 to 10 wt%) of methanol at temperatures greater than 145°F.

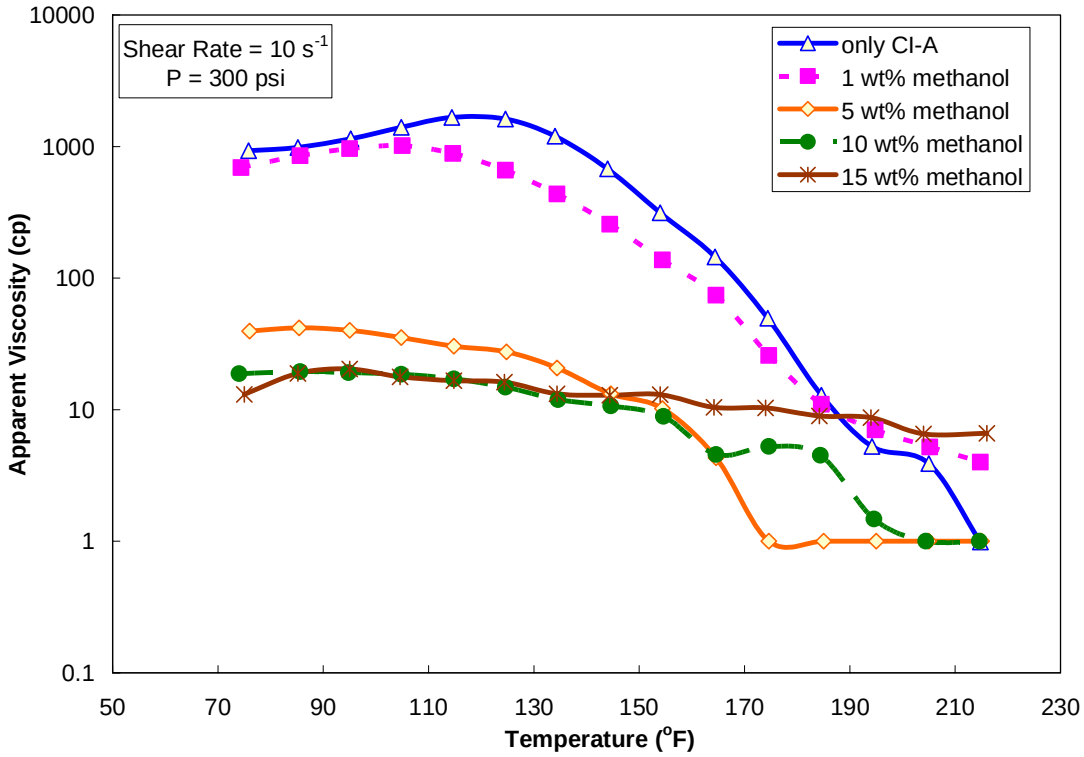


**Fig. 2.16—Effect of methanol on the apparent viscosity of spent acids (pH = 4 ~ 5). All solutions contained CI-A.**

Nasr-El-Din et al. (2008a) also reported the effect of methanol on a carboxybetaine surfactant. The addition of 1 vol% methanol increased the apparent viscosity of spent

acid at temperatures greater than 150°F. Up to 5-vol% methanol can be added to their acid system, especially at high temperatures. High concentrations of methanol (20 vol%) not only decreased the apparent viscosity of the spent-acid system, but also caused phase separation.

***Apparent Viscosity of Surfactant A in A Typical Field Application***

The results discussed thus far indicated that the apparent viscosity of this surfactant-based acid is a complex function of shear rate, temperature, acid type, and concentration. It is of interest to measure the viscosity of this acid system under typical field conditions (i.e., under typical shear rate, temperature, shear rate, and additive concentration). The following conditions were examined.

Flow of live acid in well tubulars: The initial solution contained 20 wt% HCl, 1 wt% CI-A, 0.5 wt% tetrasodium EDTA, and 4 wt% surfactant-A. The apparent viscosity was measured at room temperature.

Flow of acid in a fracture or high-permeability zone: The solution contained 20 wt% HCl, 0.25 wt% CI-A (reduced corrosion inhibitor because of adsorption on well tubulars), 0.5 wt% tetrasodium EDTA, and 4 wt% surfactant-A. The apparent viscosity was measured at 110°F.

Partially spent acid: The solution contained 10 wt% HCl, 0.25 wt% CI-A, 0.5 wt% tetrasodium EDTA, 4 wt% surfactant-A, and $CaCl_2$ that corresponds to spending 10 wt% HCl. The apparent viscosity was measured at 110°F.

Flowback of spent acid from the formation: The solution contained 0.5 wt% HCl, 0.25 wt% CI-A, 0.1 wt% tetrasodium EDTA, 2 wt% surfactant-A, and $CaCl_2$ that corresponded to spending 19.5 wt% HCl. The apparent viscosity was measured at 150°F.

**Fig. 2.17** shows how the apparent viscosity changed with shear rate for these cases. In the tubing, the apparent viscosity was nearly 10 cp at a high shear rate of 900 $sec^{-1}$. In fractures or high-permeability streaks, the apparent viscosity was approximately 20 cp at a lower shear rate of nearly 70 $sec^{-1}$. However, the apparent viscosity increased up to 700 cp at nearly 50 $sec^{-1}$ where half the HCl was consumed and a significant amount of $CaCl_2$ was generated. When acid was nearly spent, the apparent viscosity was only 50 cp at the shear rate of 1 $sec^{-1}$, which indicated reasonable cleanup following the acid treatment. It is worth mentioning that this acid was applied successfully in stimulation of water injectors and oil producers in carbonate reservoirs (Nasr-El-Din et al. 2006b-d).

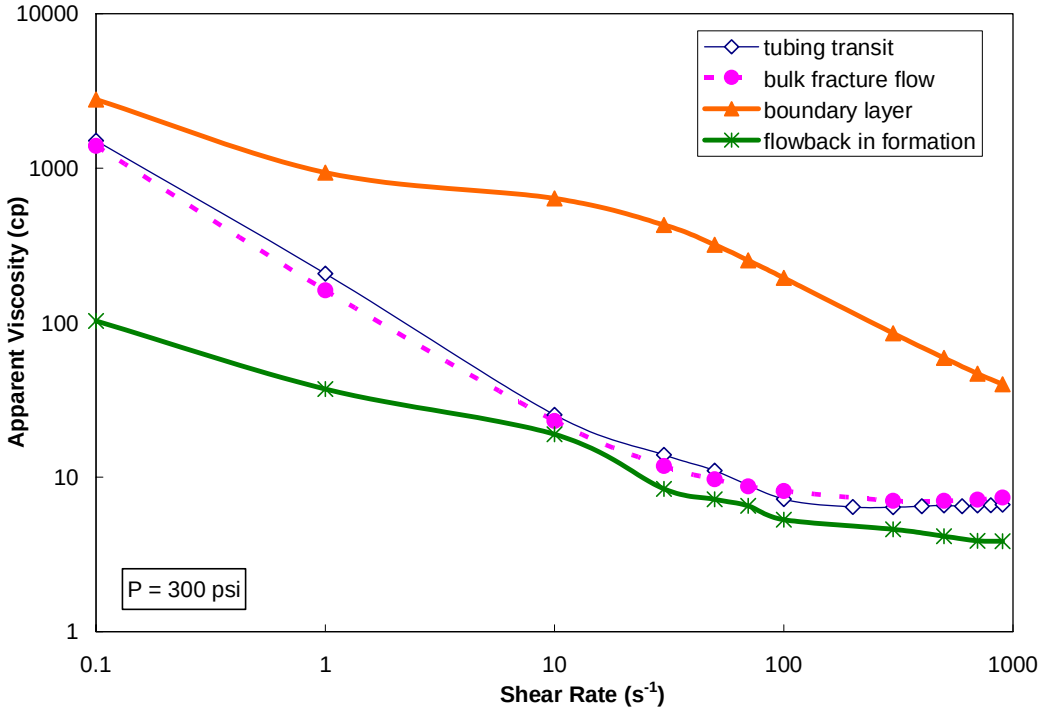


**Fig. 2.17—Applications of this VES-based acid for a life cycle of acid fracturing: tubing transit, bulk fracture flow, boundary layer and flowback in formation.**

## Conclusions

A new class of amphoteric surfactants—amidoamine oxide—was examined in this paper. The apparent viscosity of this surfactant-based acids (both live and spent) was measured as a function of temperature, shear rate, additive type, and concentration. On the basis of the results obtained, the following conclusions can be drawn about acids prepared with 4 wt% amidoamine oxide surfactant-A:

1. The apparent viscosity of surfactant-A in water was almost independent of shear-rate history.
2. Concentration of HCl in the live-acid system affected its apparent viscosity. The solution containing 12 wt% HCl showed the highest apparent viscosity.

3. Corrosion inhibitors reduced the apparent viscosity of live acids. This effect depends on the solvent used to manufacture these inhibitors.
4. Low concentrations of Fe (III) caused an increase in the apparent viscosity. Two immiscible liquids, and then a precipitate, were noted as the concentration of ferric ion was increased in live acids.
5. Acid additives can affect the apparent viscosity of spent acids. Demulsifier and mutual solvent decreased the apparent viscosity at all temperatures examined.
6. Iron-control agents reduced the apparent viscosity of surfactant-based acids. The impact of lactic acid was significant, especially at high lactic-acid concentrations. Citric acid also reduced the viscosity of surfactant-based acids but cannot be used at concentrations greater than 0.5 wt% because of precipitation of calcium citrate. EDTA slightly reduced the viscosity of surfactant-based acids. However, the solubility of EDTA in 20 wt% HCl is very low.
7. Up to 1 wt% methanol can be used with this spent-acid system at temperatures less than 175°F. Higher concentrations of methanol caused significant reduction in the apparent viscosity.

# CHAPTER III

# IMPACT OF ORGANIC ACIDS/CHELATING AGENTS ON THE RHEOLOGICAL PROPERTIES OF AN AMIDOAMINE OXIDE SURFACTANT*

## Introduction

Iron precipitation is a nightmare in oilfield, because it can reduces reservoir permeability in the near-wellbore area, causes loss of injectivity and reduces productivity of oil, gas and water supply wells. Iron can be from contaminated acid, dissolution of rust in the coiled tubing or well casing, from iron-containing minerals in the formation, from corrosion products or from the surface equipment during acid treatment.

Iron can be +2 or +3 oxidation state. Fe (II) is favored in a reducing environment. Both Fe (II) and Fe (III) can cause precipitation under certain conditions. More severe damage will occur from Fe (III) because of lower solubility in spent acid. **Fig. 3.1** shows that iron (III) hydroxide precipitates as pH is above 1 (Taylor et al. 1999), while as iron(II) hydroxide precipitates at pH > 6 (Smith et al. 1969), leading a less problem in acidizing. However, in the presence of hydrogen sulfide, iron (II) can precipitate as iron sulfide when pH is above 2. Besides, hydrogen sulfide can reduce Fe (III) to Fe (II) and

---

produce element sulfur which is not soluble in oil or water (Smith et al. 1969). When the acid is spent, iron (II) can also precipitate as iron (II) carbonate (McLeod 1984).

$$Fe^{3+} + 3OH^- \rightarrow Fe(OH)_3 \cdot mH_2O \downarrow \text{.....pH > 1}$$

$$Fe^{2+} + 2OH^- \rightarrow Fe(OH)_2 \cdot mH_2O \downarrow \text{.....pH > 6}$$

$$Fe^{2+} + H_2S \rightarrow FeS \downarrow + 2H^+ \text{.....pH > 2}$$

$$2Fe^{3+} + H_2S \rightarrow 2Fe^{2+} + 2H^+ + S \downarrow \text{.....reduction}$$

$$Fe^{2+} + CO_3^{2-} \rightarrow FeCO_3 \downarrow$$

**Fig. 3.1—Main iron precipitation reactions.**

Small amount of organic acids/chelating agents are often used in the oilfield for iron control (Crowe 1985; 1986; Hall and Dill 1988; Dill and Smolarchuk 1988). The objective of this study is to determine the effects of organic acids and chelating agents on the apparent viscosity of amidoamine oxide-based live and spent acids. Organic acids include formic acid, acetic acid, propionic acid and butyric acid. Chelating agents include α-hydroxyl carboxylic acids, such as glycolic acid, gluconic acid, lactic acid and citric acid, and high pH carboxyamino acids like tetrasodium EDTA, tetrasodium GLDA and disodium HEIDA. A second objective is to determine changes in micelle structures, and relate these changes to viscosity measurements. To the best of our knowledge, this was not examined before for this acid system.

## Experimental Studies

### *Materials*

The viscoelastic surfactant-A (amidoamine oxide) system used is a mixture of an amphoteric surfactant and solvent. Hydrochloric acid (ACS reagent grade, 36.8 wt%) and de-ionized water (resistivity = 18.2 $M\Omega \cdot cm$) at room temperature were used to prepare the acid solutions. Acid concentration was determined by titration using 1N sodium hydroxide solution. Chemical structures of organic acids and chelating agents (α-hydroxyl carboxylic acids and amino acids) are shown in **Fig. 3.2**. All acids and chelating agents were purchased from Sigma-Aldrich. Calcium carbonate was obtained from Fisher Scientific.

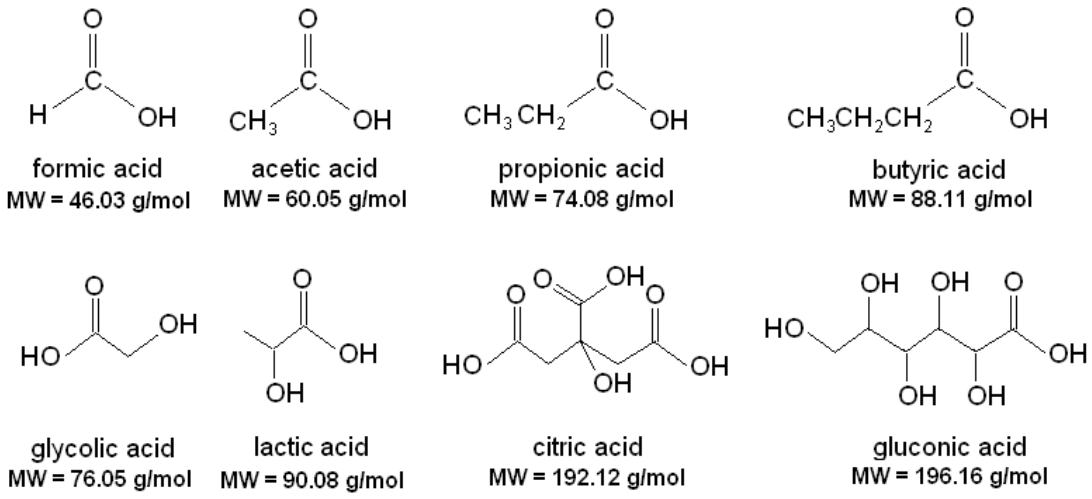


**Fig. 3.2—Structures of organic acids and chelating agents (α-hydroxyl carboxylic acids and amino acids).**

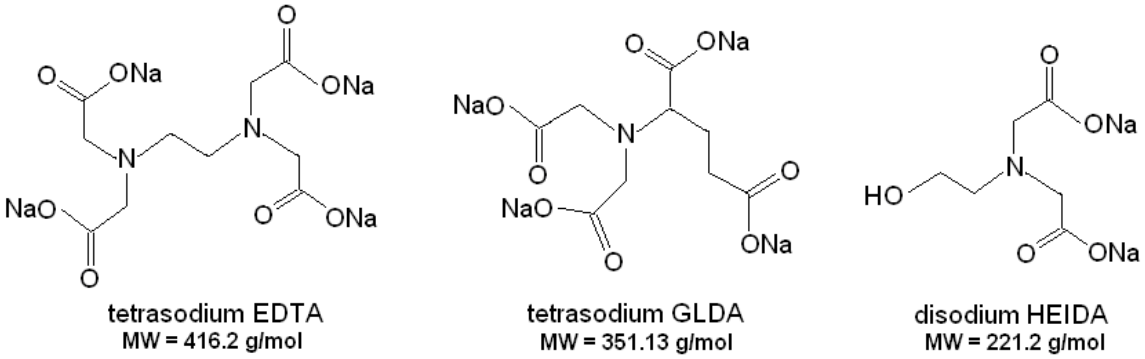


**Fig. 3.2—Continued.**

### *Fluid Systems*

Most of the experiments in this paper were performed using 20 wt% HCl, 4 wt% surfactant-A and 1 wt% corrosion inhibitor CI-A. Acid solutions with various additives were prepared such that the final acid concentration was 20 wt%.

#### *Live Surfactant-based Acid*

The live acid solution (200 g) was prepared by mixing 4 wt% surfactant-A with concentrated hydrochloric acid, followed by diluting with de-ionized water and then the resulting solution was mixed with 1 wt% corrosion inhibitor. The final HCl concentration in live acids was 20 wt%.

#### *Spent Surfactant-based Acid*

Calcium carbonate was carefully added to neutralize 20 wt% HCl and specific concentrated organic acid/chelating agent (0.055, 0.14, and 0.28 mol/l) until the pH was 4. This pH value was selected because the pH of spent acid in carbonate reservoirs is 4-

5. This is because of the buffering action of $CO_2$. A corrosion inhibitor was then added to the spent acid. Surfactant-A was added quickly as the last chemical to the spent acid mixture. A blender was used to mix them well (~ 4,000 rpm for 1-2 min).

*Removal of Air Bubbles*

A considerable number of air bubbles remained in the viscous spent acids after mixing. These bubbles were removed by centrifugation at 3,000 rpm for 30 minutes.

**Equipment**

The Grace Instrument M5600 HPHT Rheometer was used to measure the apparent viscosity of live and spent acids at different conditions. The wetted material was Hastelloy C-276, which is acid-resistant. The rheometer measured viscosity at various temperatures up to 500$^{o}$F, and shear rate of 0.00004 to 1,870 $s^{-1}$. A B5 bob was used in this work, which required a sample volume of 52 $cm^3$. A pressure of 300 psi was applied to minimize evaporation of the sample, especially at high temperatures. An Orion 950 analytical titrator was used to measure HCl concentration. The centrifuge used in this study was Z 206 A from Labnet International.

**Results and Discussions**

It was found that the addition of surfactant-A to the spent HCl solutions with an organic acid or a chelating agent solution would change the pH value significantly (**Table 3.1**). All spent acids examined in the present study were neutralized by calcium carbonate

until the pH was 4. However, after the addition of the surfactant-A, the pH of the spent acids increased to 5-6. This was mainly because of the alkaline nature of this surfactant solution, where the pH of 4 wt% surfactant solutions in deionized water was nearly 8.5.

**TABLE 3.1-- THE PH VALUES OF SPENT HCl/ORGANIC ACIDS BEFORE AND AFTER ADDING SURFACTANTS.**

| Organic Acid | Concentration (mol/l) | Concentration (wt%) | pH (before) | pH (after) |
|---|---|---|---|---|
| Formic acid | 0.055 | 0.23 | 4 | 6.2 |
| | 0.14 | 0.58 | 4 | 6.2 |
| | 0.28 | 1.15 | 4 | 6 |
| | | | | |
| Acetic acid | 0.055 | 0.3 | 4 | 6 |
| | 0.14 | 0.75 | 4 | 5.8 |
| | 0.28 | 1.5 | 4 | 5.5 |
| | | | | |
| Propionic acid | 0.055 | 0.37 | 4.1 | 5.9 |
| | 0.14 | 0.93 | 4 | 5.4 |
| | 0.28 | 1.85 | 4 | 5.1 |
| | | | | |
| Butyric acid | 0.055 | 0.44 | 4 | 6.2 |
| | 0.14 | 1.1 | 4 | 5.5 |
| | 0.28 | 2.2 | 4 | 5.3 |
| Glycolic acid | 0.055 | 0.38 | 4 | 6.1 |
| | 0.14 | 0.95 | 4 | 6 |
| | 0.28 | 1.9 | 4 | 5.9 |
| | | | | |
| Lactic acid | 0.055 | 0.45 | 4 | 5.9 |
| | 0.14 | 1.13 | 4 | 6 |
| | 0.28 | 2.25 | 4 | 5.8 |
| | | | | |
| Citric acid | 0.055 | 0.96 | 4 | 6 |
| | 0.14 | 2.4 | 4 | 6.1 |
| | 0.28 | 4.8 | 4 | 5.8 |
| | | | | |
| Gluconic acid | 0.055 | 0.98 | 4 | 5.6 |
| | 0.14 | 2.45 | 4 | 5.2 |
| | 0.28 | 4.9 | 4 | 4.9 |

| TABLE 3.1—CONTINUED. | | | | |
|---|---|---|---|---|
| Tetrasodium EDTA | 0.055 | 2.08 | 4 | 6.2 |
| Tetrasodium GLDA | 0.14 | 1.76 | 4 | 5.8 |
| Disodium HEIDA | 0.28 | 1.74 | 4 | 5.7 |

***Effect of Temperature on the Apparent Viscosity of Live surfactant-based Acids***

**Fig. 3.3** shows the effect of temperature on the apparent viscosity of live acid system (20 wt% HCl, 1 wt% corrosion inhibitor CI-A and 4 wt% surfactant-A) at a shear rate of 10 $s^{-1}$ and 300 psi. The viscosity of live surfactant-based acid was low. As a result, the effects of organic acids and chelating agents on the viscosity of live acids were not evaluated. The low viscosity of live acid indicates that this acid system can be pumped into the formation using coiled tubing.

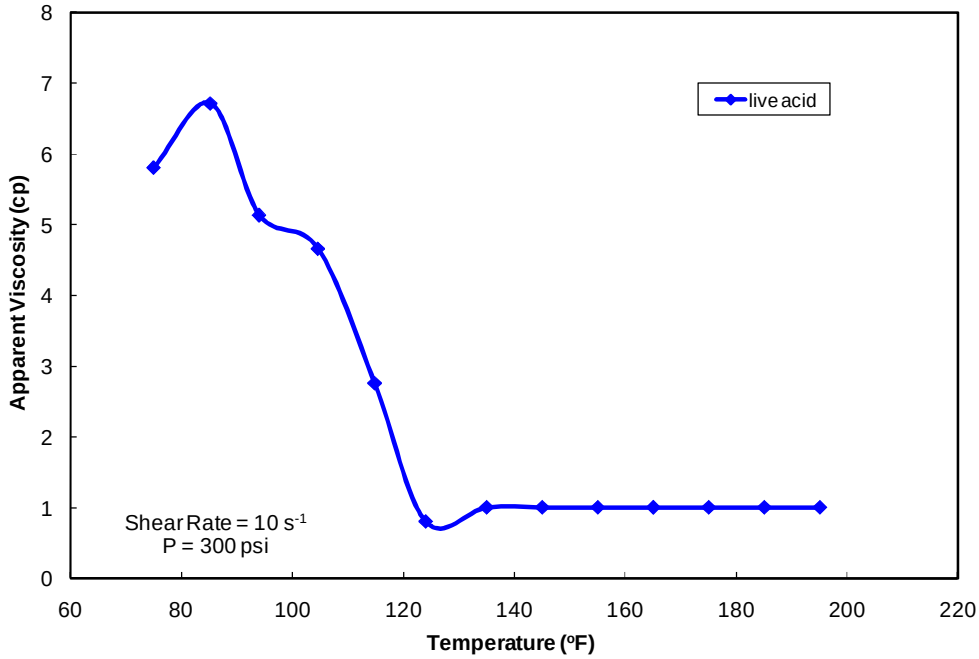


**Fig. 3.3—Effect of temperature on the apparent viscosity of live acid (20 wt% HCl, 1 wt% corrosion inhibitor CI-A and 4 wt% surfactant-A) at a shear rate of 10 $s^{-1}$ and 300 psi.**

***Effect of Organic Acids on the Apparent Viscosity of Spent Surfactant-based Acids***

**Figs. 3.4-3.6** show the effect of short-chain organic acids on the apparent viscosity of spent acids. The viscosity was measured at a shear rate of 10 $s^{-1}$ and a pressure of 300 psi. Four organic acids were tested including: formic, acetic, propionic, and butyric at 0.055 (Fig. 3.4), 0.14 (Fig. 3.5), and 0.28 mol/l (Fig. 3.6). For the spent HCl acid without organic acid or chelates, the apparent viscosity reached a maximum of 1,650 cp at 120°F, and then decreased as the temperature was increased. At temperatures greater than 170°F, the viscosity was low, and as a result, this system should not be used at higher temperatures.

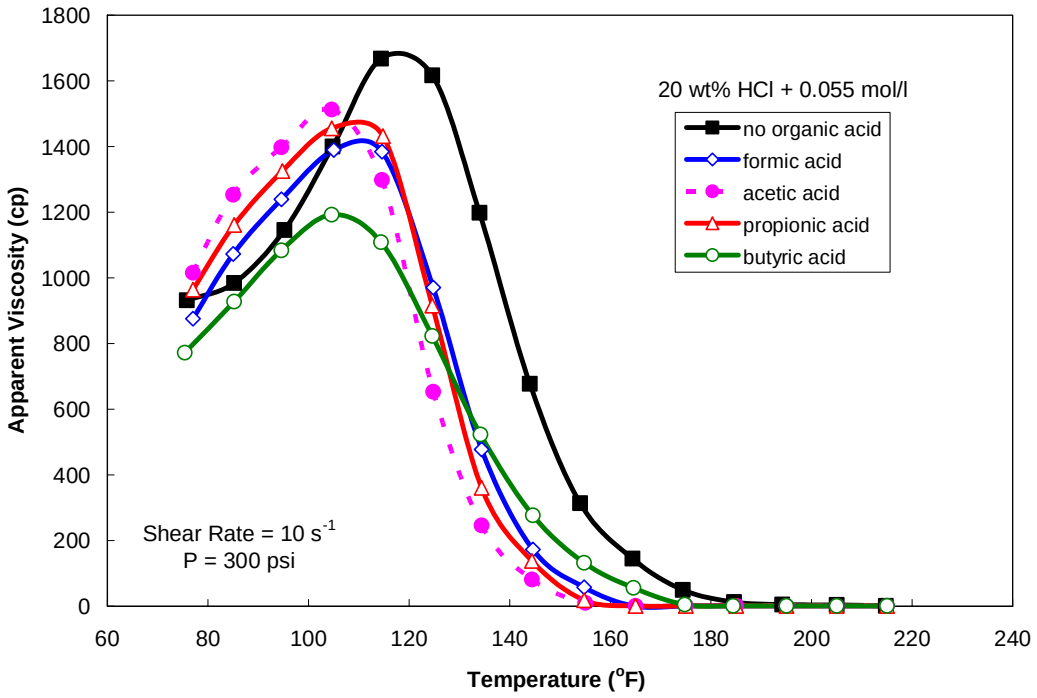


**Fig. 3.4—Effect of organic acids (0.055 mol/l) on the apparent viscosity of spent acids.**

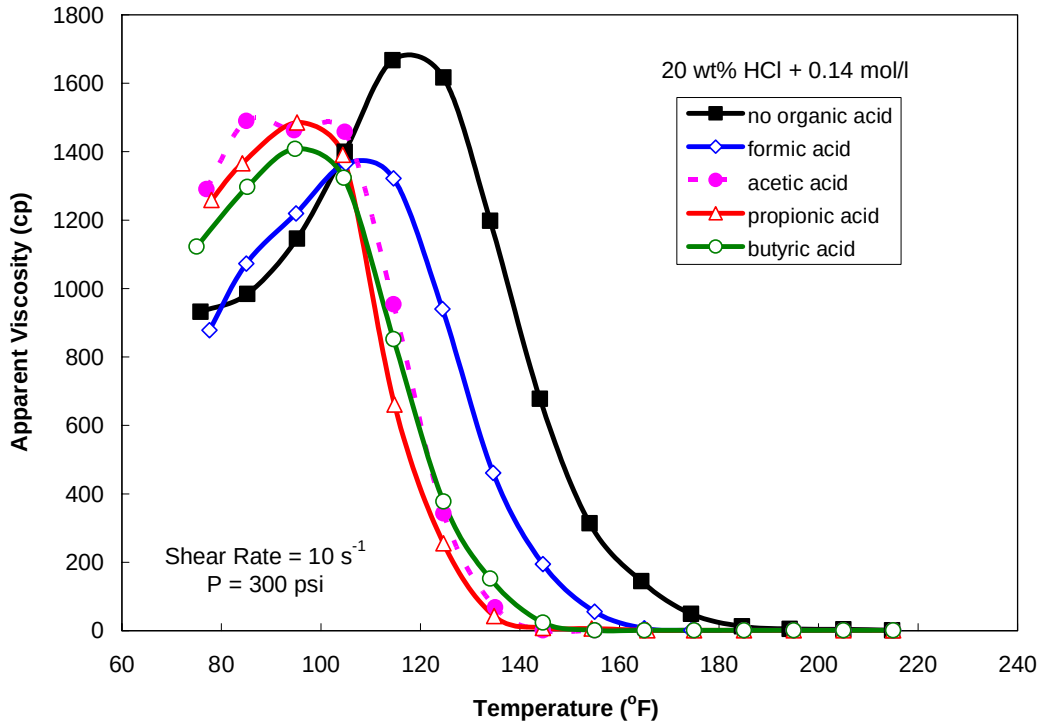


**Fig. 3.5—Effect of organic acids (0.14 mol/l) on the apparent viscosity of spent acids.**

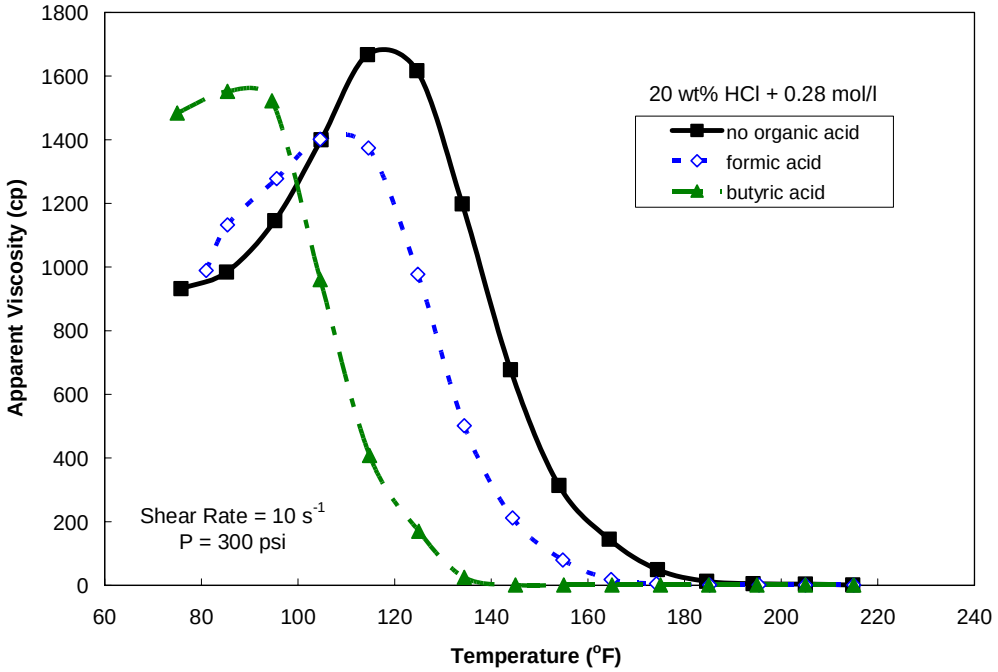


**Fig. 3.6—Effect of organic acids (0.28 mol/l) on the apparent viscosity of spent acids at a shear rate of 10 $s^{-1}$ and 300 psi.**

The addition of formic acid to spent surfactant-based acids reduced its apparent viscosity. Acetic acid or propionic acid decreased the apparent viscosity of spent acids. Butyric acid reduced the maximum apparent viscosity and the temperature range where the surfactant-A can be used.

Fig. 3.5 shows that the spent acid system with 0.14 mol/l formic acid had a much wider temperature range where the surfactant-A can be used. Spent surfactant-based acid systems containing 0.14 mol/l formic acid did not cause further reduction in the apparent viscosity compared to the solution with 0.055 mol/l formic acid. The gel made of 0.14 mol/l acetic/propionic acids showed lower apparent viscosity than the system made with 0.055 mol/l acetic acid/propionic acids.

Fig. 3.6 shows the effect of formic acid and butyric acid each at 0.28 mol/l on the apparent viscosity of spent acids. Phase separation was observed for the systems with 0.28 mol/l acetic acid or propionic acid (**Fig. 3.7**). Therefore, the effect of these two acids was not examined. Butyric acid at 0.28 mol/l reduced the temperature range where the surfactant-A can be used from 75-200 to 75-140$^{o}$F.

Fig. 3.7 shows white calcium precipitate at the bottom of sample tubes. When more concentrated organic acid was used, more precipitation was observed. The spent surfactant-based acid system with 0.28 mol/l acetic acid/propionic acid showed two immiscible liquids besides the precipitation.

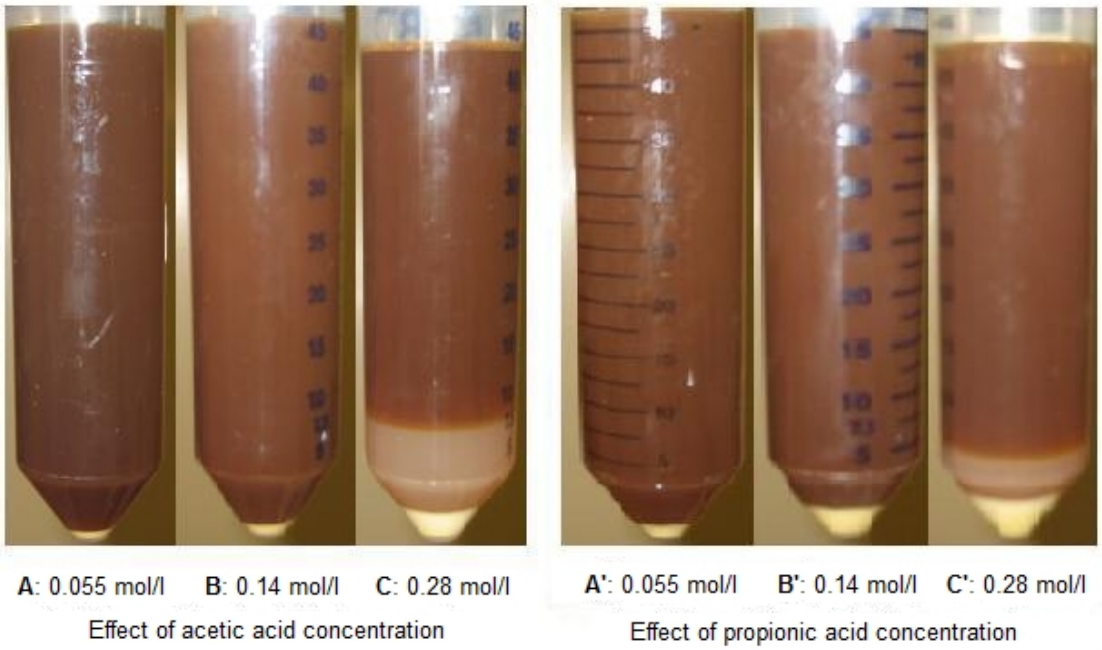


**Fig. 3.7—Effects of acetic acid/propionic acid concentrations on spent acids. Tubes A, B, C and A', B', C' show white calcium precipitation at the bottom. Tubes C and C' show two immiscible phases and white precipitation.**

**Fig. 3.8** indicates that homogenous gels were obtained for spent surfactant-based HCl/butyric acid, even though 0.28 mol/l butyric acid was used. A white precipitate was observed at the bottom of sample tubes.


**Fig. 3.8—Effect of butyric acid concentration on spent acids. Tubes A, B and C show homogeneous gel solutions and white calcium precipitation at the bottom.**

The results shown in Figs. 3.4-3.8 indicate that the addition of simple organic acids reduced the maximum viscosity of surfactant-based acids when this amine oxide surfactant-A was used. This trend was noted with all organic acids examined, except formic acid where the effect of formic acid concentration was not significant. The impact of increasing the concentration of formic acid on the apparent viscosity of spent acid may be explained in terms of the small stability constant between $Ca^{2+}$ ion and formate ion, which means that the effect of increasing the concentration of formate ion on the micelles shape was not significant.

***Effect of Chelating Agents (α-Hydroxyl Carboxylic Acids) on Spent Surfactant-based Acids***

Usually, α-hydroxyl carboxylic acids are used with HCl as iron control agents. It is of interest to examine their effect on the apparent viscosity of spent HCl acids. **Figs. 3.9 to 3.11** show the effects of glycolic, lactic, citric, and gluconic acids on the apparent viscosity of spent surfactant-based acids. The maximum temperature at which these types of surfactant-based systems that contained 0.055 mol/l glycolic acid was 150°F. A lower maximum temperature was found when lactic acid was used instead of glycolic acid. The apparent viscosity of spent acid made with 0.055 mol/l gluconic acid decreased during sample heating and the highest temperature that this surfactant can be used is 115°F.

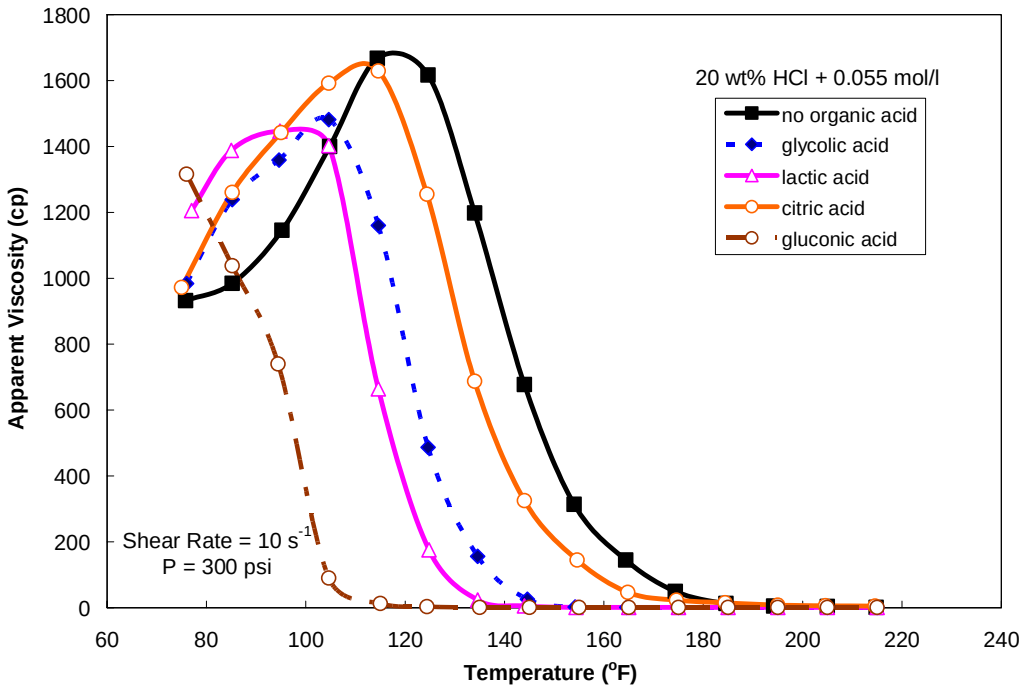


**Fig. 3.9—Effect of chelating agents (α-hydroxyl carboxylic acids, 0.055 mol/l) on the apparent viscosity of spent acids at a shear rate of 10 $s^{-1}$ and 300 psi.**

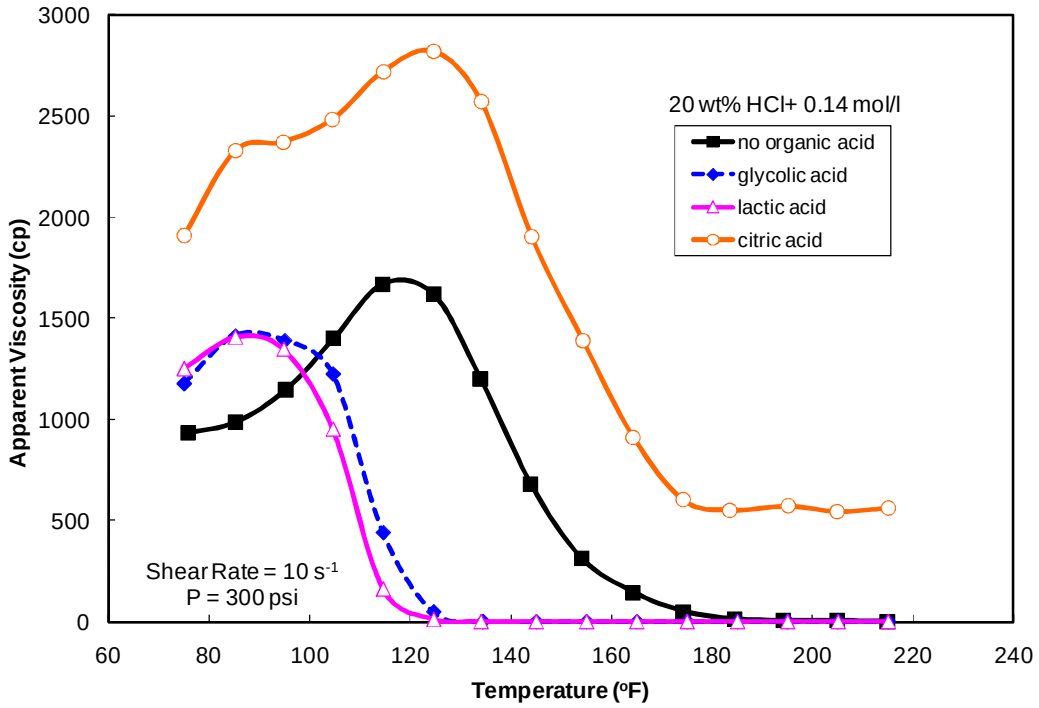


**Fig. 3.10—Effect of chelating agents (α-hydroxyl carboxylic acids, 0.14 mol/l) on the apparent viscosity of spent acids at a shear rate of 10 $s^{-1}$ and 300 psi.**

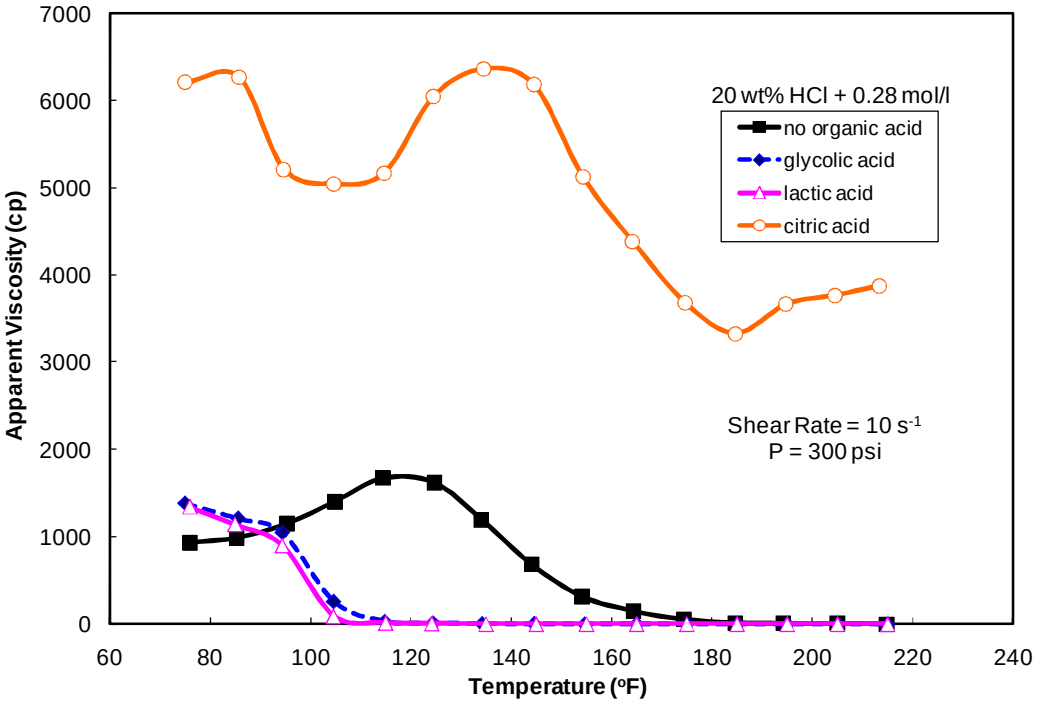


**Fig. 3.11—Effect of chelating agents (α-hydroxyl carboxylic acids, 0.28 mol/l) on the apparent viscosity of spent acids at a shear rate of 10 $s^{-1}$ and 300 psi.**

The behavior of citric acid was significantly different from other acids that were tested in this paper. **Fig. 3.12** shows that the color of the spent acid became lighter as more citric acid was added, because more white calcium citrate was generated. The calcium citrate precipitate remained suspended in the spent surfactant-based acid and formed a very viscous mixture. As shown in **Fig. 3.13**, the maximum apparent viscosity of spent acid with 0.28 mol/l citric acid was two times greater than that of the spent acid made by 0.14 mol/l citric acid, which was at least double the viscosity compared to the original spent surfactant-based acid. Besides, the addition of citric acid significantly widened the temperature range that amidoamine oxide can be used. It should be noted that the apparent viscosity was over 3,000 cp for the spent acid with 0.28 mol/l citric acid even though the temperature was 215$^{o}$F. However, calcium citrate can cause formation damage and subsequent loss of well performance. It should be noted that the apparent viscosity of spent acid containing 0.28 mol/l glycolic acid or 0.28 mol/l lactic acid decreased when heated to 215$^{o}$F. Gluconic acid at 0.14/0.28 mol/l was not examined because of phase separation noted (**Fig. 3.12**).

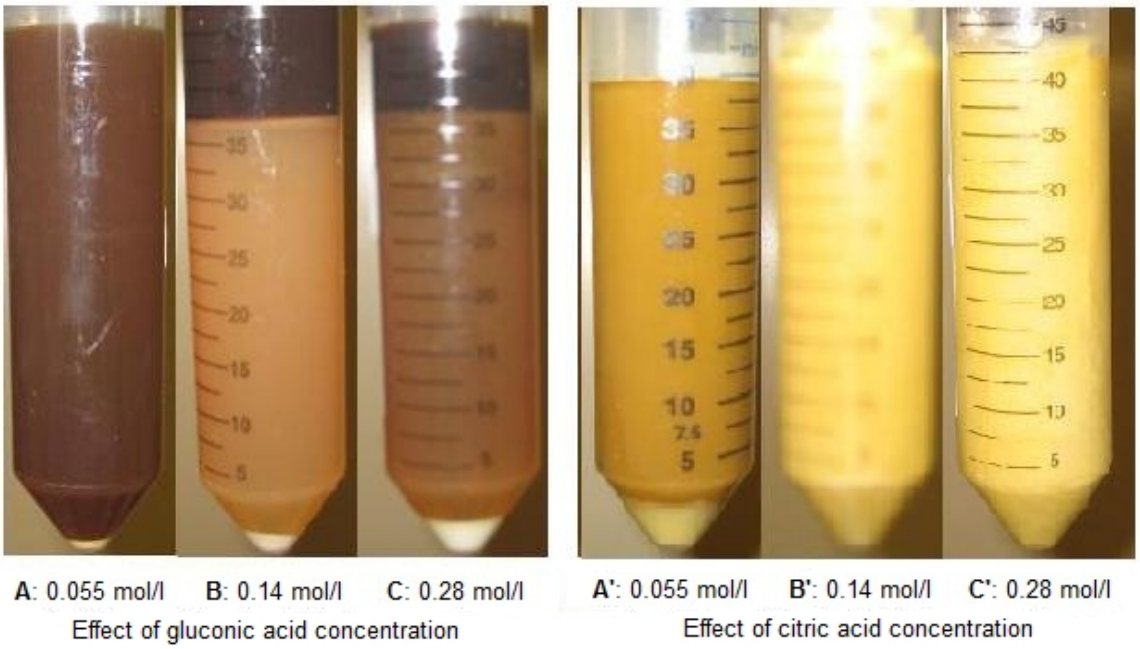


**Fig. 3.12—Effects of gluconic acid/citric acid concentration on spent acids. Tube A shows homogeneous gel. Tubes B and C show two immiscible phases and white precipitate at the bottom. Tubes A', B' and C' were spent acids made with citric acid and had yellow to light yellow color.**

The results show that the addition of chelating agents significantly reduced the viscosity of spent acids. This reduction in viscosity increased with the number of carbon atoms in the acid. All these rules are not applicable to citric acid, as a very viscous suspension was noted because of the precipitation of calcium citrate.

As described above, the addition of organic acids/chelating agents can significantly influence the rheological properties of spent acids because they can rearrange the micelles and cause the shape changes. Cryo-TEM (transmission electron microscopy) tests were conducted in this study to examine how these additives affect the shape of the micelles.

The samples should be frozen before TEM tests because a thin amorphous film needs to be obtained. Spent acids were very viscous; it was not possible to freeze them without dilution. **Figs. 3.13a and 3.13b** show photomicrographs of spent acids with and without 0.28 mol/l glycolic acid. These two samples were diluted four times using deionized water. The sample without glycolic acid contained numerous elongated linear micelles, whereas, a far fewer visible micelles appeared in the sample with glycolic acid. These results indicate that the addition of glycolic acid to the spent acid decreased the size and number of the rod-shaped micelles. Therefore, the apparent viscosity of the spent acid decreased because of the reduced amount of elongated micelles.

(a) 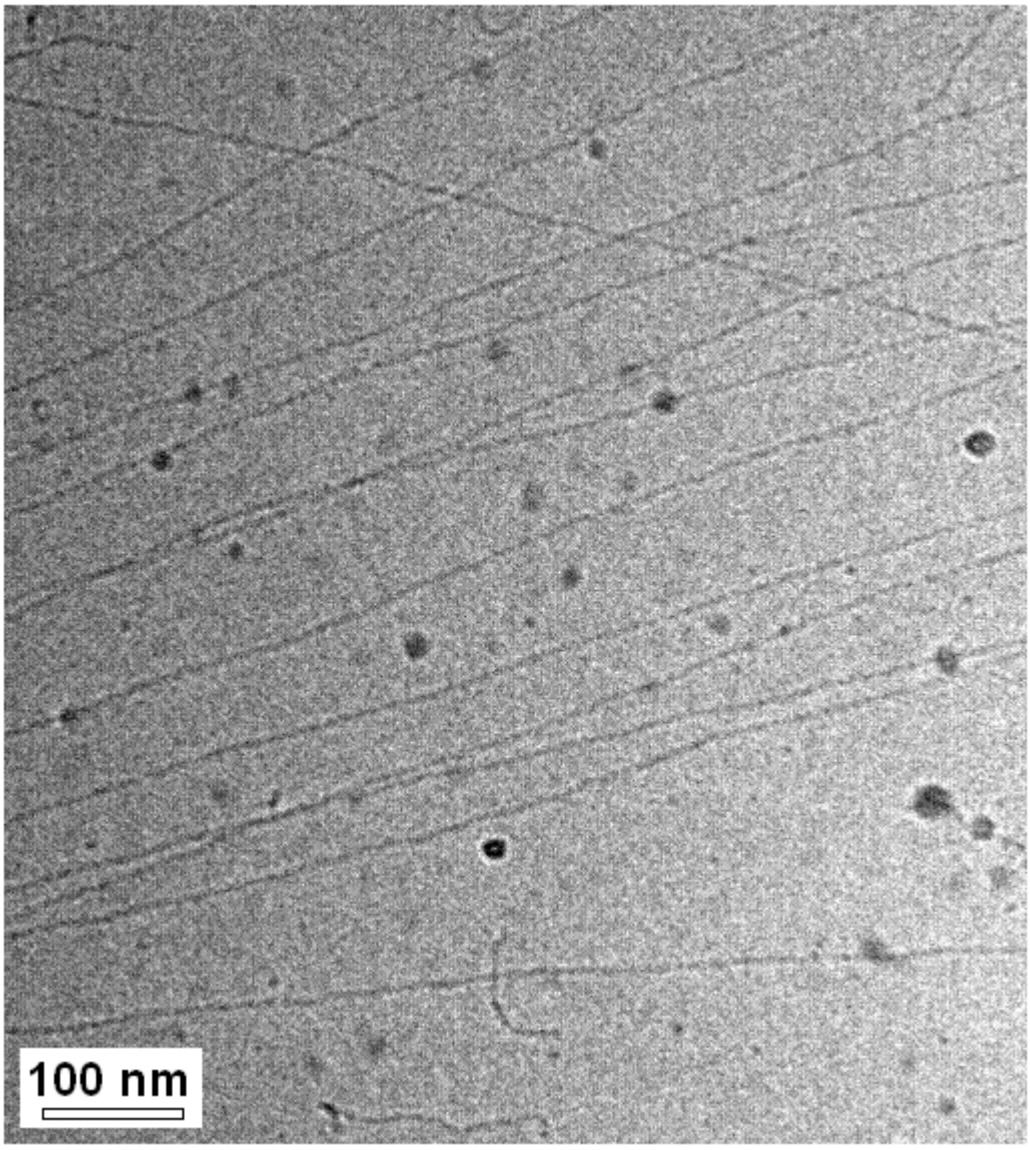


**Fig. 3.13—a) TEM image of the spent acid sample without any organic acids/chelating agents.**

(b)

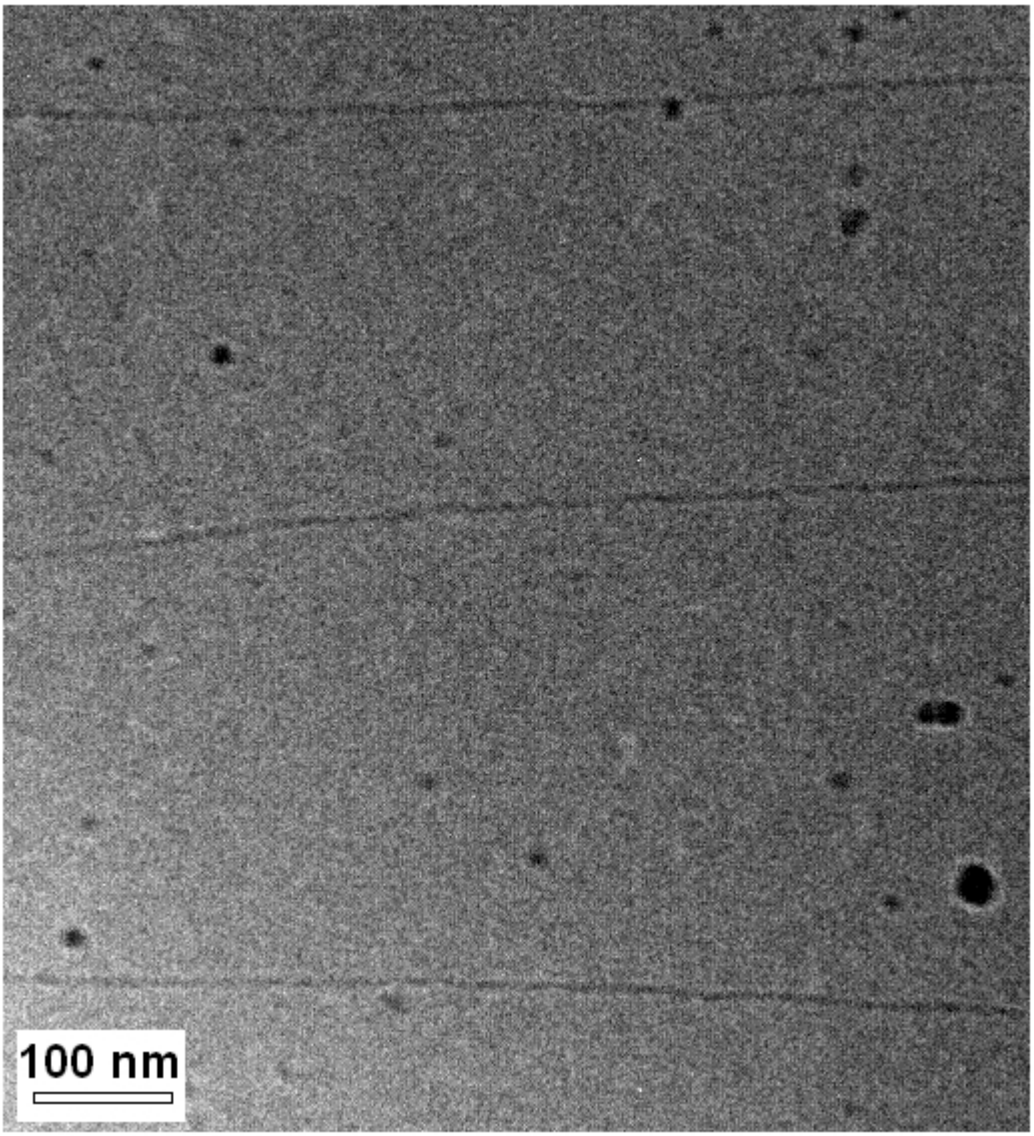


**Fig. 3.13—Continued. b) TEM image of the spent acid sample with 0.28 mol/l glycolic acid. (Note: the samples were diluted with four times the volume of water).**

### *Effect of Chelating Agents (Amino Acids) on Spent Surfactant-based Acids*

Three amino acids were examined in this paper: tetrasodium EDTA, tetrasodium GLDA and disodium HEIDA (Fig. 3.2). **Fig. 3.14** shows the effects of each of the three chelants at 0.055 mol/l on the apparent viscosity of spent acids. The narrowed temperature ranges

were obtained after adding these amino acids. The highest temperature at which this surfactant-A can be used in spent acid with disodium HEIDA was only 145°F. Among these three-acid systems, the highest apparent viscosity was obtained with the spent acid that contained tetrasodium GLDA at 105°F.

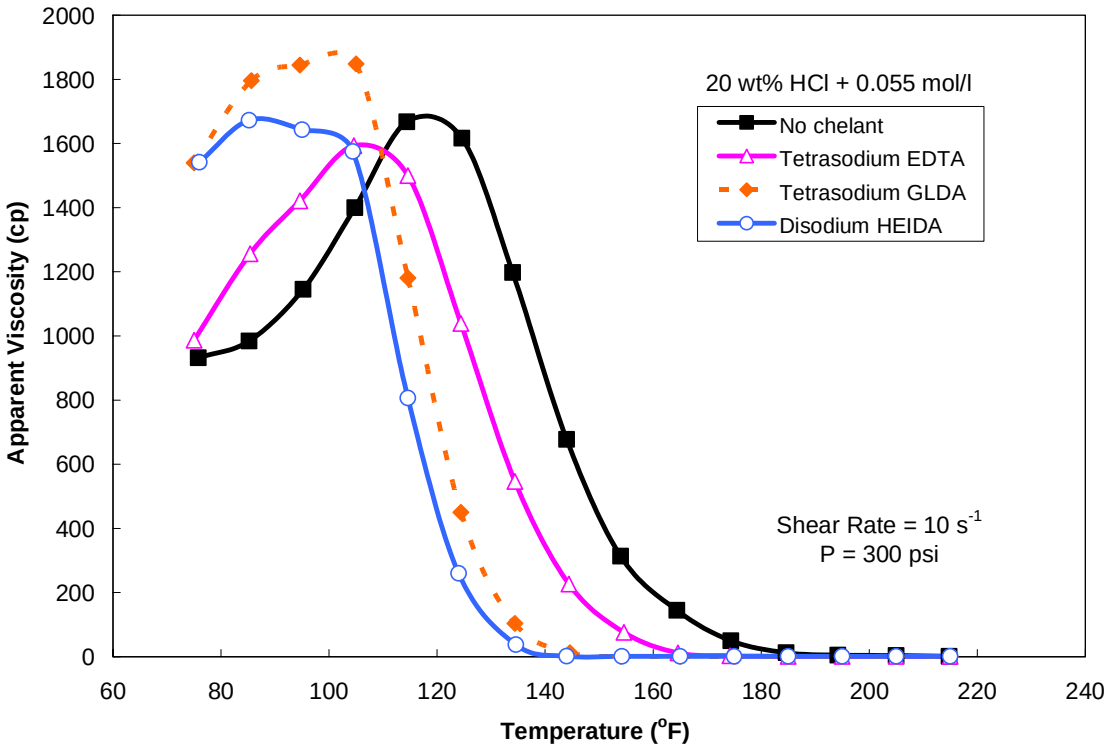


**Fig. 3.14—Effect of chelating agents (amino acids, 0.055 mol/l) on the apparent viscosity of spent acids at a shear rate of 10 $s^{-1}$ and 300 psi.**

Nine water molecules surround a calcium ion in aqueous solutions, which means that nine chelating functional groups can replace water and form a complex (Bakken and Schöffel 1996). In the spent acid system, $Ca^{2+}$ was already chelated by organic acids/chelating agents, thus, less concentration of $Ca^{2+}$ was available to form rod-shaped micelles, causing the viscosity of spent acid to decrease. In addition, spherical micelles

may co-chelate $Ca^{2+}$ with organic acids/chelating agents and, as a result, the concentration of spherical micelles available to form long rod-shaped micelles will be less. This also can reduce the viscosity of the spent acid.

***Effect of the Surfactant Concentration on Spent Surfactant-based Acids***

The results obtained from the present study show that the addition of organic acid/chelating agents to the spent surfactant-based acid reduced its apparent viscosity. Additionally, the temperature range for effective use of the surfactant-A was narrowed. Therefore, more concentrated surfactant should be used to compensate for the reduced viscosity caused by the addition of an organic acid or a chelating agent. **Figs. 3.15 and 3.16** show that using 6 wt% surfactant-A instead of 4 wt% increased the apparent viscosity of spent acids, and widened the temperature range where this surfactant-based system could be used. The obtained maximum apparent viscosity was doubled when the surfactant concentration was increased from 4 to 6 wt%. It should be noted, however, that increasing the surfactant concentration should be pursued with extreme caution, and only after conducting compatibility tests with the native hydrocarbons, wettability tests with reservoir rocks and rheological tests at downhole conditions.

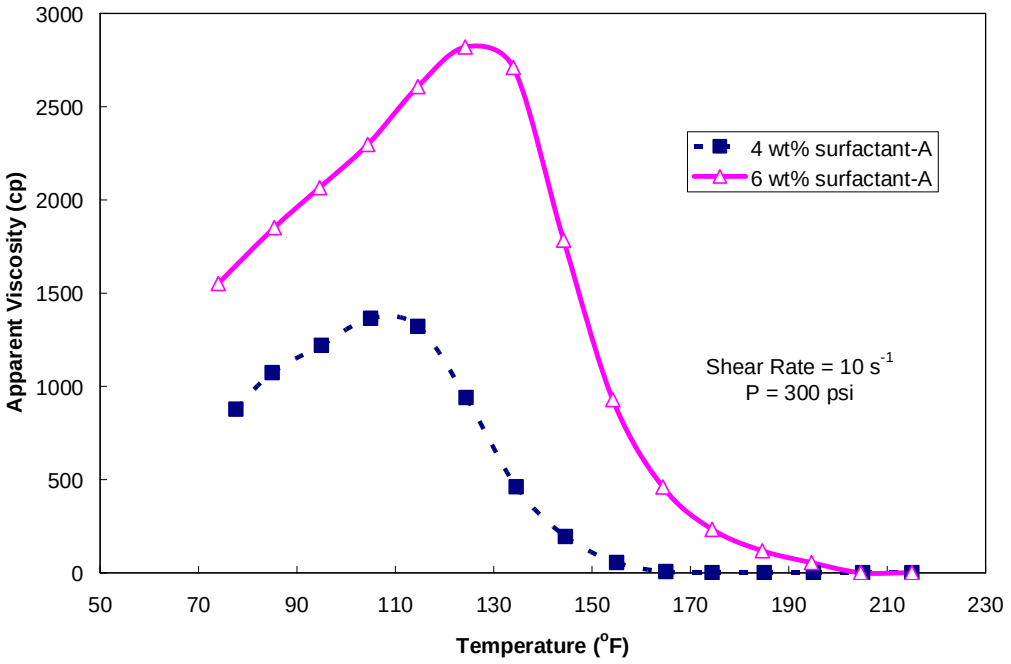


**Fig. 3.15—Effect of the surfactant concentration on the apparent viscosity of the spent acid (made by 20 wt% HCl and 0.14 mol/l formic acid) at a shear rate of 10 $s^{-1}$ and 300 psi.**

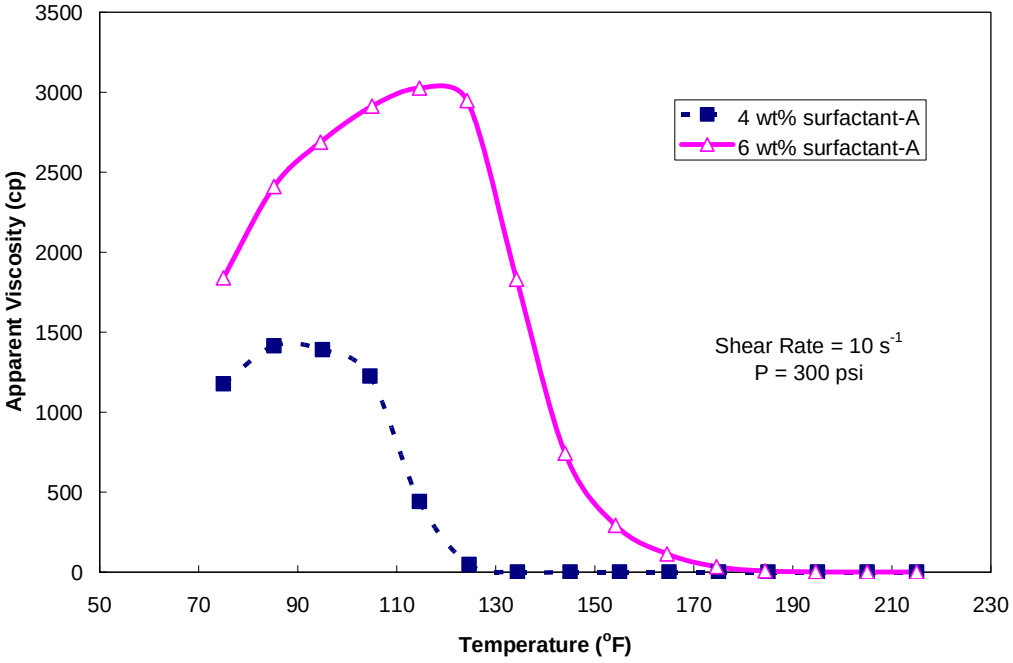


**Fig. 3.16—Effect of the surfactant concentration on the apparent viscosity of the spent acid (made by 20 wt% HCl and 0.14 mol/l glycolic acid) at a shear rate of 10 $s^{-1}$ and 300 psi.**

## Conclusions

The effects of low concentrations of organic acids and chelating agents on the apparent viscosity of an amidoamine oxide surfactant-A were examined in this work. Eleven organic acids/chelating agents were tested in this paper. Based on the results obtained, the following conclusions can be drawn:

1. The addition of organic acids/chelating agents to the spent acid reduced its apparent viscosity.
2. When more concentrated organic acids were used, less apparent viscosity was obtained. However, this did not apply to formic acid.
3. For spent acid systems with α-hydroxyl carboxylic acids, the viscosity of spent acids decreased with an increase in the number of carbon atoms in the acid.
4. The addition of citric acid to the spent acid not only increased the apparent viscosity, but it also broadened the temperature range that surfactant can be used, due to the generation of suspended solids of calcium citrate. However, calcium citrate precipitate can cause formation damage. Other organic acids did form a precipitate in spent acids. Therefore, laboratory testing of all additives with viscoelastic surfactant acid systems should be done prior to field use.
5. More concentrated surfactant-A should be added to the acid system to compensate for the reduced viscosity caused by organic acids or chelating agents. Increasing the surfactant concentration should be pursued with caution, and only after conducting qualifying laboratory tests.

6. TEM photomicrographs confirmed that the addition of organic acid to the spent acid generated fewer elongated micelle structures and resulted in less apparent viscosity.

# CHAPTER IV

# IMPACT OF CORROSION INHIBITORS ON RHEOLOGICAL PROPERTIES AND PHASE BEHAVIOR OF AMIDOAMINE OXIDE SURFACTANTS-BASED ACIDS

## Introduction

A good surfactant-based acid should have the following properties: thermal stability, compatibility with cations, low viscosity in live acids but high viscosity in spent acids, ease to be removed by internal or external breakers, and no harm to the environment. Corrosion inhibitors must be added to the acid system to protect well tubulars and minimize Fe contamination. The components of corrosion inhibitor usually contain short-chain alcohols (e.g. isopropyl alcohol) that can significantly affect the properties of surfactant-based acids. Therefore, corrosion inhibitor plays an important role in evaluating acid systems.

Two amine oxides (surfactant-A and surfactant-AW) will be discussed in this chapter. They are positively charged at low pH and deprotonated at higher pH. Three different corrosion inhibitors (CI-A, CI-28 and CI-5) were tested in surfactant-based acids. A HPHT rheometer was used to measure the apparent viscosity of surfactant-based water system, live acids and spent acids. Measurements were made at temperatures from 75 to 300$^{o}$F, at a shear rate of 10 $s^{-1}$ at 300 psi. The compositions of surfactants and corrosion inhibitors are shown in **Table 4.1**.

| TABLE 4.1--COMPOSITION OF SURFACTANTS AND CORROSION INHIBITORS | | |
|---|---|---|
| **Additive** | **Main Components** | **Concentration (wt%)** |
| surfactant-A | amides, tallow, n-[3-dimethylamino)propyl], n-oxides | 50-65 |
| | 1,2-propanediol | 25-40 |
| | water | 5-10 |
| surfactant-AW | amides, tallow, n-[3-dimethylamino)propyl], n-oxides | 40-60 |
| | 1,2-propanediol | 40-60 |
| | water | 5-10 |
| Corrosion inhibitor-A | isopropanol | 10-30 |
| | dimethylformamide | 10-30 |
| | propargyl alcohol | 5-10 |
| | substituted alcohol | 1-5 |
| | haloalkyl heteropolycycle salt | 10-30 |
| | quaternary ammonium compound | 10-30 |
| | oxyalkylated alcohol | 10-30 |
| Corrosion inhibitor-28 | proprietary alkoxylated fatty polyamines | 38 |
| | proprietary fatty amines | 28 |
| | propargyl alcohol | 15 |
| | butanol | 8 |
| | formaldehyde | 6 |
| | acetic acid | 5 |
| Corrosion inhibitor-5 | ethoxylated fatty amines | 37 |
| | fatty amines | 28 |
| | propargyl alcohol | 15 |
| | acetic acid | 5 |
| | formaldehyde | 6 |
| | water | 9 |

It should be noted that surfactant-AW contains more 1,2-propanediol than surfactant-A. Based on the compositions, it should be noted that all of these corrosion inhibitors contain propargyl alcohol, however, there is more concentrated short chain alcohol in corrosion inhibitor-A, and more concentrated butanol in corrosion inhibitor-28.

## Experimental Studies

### *Materials*

Two viscoelastic surfactant (amidoamine oxide) systems were examined in this paper: surfactant-A and surfactant-AW. For each surfactant system, it is a mixture of an amphoteric surfactant and solvent. The activities of surfactant-A and surfactant-AW are 50% and 40%, respectively. Hydrochloric acid (ACS reagent grade, 36.8 wt%) and de-ionized water (resistivity = 18.2 $M\Omega \cdot cm$) were used to prepare the acid solution. Acid concentration was determined by titration using 1N sodium hydroxide solution. Three corrosion inhibitors were used: CI-A, CI-28 and CI-5.

### *Fluid Systems*

Most of the experiments in this paper were performed using 20 wt% HCl, 4-6 vol% viscoelastic surfactant (concentrations based on various activities) and 1 vol% corrosion inhibitor. Acid solutions with various additives were prepared such that the final acid concentration was 20 wt%.

#### *Live Surfactant-based Acid*

The live acid solution (200 g) was prepared by mixing 4-6 vol% viscoelastic surfactant with concentrated hydrochloric acid, followed by diluting with de-ionized water and then the resulting solution was mixed with 1 vol% corrosion inhibitor. Every effort was made not to contaminate the acid with iron.

*Spent Surfactant-based Acid*

Calcium carbonate was carefully added to neutralize 20 wt% HCl until pH was 4-5. Corrosion inhibitor was then added to the spent acid. A blender was used to mix these solutions. The viscoelastic surfactant was added quickly as the last additive to the spent acid mixture. The whole mixture was blended well at a high shear rate (~ 4,000 rpm) for 1-2 min.

*Removal of Air Bubble*

A considerable number of air bubbles remained in the viscous live and spent acids after mixing. These bubbles were removed by centrifuging for 30 minutes at 2,500 rpm.

***Equipment***

The Grace Instrument M5600 HPHT rheometer was used to measure the apparent viscosity of live and spent acids under different conditions. The wetted material is Hastelloy C-276, which is acid-resistant. The rheometer can measure viscosity at various temperatures up to 500 $^{o}$F, over shear rate of 0.00004 to 1,870 $s^{-1}$. A B5 bob was used in this work which requires a sample volume of 52 $cm^3$. A pressure of 300 psi was applied to minimize evaporation of the sample, especially at high temperatures. Orion 950 analytical titrator was used to measure HCl concentration. The centrifuge used in this study was Z 206 A from Labnet International.

## Results and Discussions

### *Apparent Viscosity of Amidoamine Oxide Surfactants in Water*

**Fig. 4.1** shows the apparent viscosity as a function of temperature for solutions containing 4-5 vol% viscoelastic surfactants at a shear rate of 10 $sec^{-1}$ and at 300 psi. It should be noted that the amount of active species in the system with 4 vol% surfactant-A equals that in the acid made by 5 vol% surfactant-AW. Apparently, the water system with surfactant-A shows a much higher viscosity than the solution made with surfactant-AW. For both of these water systems, the apparent viscosity increased and reached a maximum. The maximum value obtained was approximately twice that obtained at room temperature. After that, the apparent viscosity rapidly decreased as temperature was increased to 195°F. At that temperature, the solution had an apparent viscosity similar to water.

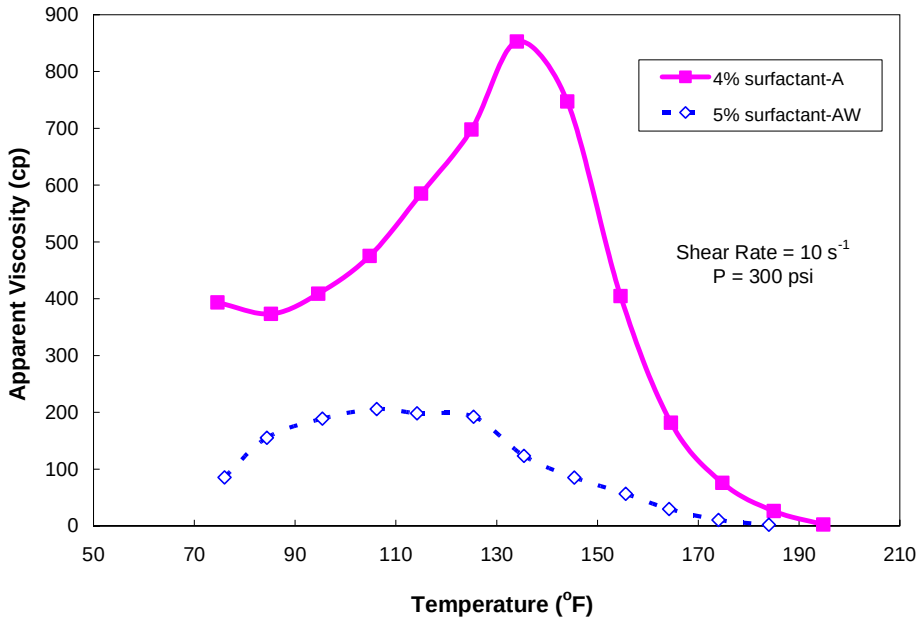


**Fig. 4.1—Effect of temperature on water systems made by amidoamine oxide surfactants.**

***Apparent Viscosity of Amidoamine Oxide Surfactants in Live Acids***

Various concentrations of HCl can result in significantly different apparent viscosities of viscoelastic surfactants in live HCl acid solutions (Nasr-El-Din et al. 2008a; Li et al. 2010a). **Fig 2.7** shows how the apparent viscosity behaves in live acids (with 4 vol% surfactant-A, 1 vol% CI-A) at various HCl concentrations. The results indicate that the acid that contained 12 wt% HCl gave the highest apparent viscosity. Phase separation was observed when HCl concentrations were in the range of 4-7 wt%.

**Fig. 4.2** shows that live acids prepared with surfactant-AW have similar trends, even though different surfactant concentrations (5-6 vol% surfactant-AW) and corrosion inhibitors (CI-28/CI-5) were used. Low viscosity was observed if HCl concentrations were higher than 15 wt% or lower than 1 wt%. However, the apparent viscosity of live acids increased significantly if HCl concentrations were 3-12 wt%. The maximum apparent viscosity was obtained at 5 wt% HCl. Compared to the systems made by surfactant-A and CI-A, surfactant-AW and CI-28/CI-5 have better compatibility in HCl: live acids were all homogeneous no matter what HCl concentration was used. Besides, it was noted that higher apparent viscosity was achieved if more concentrated surfactant-AW was applied.

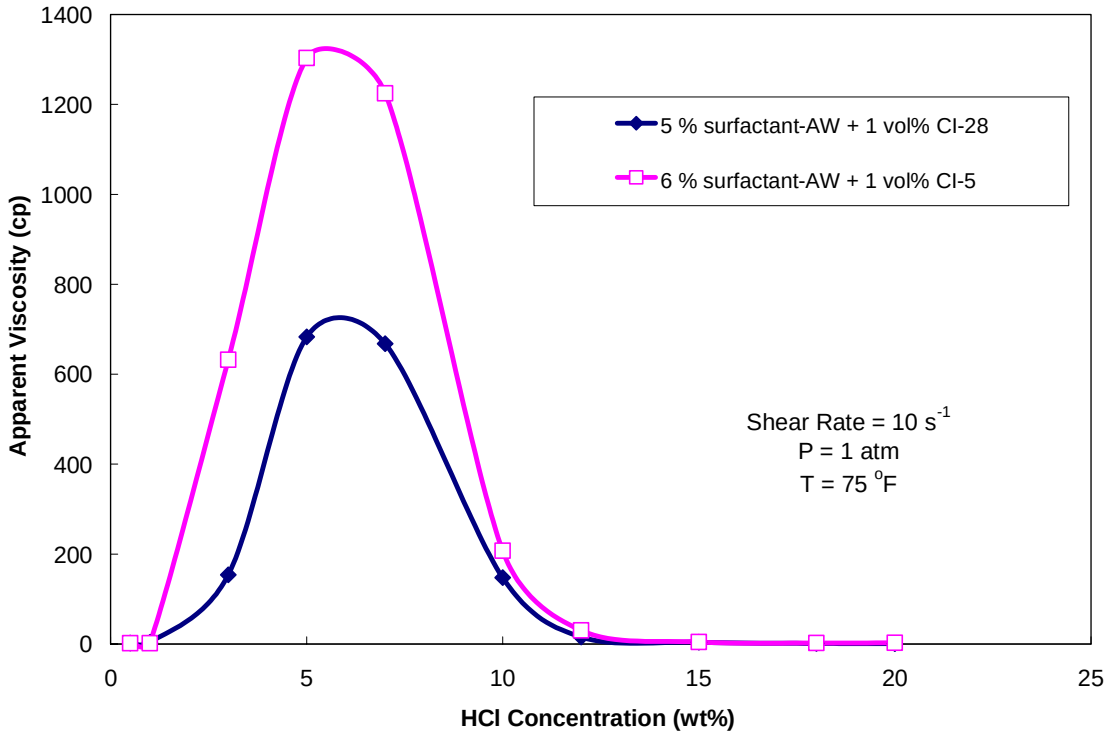


**Fig. 4.2—Effect of HCl concentrations on live acids containing surfactant-AW.**

### *Rheological Properties of Amidoamine Oxide Surfactants in Spent Acids*

*Effect of Corrosion Inhibitors on the Apparent Viscosity*

The apparent viscosity of spent acids was measured as a function of temperature at a shear rate of 10 $s^{-1}$ and 300 psi. Spent acid samples were heated from room temperature until 250 °F. **Figs. 4.3 and 4.4** show the comparison between surfactant-based spent acids with and without corrosion inhibitors. It can be seen that the apparent viscosity of systems without any corrosion inhibitor was much higher than that of spent acid containing corrosion inhibitor, especially at high temperatures. The temperature range that the surfactant can be effectively used was broadened if no corrosion inhibitor was added.

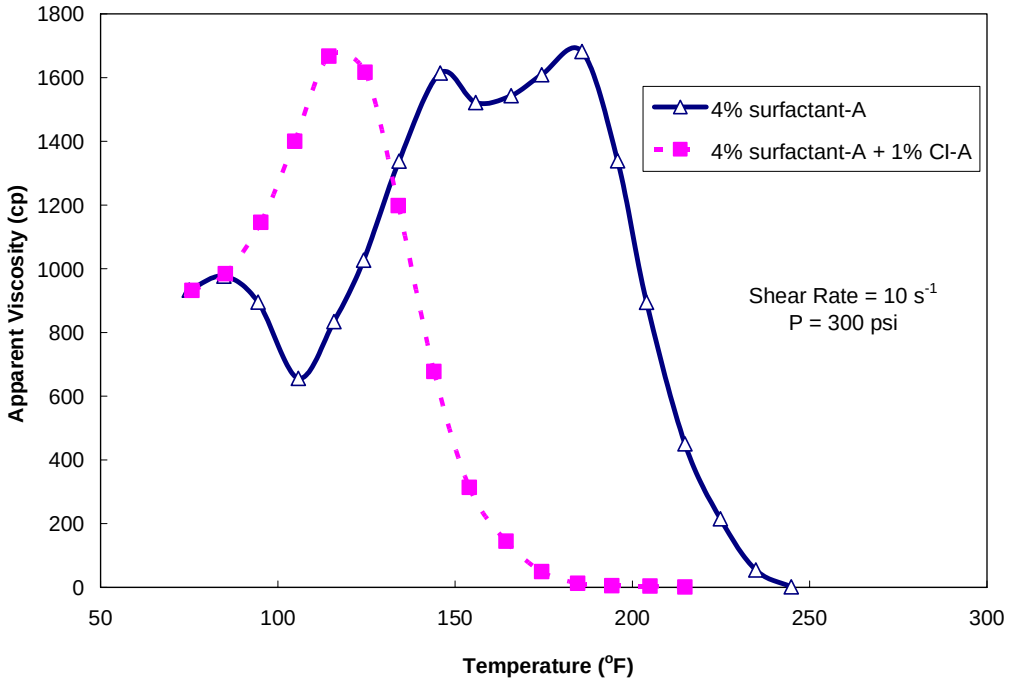


**Fig. 4.3—Effect of corrosion inhibitor CI-A on the apparent viscosity of spent acids containing 4 vol% surfactant-A.**

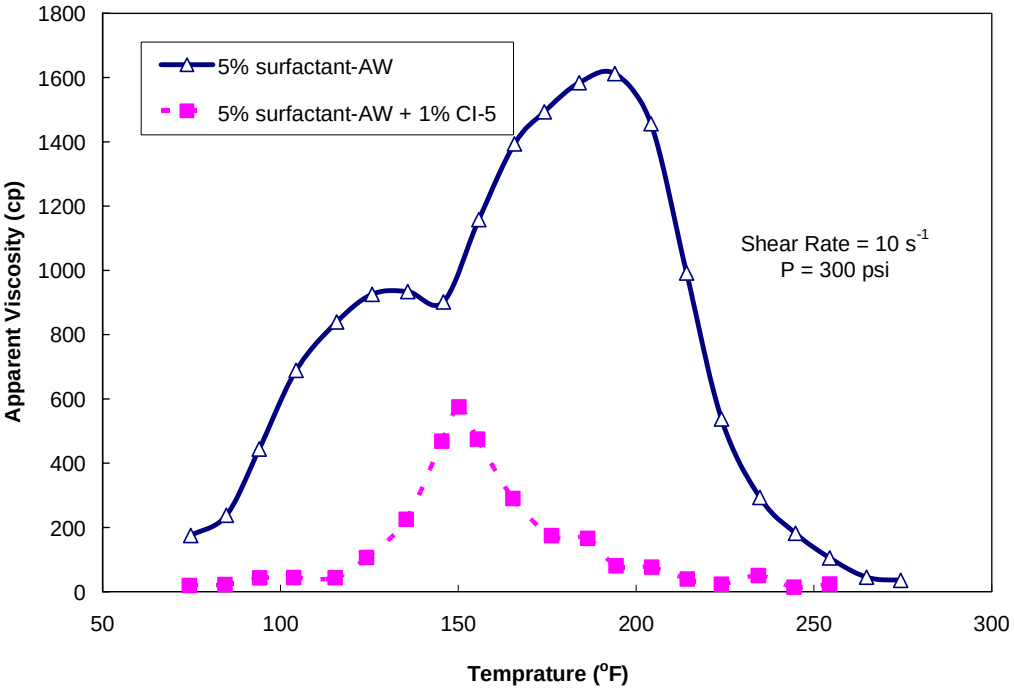


**Fig. 4.4—Effect of corrosion inhibitor CI-5 on the apparent viscosity of spent acids containing 5 vol% surfactant-AW.**

*Effect of Corrosion Inhibitors on G' and G''*

The oscillatory tests were done for spent acids. G' (elastic modulus) and G'' (viscous modulus) were measured as a function of temperature at frequency of 1 Hz and 300 psi. **Figs. 4.5 and 4.6** show that the addition of corrosion inhibitor to the spent acids significantly affected G' and G''. It can be seen that for spent acids without any corrosion inhibitors, the elasticity was predominate rather than the viscosity at temperatures of 130-190 $^{o}$F. However, for spent acids made with corrosion inhibitors, the viscous modulus (G'') was higher than the elastic modulus (G') at almost all the examined temperatures.

In a word, the addition of corrosion inhibitor to surfactant-based acids significantly affected their rheological properties; therefore it is very important to examine the influence of corrosion inhibitors before applied in the field.

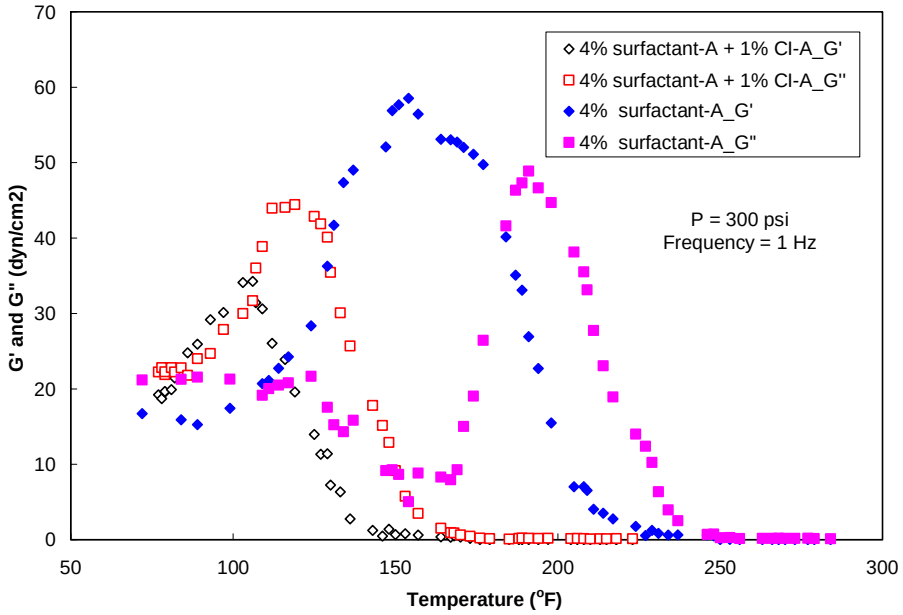


**Fig. 4.5—Effect of corrosion inhibitor CI-A on G' and G" of spent acids containing 4 vol% surfactant-A.**

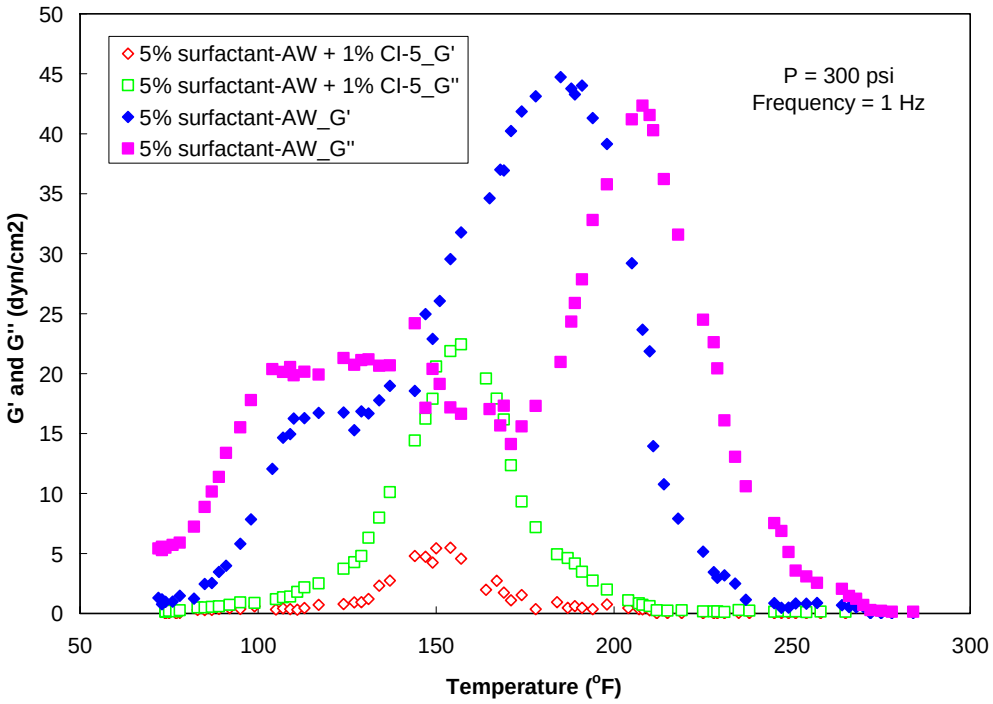


**Fig. 4.6—Effect of corrosion inhibitor CI-5 on G' and G'' of spent acids containing 5 vol% surfactant-AW.**

*Effect of Corrosion Inhibitor on the Micelle Structure*

Cryo-TEM tests were conducted on the spent acids containing 5 vol% surfactant-AW. The samples were frozen by liquid nitrogen before taken any imagine. Compared to TEM tests in Chapter III (Fig. 3.13), the samples made by surfactant-AW were not diluted due to the low viscosity (only 18 cp at room temperature). **Fig. 4.7a** shows that there were a large number of 100 nm long curly micelles, while much fewer micelles were observed in **Fig. 4.7b**, indicating that the addition of corrosion inhibitor CI-5 to the spent acid can prevent the micelle formation, and cause the less apparent viscosity.

**(a)**

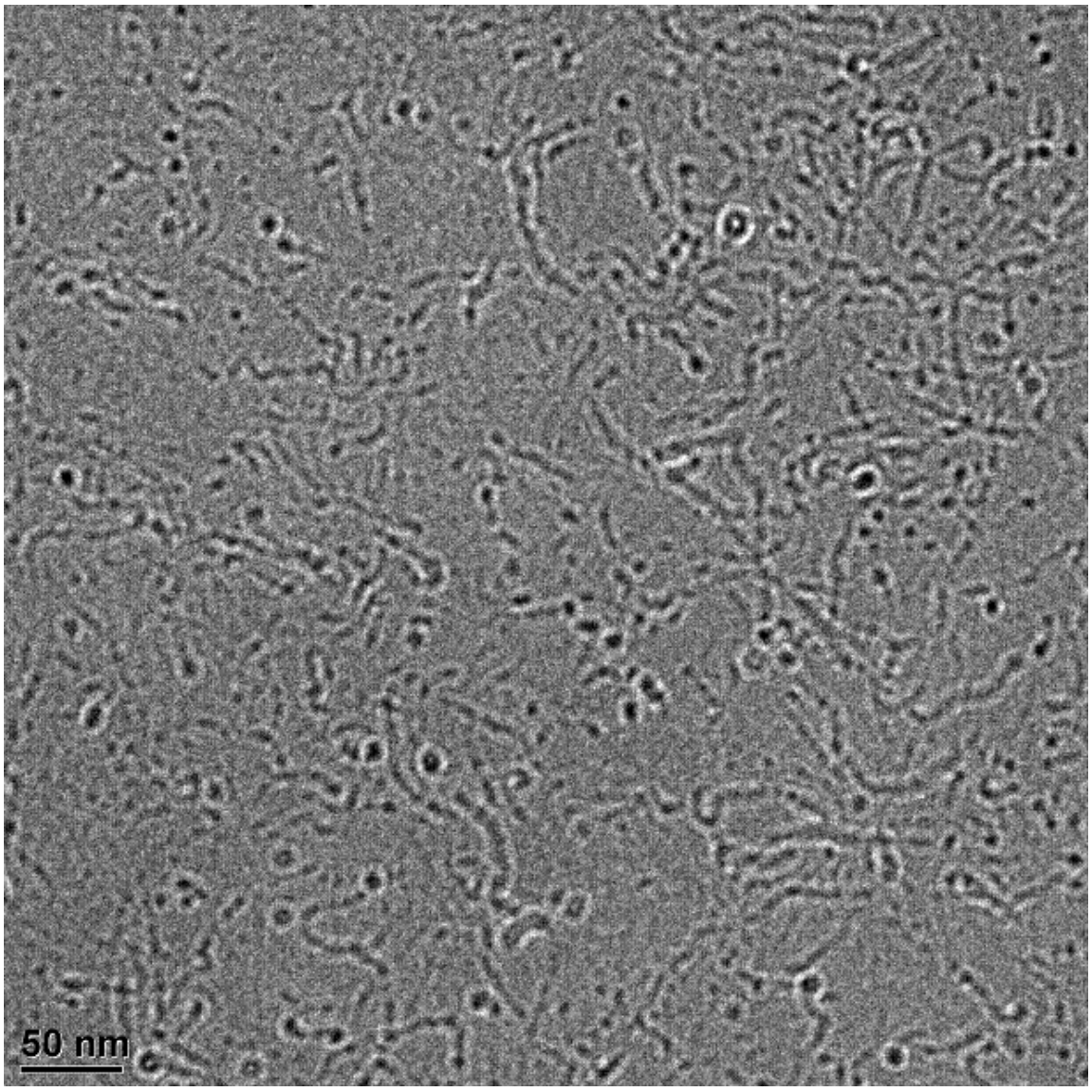


**Fig. 4.7—a) TEM image of the spent acid sample containing 5 vol% surfactant-AW only.**

**(b)**

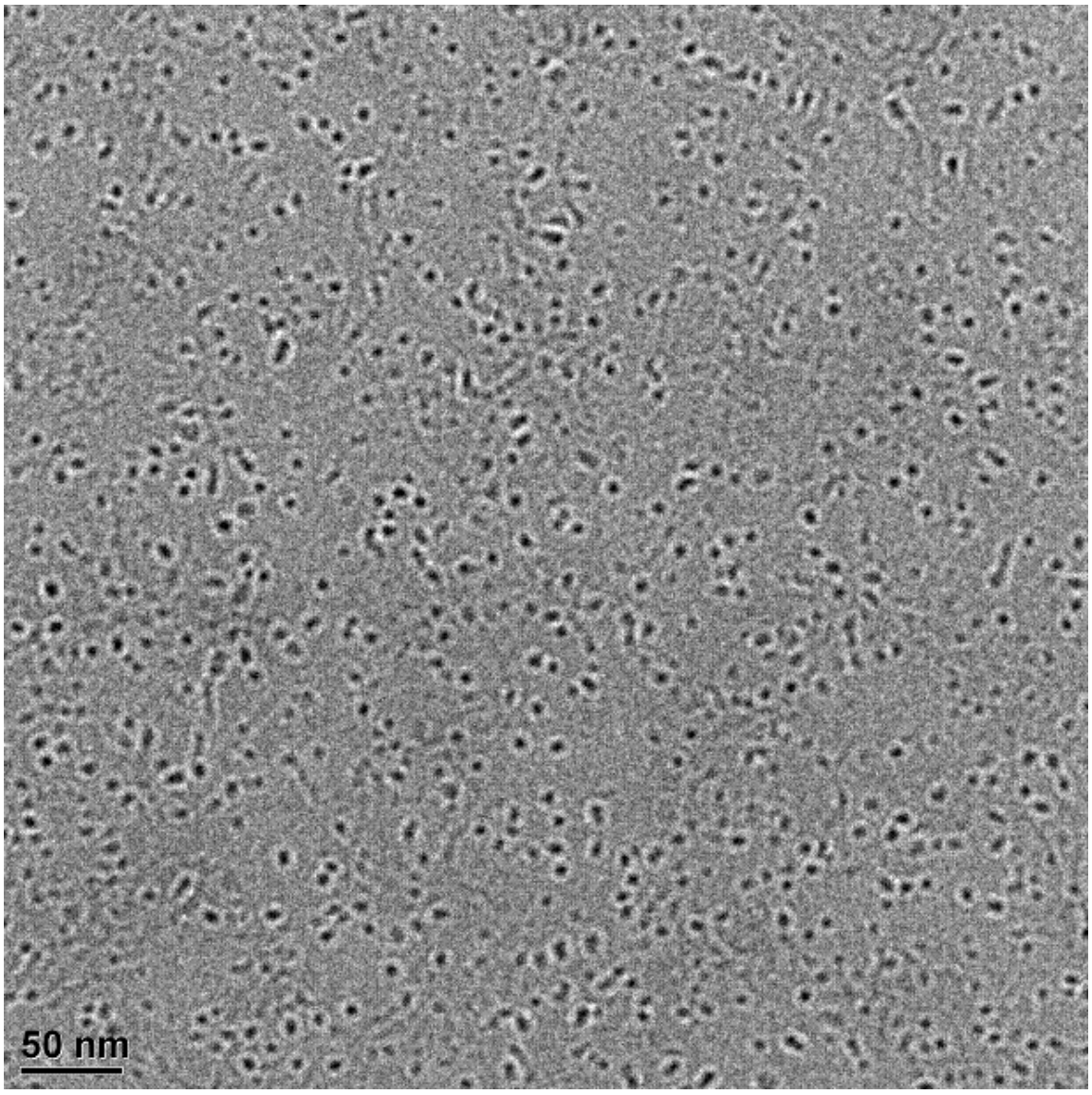


**Fig. 4.7—Continued. b) TEM image of the spent acid sample containing 5 vol% surfactant-AW and 1 vol% CI-5. (Note: the black dots in the TEM imagines are the ice contamination).**

*Compatibility Tests*

Six experiments were done and prepared by different surfactants and corrosion inhibitors. **Fig. 4.8** shows how six samples looked like after the heating up process. The result shows that as long as CI-A was used in the surfactant-based acids, two phases were observed immediately after samples were heated up to 250 $^{o}$F. On the other hand, corrosion inhibitor-28 and corrosion inhibitor-5 have better compatibility with amidoamine oxide surfactants: no immiscible fluids were found out right after the heating up process, but spent acids made by surfactant-A showed phase separation after couple of days. Therefore, spent acids containing surfactant-AW and CI-28/CI-5 were the most stable system at high temperatures.

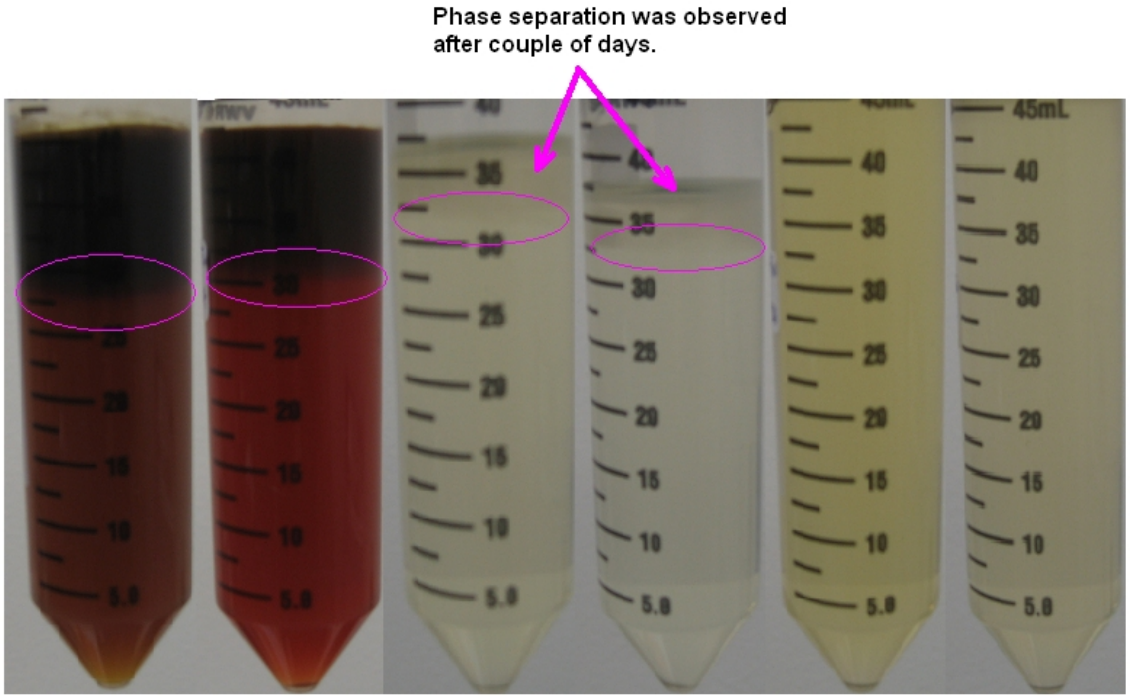


| 4% surfactant-A | 5% surfactant-AW | 4% surfactant-A | 4% surfactant-A | 6% surfactant-AW | 6% surfactant-AW |
|---|---|---|---|---|---|
| 1% CI-A | 1% CI-A | 1% CI-28 | 1% CI-5 | 1% CI-28 | 1% CI-5 |

**Fig. 4.8—Compatibility between surfactants and corrosion inhibitors.**

*Effect of Corrosion Inhibitors on Surfactant-A-based Spent Acids*

**Fig. 4.9** shows the rheological properties of spent acids made by 4 vol% surfactant-A. For the spent HCl acid with CI-A, the apparent viscosity reached a maximum of 1,650 cp at 120°F, and then decreased as the temperature was increased. The similar trends were observed for spent acids made by CI-28/CI-5, but much less viscosity was noted. The maximum temperature that surfactant-A can be effectively used was no more than 200°F, no matter what corrosion inhibitor was used.

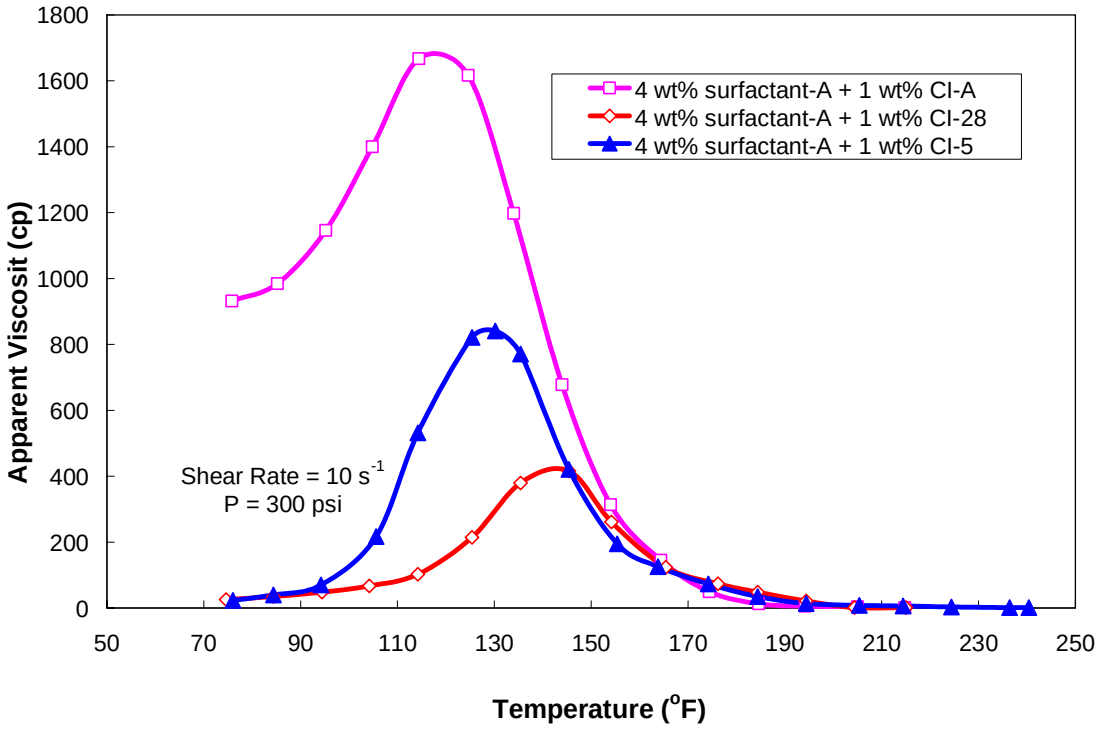


**Fig. 4.9—Effect of corrosion inhibitors on surfactant-A-based spent acids.**

*Effect of Corrosion Inhibitor CI-A on Amidoamine Oxide-based Spent Acids*

**Fig. 4.10** shows how CI-A affected the apparent viscosity of amidoamine oxide-based spent acids. It can be seen that if the same amount of corrosion inhibitor CI-A was applied, the apparent viscosity of spent acid with 4 vol% surfactant-A was much higher than that of the acid made by 5 vol% surfactant-AW, even though the amounts of active species in these two systems were equal.

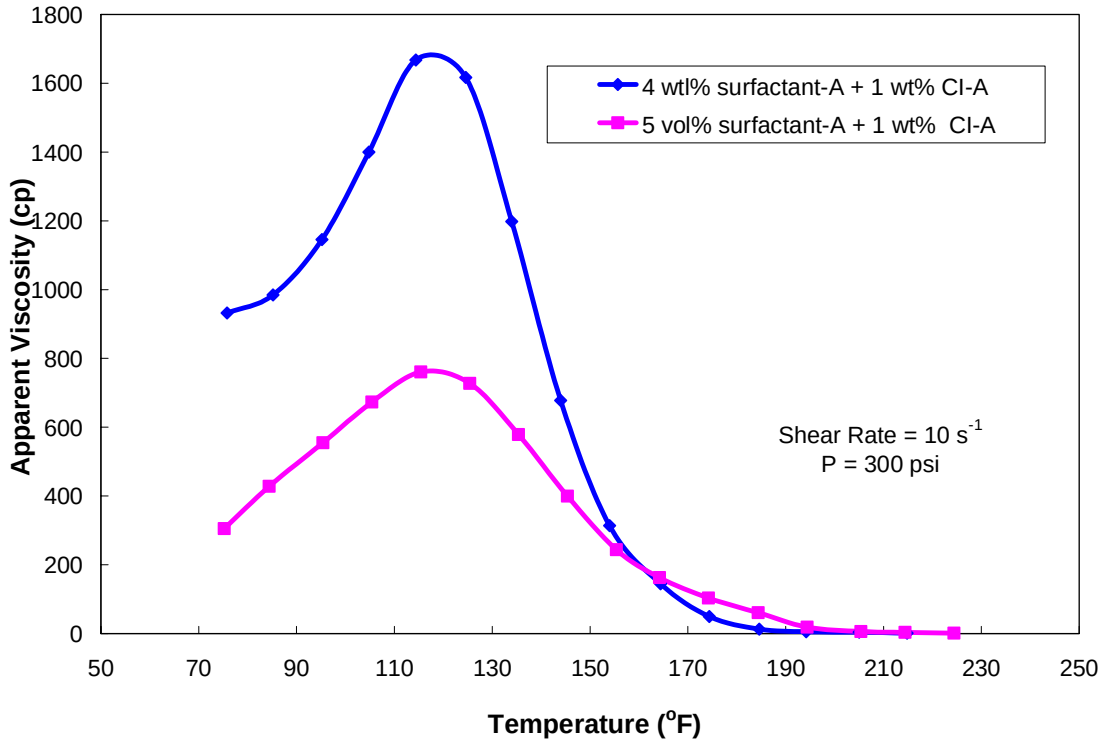


**Fig. 4.10—Effect of corrosion inhibitor CI-A on amidoamine oxide-based spent acids.**

*Effect of Corrosion Inhibitors on Surfactant-AW-based Spent Acids*

**Fig. 4.11** shows the effects of corrosion inhibitors -28 and -5 on the rheological properties of spent acids containing 6 vol% surfactant-A. As mentioned earlier in **Fig. 4.9**, these two spent acids were most stable systems and showed highest compatibility. The results indicate that the spent acid with corrosion inhibitor-5 showed the better performance-much higher viscosity than the system with CI-28 and the maximum apparent viscosity was obtained as 735 cp at 160°F.

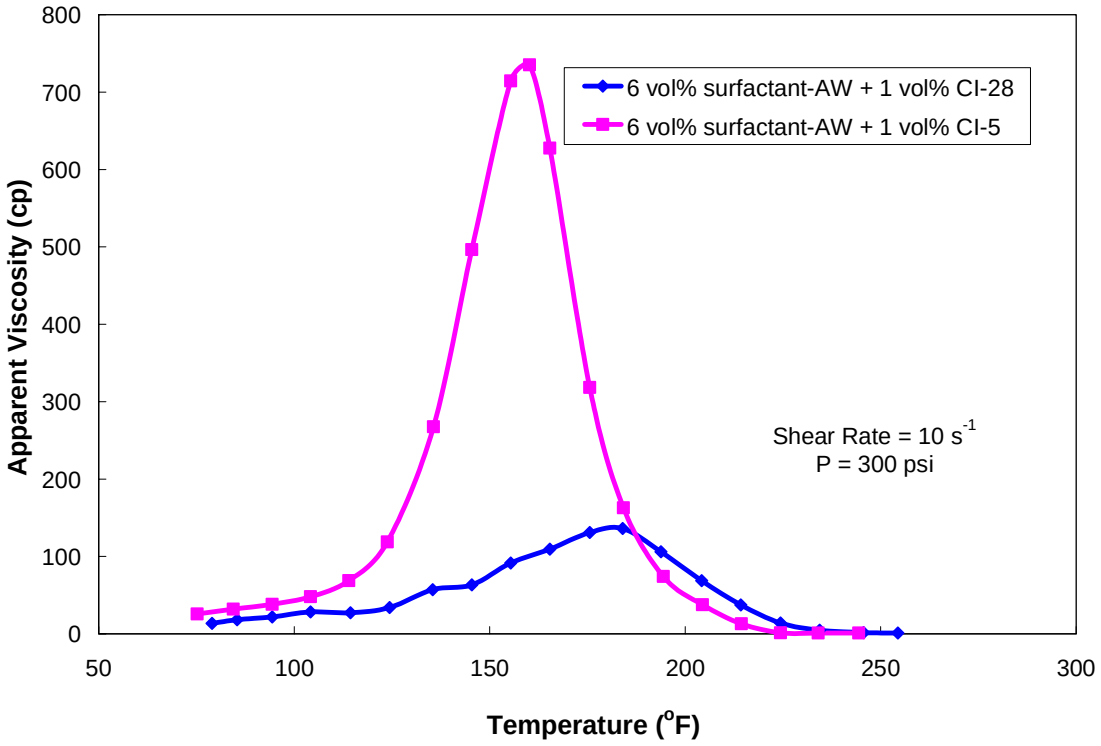


**Fig. 4.11—Effect of corrosion inhibitors on surfactant-AW-based spent acids**.

*Effect of Corrosion Inhibitor-5 on Amidoamine Oxide-based Spent Acids*

**Fig. 4.12** shows how 1 vol% corrosion inhibitor-5 affected the apparent viscosity of amidoamine oxide-based spent acids. All of these acid systems had similar trends of apparent viscosity as a function of temperature. The viscosity increased first as spent acids were heated up until it reached the maximum, and then the viscosity dropped down. The difference among these systems was the optimal temperature when the maximum apparent viscosity can be obtained and it varied based on their rheological properties. The results in Fig 4.11 indicate that if corrosion inhibitor-5 was used, the spent acid system containing 4 vol% surfactant-A can be effectively used at temperatures lower than 145 $^{o}$F, whereas the acids prepared by 5-6 vol% surfactant-AW can be efficiently applied at higher temperatures (145 ~ 220$^{o}$F).

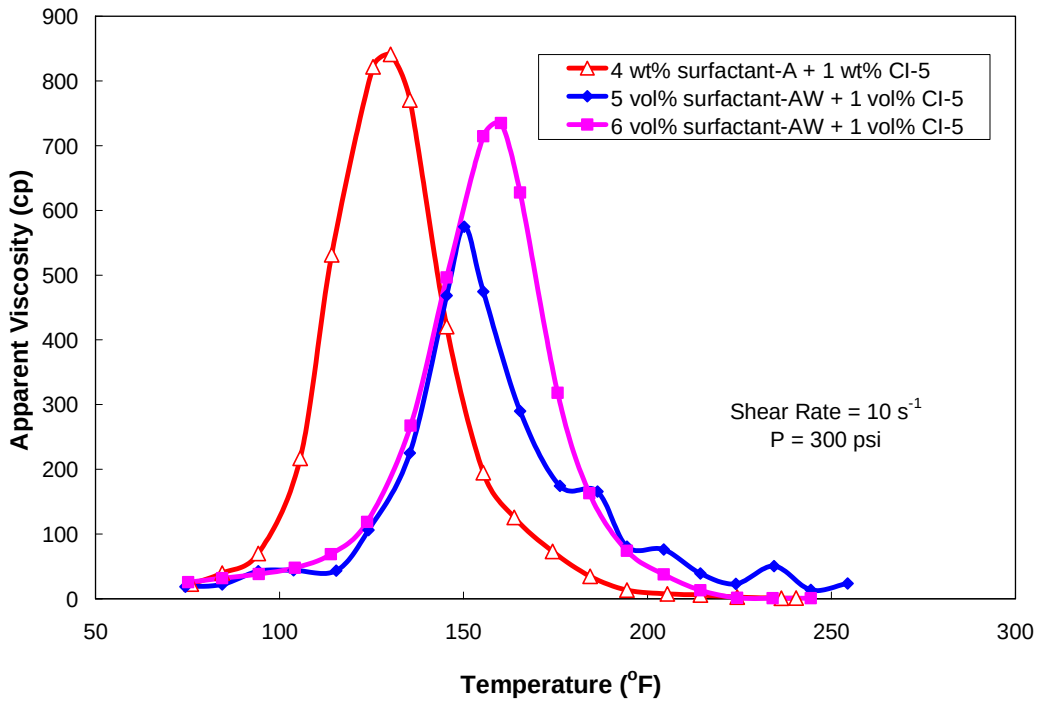


**Fig. 4.12—Effect of corrosion inhibitor CI-5 on amidoamine oxide-based spent acids.**

*Thermal Stability*

It is very important to look into the thermal stability of surfactant-based acids. The viscosity of acids should be stabilized at high temperature for a certain time which is long enough for the acidizing treatment. **Fig. 4.13** shows how apparent viscosity of spent acid (contains 5 vol% surfactant-AW and 1 vol% CI-5) changes with the time at 150 and 190 $^{o}$F, shear rate of 10 $s^{-1}$ and 300 psi. The result indicates that the viscosity of spent acid can be kept for 100 min. The system was thermal stable and can be effectively used in the field.

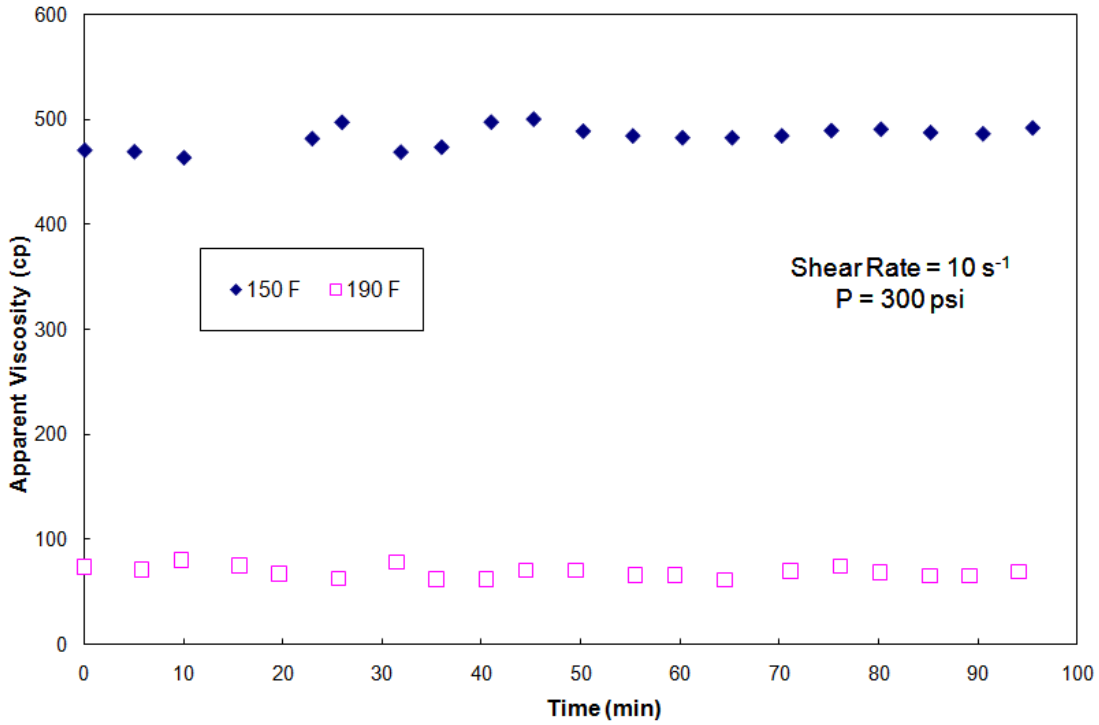


**Fig. 4.13—Thermal stability of the spent acid containing 5 vol% surfactant-AW and 1 vol% CI-5.**

**Conclusions**

The effects of corrosion inhibitors on the rheological properties of amidoamine oxide surfactants-based acids were examined in this chapter. Three different corrosion inhibitors and two amidoamine oxide surfactants were tested. Based on the results obtained, the following conclusions can be drawn:

1. Compared to surfactant-based acids made with corrosion inhibitor CI-28 or CI-5, the acids prepared with corrosion inhibitor-A showed a much higher viscosity, but less thermal stability.
2. Although corrosion inhibitor-28 had a good compatibility with surfactants, it adversely influenced the rheological properties of surfactant-based acids.
3. Cryo-TEM tests showed the addition of corrosion inhibitor to the spent acid prevented the rod-like micelle formation.
4. If corrosion inhibitor CI-5 was used to prepare surfactant-based acids, the system with surfactant-AW can be effectively used at higher temperatures (>150$^{o}$F); whereas acids prepared with surfactant-A can be efficiently applied at lower temperatures (<150$^{o}$F).
5. The spent acid with 5 vol% surfactant-AW and 1 vol% CI-5 showed good thermal stability at high temperatures. The apparent viscosity can be stabilized for 100 min at 150 and 190 $^{o}$F.

# CHAPTER V

# REACTION KINETICS BETWEEN SURFACTANT-BASED ACIDS WITH CALCITE BY USING ROTATING DISK APPARATUS

## Introduction

The rotating disk apparatus is used to study heterogeneous reactions. This system allows the determination of rock dissolution rate, reaction rate constants, reaction order and diffusion coefficients. This instrument has been used extensively to investigate the reaction of HCl, organic acids, and chelating agents with carbonate rocks (**Table 5.1**).

**TABLE 5.1—LITERATURE REVIEW OF STUDIES USING RDA**

| Author | Rock type | Reactive system |
|---|---|---|
| Lund et al. (1975) | Calcite | HCl |
| Anderson (1991) | Dolamite | HCl |
| Alkattan et al. (1998) | Dolomite/limestone | HCl |
| Fredd and Fogler (1998a,b,c) | Calcite | EDTA; Acetic acid |
| Gautelier et al. (1999) | Dolamite | HCl |
| Conway et al. (1999) | Calcite/dolomite | Straight/gelled/emulsified HCl |
| Alkattan et al. (2002) | Calcite | HCl |
| Burns (2002) | Calcite | Polyaspartic acid |
| Frenier et al. (2004) | Calcite/dolomite | HEDTA |
| Buijse et al. (2004) | Calcite | HCl; Acetic acid; Formic acid |
| Taylor et al. (2004a) | Calcite/dolomite | HCl + additives |
| Taylor et al. (2004b) | Dolomite | HCl + additives |
| Al-Mohammad et al (2006) | Calcite | Surfactant based HCl |
| Nasr-El-Din et al. (2007) | Cement | HCl |
| Al-Khaldi et al. (2007) | Calcite | Citric acid |
| Nasr-El-Din et al. (2008b) | Calcite | Gelled HCl |
| Nasr-El-Din et al. (2009) | Calcite | Surfactant based HCl |
| Rabie et al. (2010) | Limestone/chalk | Gelled HCl |

***Mechanism***

Dissolution of calcite consists of three primary steps (**Fig. 5.1**): 1) mass transfer of the reactant from the bulk fluid to the solid-liquid interface, 2) heterogeneous reaction with $CaCO_3$ solid at the interface, and 3) mass transfer of products from the surface back out into the bulk.

During dissolution, one of these three processes may be significantly slower than the other two, and is considered to be the rate-limiting mechanism. As such, the overall dissolution rate is equal to the rate of the slowest step. Thus, the dominant mechanism for dissolution may be mass transfer, surface reaction or a combination of the two depending on pH, reactant concentration, and disk rotating speed.

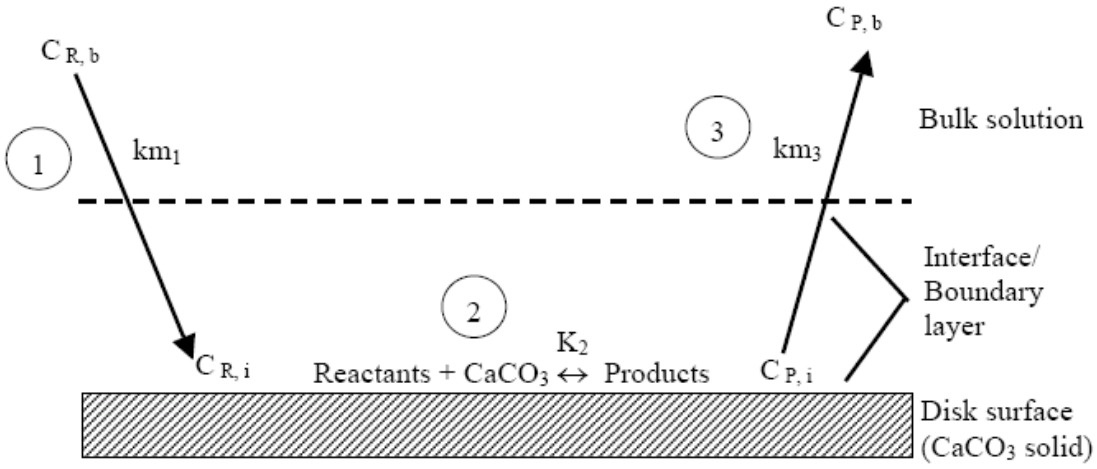


**Fig. 5.1—Dissolution of calcite (Burns 2002).**

*Mass Transfer to the Rotating Disk Surface*

Levich (1962) solved the Navier-Stokes and Continuity equation to evaluate the mass transfer of species from a bulk solution to the surface of a rotating disk. The key assumption for modeling the fluid dynamics and mass transfer is that the disk is

sufficiently large so that the edge effect is negligible. The mass transfer flux of a species *j* can be expressed as

$$J_j = K_{mtj}\left(C_{Bj} - C_{Sj}\right) \quad \text{Eq. 5.1}$$

where $K_{mtj}$ is the mass transfer coefficient, $C_{Bj}$ is the concentration of a species *j* in the bulk solution, and $C_{Sj}$ is its concentration at the interface. The mass transfer coefficient can be determined for Newtonian fluids under laminar flow conditions ( $\mathrm{Re} \le 3\times10^5$ and $Sc > 100$ ) using Eq. (5.2):

$$K_{mt} = \frac{(0.62048)(Sc^{2/3})\sqrt{\omega\nu}}{1 + (0.2980)Sc^{-1/3} + (0.14514)Sc^{-2/3}} \quad \text{Eq. 5.2}$$

where $Sc$ is Schmidt number ( $\nu / D$ ), $\nu$ is the kinematic viscosity ( $\mu / \rho$ ) , $D$ is the diffusion coefficient, $\omega$ is the disk rotational speed.

In this expression, it is important to note that under mass transfer limitation, a linear relationship will exist between dissolution rate and the square root of rotating speed ( $\omega^{1/2}$ ).

For an example in **Fig. 5.2**, the dissolution rate increases linearly with $\omega^{1/2}$ at low disk rotating speeds, due to the mass transfer limitation, while as, at high rotating speeds, the dissolution is constant, because the reaction rate in this regime is limited by the surface reaction rate.

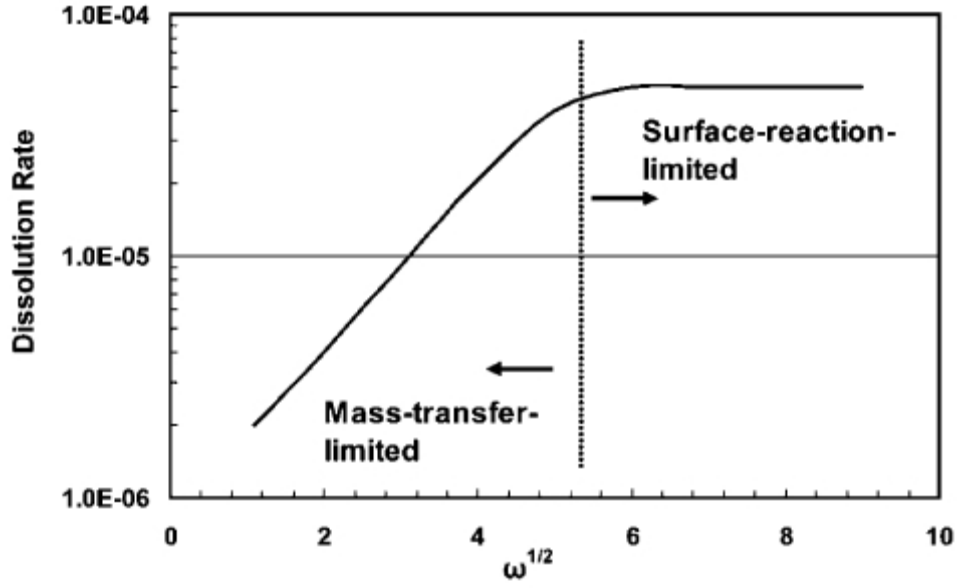


**Fig. 5.2—An example of rock dissolution rate vs $\omega^{1/2}$ (Taylor 2004a).**

For non-Newtonian fluids, Hansford and Litt (1968) solved the convective diffusion equation and the Reynolds and Schmidt numbers were modified to take into account the shear dependence of the power-law "viscosity",

$$\mu = K\dot{\gamma}^{n-1} \quad \text{.....Eq. 5.3}$$

where $K$ is power-law consistency index, $\dot{\gamma}$ is the shear rate and n is power law index. The modified Reynolds and Schmidt numbers become:

$$\mathrm{Re} = \frac{r^2\omega^{2-n}}{N} \quad \text{.....Eq. 5.4}$$

and $$Sc = \frac{N\omega^{n-1}}{D} \quad \text{.....Eq. 5.5}$$

where $N$ is $K/\rho$ and $r$ is the radius of the disk.

The average mass flux to the solid surface can then be determined:

$$J = \frac{ShD}{r}(C_b - C_s) \quad \text{.....Eq. 5.6}$$

where *Sh* is known as Sherwood number and expressed by

$$Sh = \phi(n) Sc^{1/3} \mathrm{Re}^{1/3[(n+2)/(n+1)]} \quad \text{.....Eq. 5.7}$$

where $\phi(n)$ is the function that depends on n and the wall radial velocity gradient. Values of $\phi(n)$ are given in **Table 5.2**:

| TABLE 5.2-- VALUES OF ø(n) AS A FUNCTION OF n | | | | | | | |
|---|---|---|---|---|---|---|---|
| n | 0.2 | 0.4 | 0.5 | 0.6 | 0.8 | 1 | 1.3 |
| ø(n) | 0.695 | 0.662 | 0.655 | 0.647 | 0.633 | 0.62 | 0.618 |

Finally, the average mass flux of a solute diffuses from the bulk of solution to the solid surface as a function of the disk rotating disk speed $\omega$, bulk concentration $C_b$, diffusivity D, and the power-law parameters n and K can be obtained as follows:

$$J = \left[ \phi(n) \left( \frac{K}{\rho} \right)^{\frac{-1}{3(1+n)}} (r)^{\frac{(1-n)}{3(1+n)}} (\omega)^{\frac{1}{1+n}} D^{2/3} \right] (C_b - C_s) \quad \text{.....Eq. 5.8}$$

***pH***

Mass transfer from a viscoelastic surfactant-based acid to calcite is very complicated. The viscosity of the gel is a function of many parameters, including pH and $Ca^{2+}$ concentration. The bulk solution contains high acid concentration and its pH is nearly zero. However, on the rock surface, the acid spent and the pH is approximately 4.5. Therefore, the pH goes through a transition across the diffusion boundary layer from nearly zero to 4.5 (**Fig. 5.3**). The viscosity of the fluid inside the boundary layer also

varies making the diffusion process vary spaciously. Consequently, the diffusivity calculated in the present study is an averaged value of multiple diffusivity values as the hydrogen ions is transferred from the bulk fluid to the rock surface.

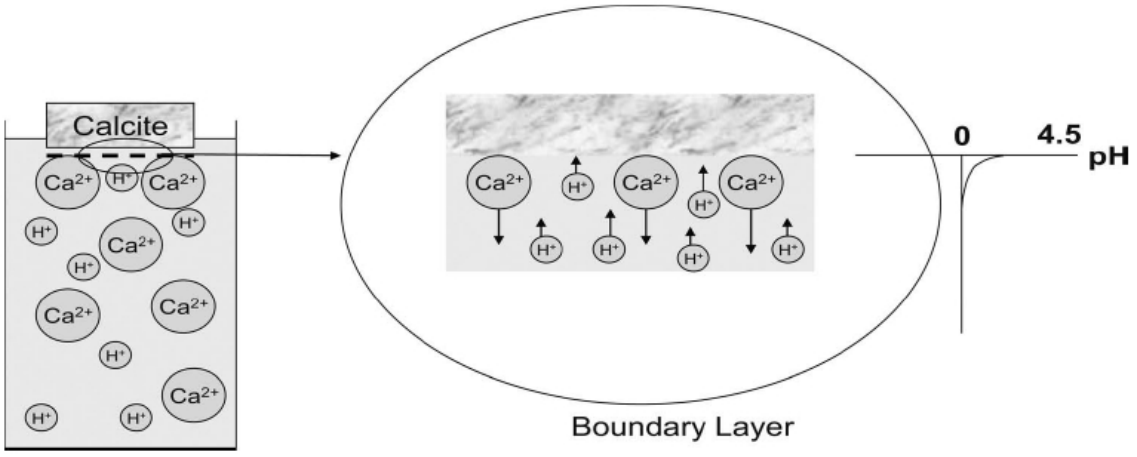


**Fig. 5.3—pH diagram in the bulk solution and the boundary layer (Nasr-El-Din et al. 2009).**

***Flow Patterns***

The addition of a viscoelastic surfactant or polymer to regular HCl acid can change the type of fluid from Newtonian to Non-Newtonian fluid. Surfactant-based acids exhibit shear thinning behavior, and they resemble polymer solutions examined by Hansford and Litt (1968). As a result, the flow pattern in the rotating disk will vary with the rotational speed. This variation will affect the react of the acid with the calcite disk. Hansford and Litt (1968) studies flow of non-Newtonian fluid in a rotating disk and mentioned three types of flow patterns: (1) Reverse flow at low rotational speeds, (2) Toroidal flow at intermediate rotational speeds, and (3) Centrifugal flow at higher rotational speeds. The schematic diagram of the three patterns is shown below in **Fig. 5.4**.

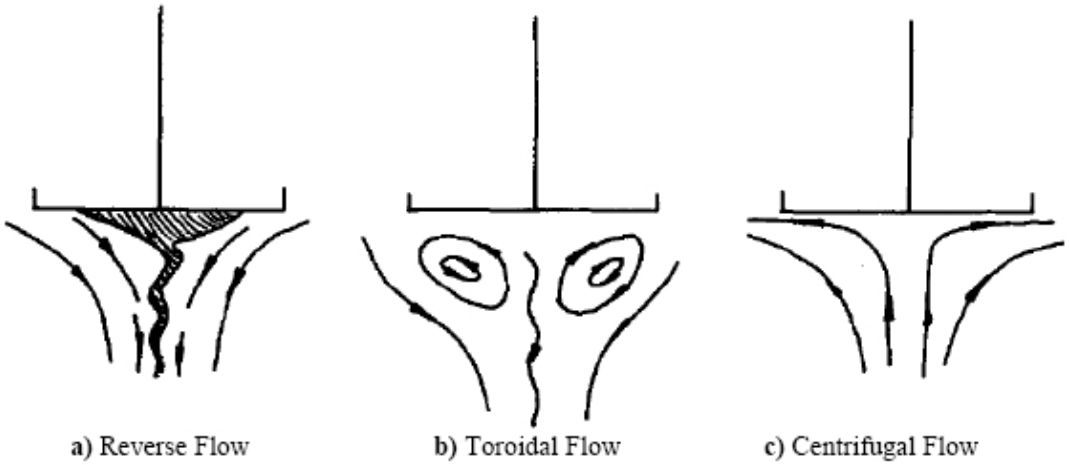


**Fig. 5.4—Flow patterns of non-Newtonian fluid in rotating disk.**

## Experimental Studies

### *Materials*

The viscoelastic surfactant-AW system was examined and it is a mixture of an amphoteric surfactant and solvent. Hydrochloric acid (ACS reagent grade, 36.8 wt%) and de-ionized water (resistivity = 18.2 $M\Omega \cdot cm$) were used to prepare the acid solution. Acid concentration was determined by titration using 1N sodium hydroxide solution.

### *Fluid Systems*

The live acid solution (500 ml) was prepared by mixing 6 vol% surfactant-AW with concentrated hydrochloric acid, followed by diluting with de-ionized water and then the resulting solution was mixed with 1 vol% corrosion inhibitor-5. Every effort was made not to contaminate the acid with iron. Acid solutions with various additives were prepared such that the final acid concentration was 7 or 20 wt%.

***Equipment***

Reaction rate experiments were performed using rotating disk apparatus RDA-100. Dessert limestone was tested in this chapter and cut by the dimension of 1.5'' diameter and 1'' thickness. The disks were fixed in the core holder assembly in the reactor vessel using heat-shrinkable Teflon tubing. Reaction fluid was poured in the reservoir vessel and both were heated up to the desired temperatures. Compressed $N_2$ was used to pressurize the reservoir vessel to a pre-determined pressure that is sufficient to transfer the acid to the reactor vessel and results in a reactor pressure of 1500 psig. Pressure greater than 1000 psig is necessary in the reaction vessel to ensure that the evolved $CO_2$ is kept in solution and does not affect the system hydrodynamic and the dissolution rate. The rotational speed was then set up to the selected value and the time is started by the moment at which the valve between the reservoir and the reactor vessels is opened. Samples, each of approximately 2 ml, were withdrawn at equal interval of 2 minutes up to 20 minutes. Be careful that lots of foam will be generated due to the surfactant. Calcium concentrations in the samples were measured using Perkin-Elmer atomic absorption. In addition, the calcite surface exposed to acidic solutions was photographed to examine the etching pattern on the surface of calcite disks. A new core sample was used for each experiment. The rate of calcium production along with the initial area of the sample was used to determine the dissolution rate. The experiments aimed to study the effect of temperature (75, 120, and 170$^{o}$F) and rotational speed (100-1800 rpm) on the reaction rate, and to determine the reaction rate and mass transfer parameters in both mass-transfer and surface-reaction limited regimes.

## Results and Discussions

### *Apparent Viscosity of Live Acids*

The apparent viscosity of live acid (20 wt% HCl, 6 vol% surfactant-AW, and 1 vol% CI-5) was examined at three different temperatures (75, 120 and 170$^{o}$F). They are all Newtonian fluid and the results were listed in **Table 5.3**. It indicates that surfactant-based 20 wt% HCl can be injected without any difficulty due to its low viscosity.

**TABLE 5.3--VISCOSITY OF SURFACTANT-BASED ACID AT VARIOUS TEMPERATURES USING CAPILLARY VISCOMETER**

| Temperature ($^{o}$F) | Time (s) | Viscosity (cp) |
|---|---|---|
| 75 | 197 | 2.14336 |
| 120 | 149 | 1.62112 |
| 170 | 112 | 1.21856 |

The rheological properties of live acid with 7 wt% HCl, 6 vol% surfactant-AW, and 1 vol% CI-5 were plotted in **Fig. 5.5** and it can be seen that this live acid was shear thinning fluid at room temperature and 120 $^{o}$F, however, once the temperature was increased up to 170 $^{o}$F, the surfactant-based 7 wt% HCl acid became Newtonian fluid and the viscosity was 22 cp.

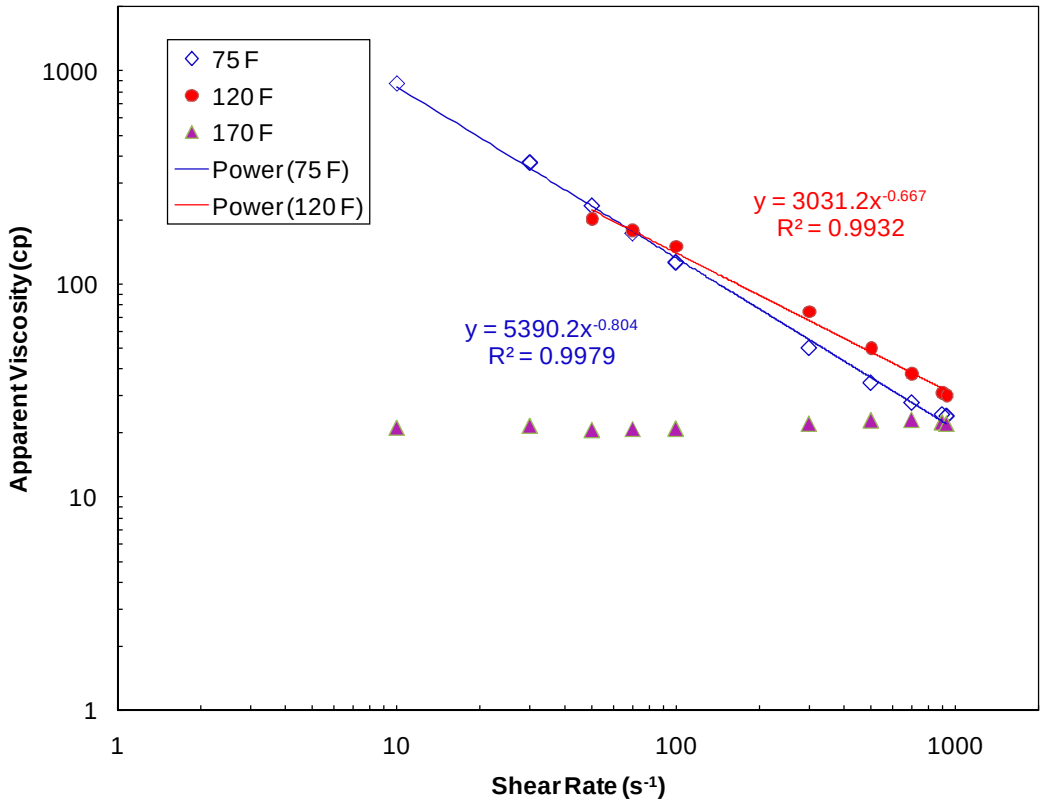


**Fig. 5.5—Viscosity of surfactant-based live acid (7 wt% HCl, 6vol% surfactant-AW and 1 vol% corrosion inhibitor CI-5) at various shear rates.**

### *Surfaces of the Disks after Reaction*

**Fig. 5.6a** shows the surface of three different disks exposed to 20 wt% HCl and 6 vol% surfactant-AW at 170°F, and variable rotating speed. At 200 rpm, there was a stagnation zone at the middle of the disk. There was a spiral with grooves on the surface of the disk. The size of the stagnation zone decreased at higher rotating spends. No photos were taken at rotating speed above 1000 rpm, because the reaction was so vigorous and almost the entire disk was dissolved in the acid.

**Fig. 5.6b** show the surface of three different disks exposed to 20 wt% HCl, 6 vol% surfactant-AW and 1 vol% CI-5 at 500 rpm but variable temperatures. At room temperature, there was a stagnation zone at the middle of the disk and grooves need the edge of the disk. The size and depth of the grooves increased at higher temperatures.

**Fig. 5.6c** shows the surface of disks exposed to 7 wt% HCl, 6 vol% surfactant-AW and 1 vol% corrosion inhibitor-5 at 500 rpm. At 120 $^{o}$F, the surface was very flat. Whileas, at 170 $^{o}$F, a stagnation zone and grooves were observed. If 5 wt% mutual solvent was added to this surfactant-based 7 wt% HCl, the size of stagnation zone was decreased and the grooves became deeper. With the addition of 1 wt% citric acid, the shallow grooves were noted at the surface of the disk. If 0.03 wt% $FeCl_3$ was additionallu used in this acid, the surface was yellowish and shallow grooves were obtained.

(a)

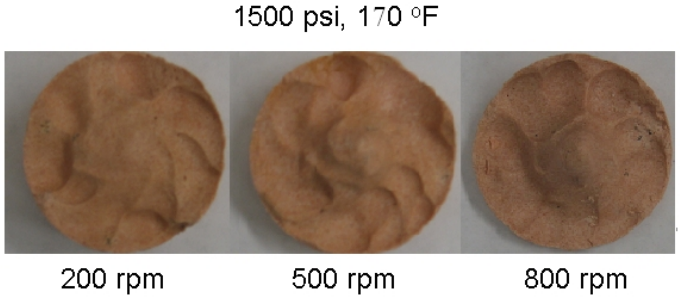


**Fig. 5.6—a) Surface of three different disks exposed to 20 wt% HCl and 6 vol% surfactant-AW at 170 $^{o}$F, and variable rotating speed.**

(b)

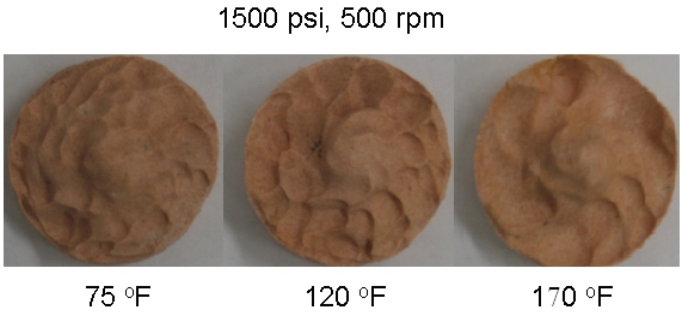


(c)

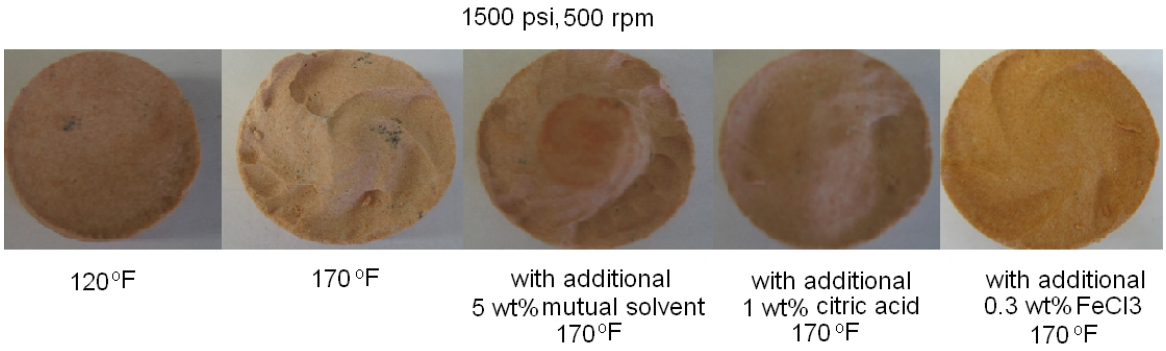


**Fig. 5.6—Continued. b) Surface of three different disks exposed to 20 wt% HCl and 6 vol% surfactant-AW at 500 rpm but variable temperatures. c) Surface of different disks exposed to 7 wt% HCl, 6 vol% surfactant-AW and some acid additives at 120, 170 °F, and 500 rpm.**

### *Dissolution Rate*

**Fig. 5.7** shows the concentration of calcium ion in collected samples as a function of time. Four experiments were conducted at a pressure of 1500 psi and temperature of 170 °F. The result indicates that Ca concentration linearly increased with the time. More Ca was dissolved when the rotating speed increased.

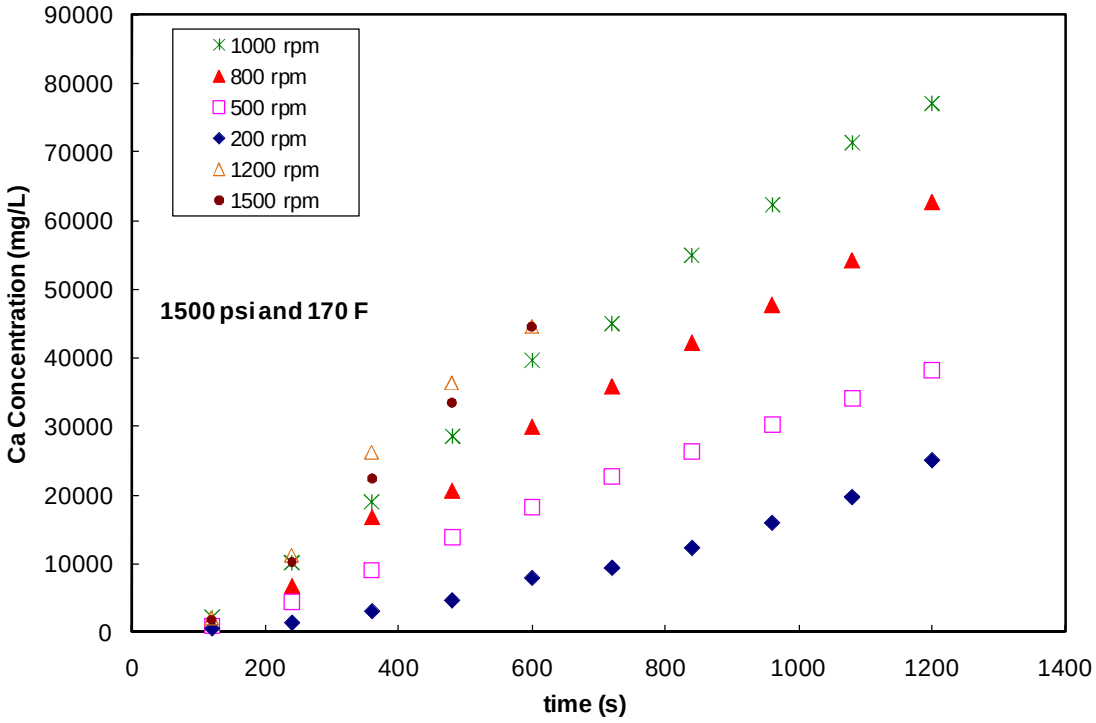


**Fig. 5.7—Ca concentration at various disk rotating speed for 20 wt% HCl, 6 vol% surfactant-AW and 1 vol% corrosion inhibitor-5 at 1500 psi and 170°F.**

The linear fitting lines based on the first few point are shown in **Fig. 5.8**. The dissolution rate (**Eq. 5.9**) can be determined from the slope of the linear portion of the calcium concentration vs. time relationship and the initial surface area of the disk surface exposed to the acid.

$$\text{Dissolution Rate} = \frac{d[Ca]}{Adt} \quad \text{.....Eq. 5.9}$$

where $A$ is the surface area of the disk and equals $\pi r^2$.

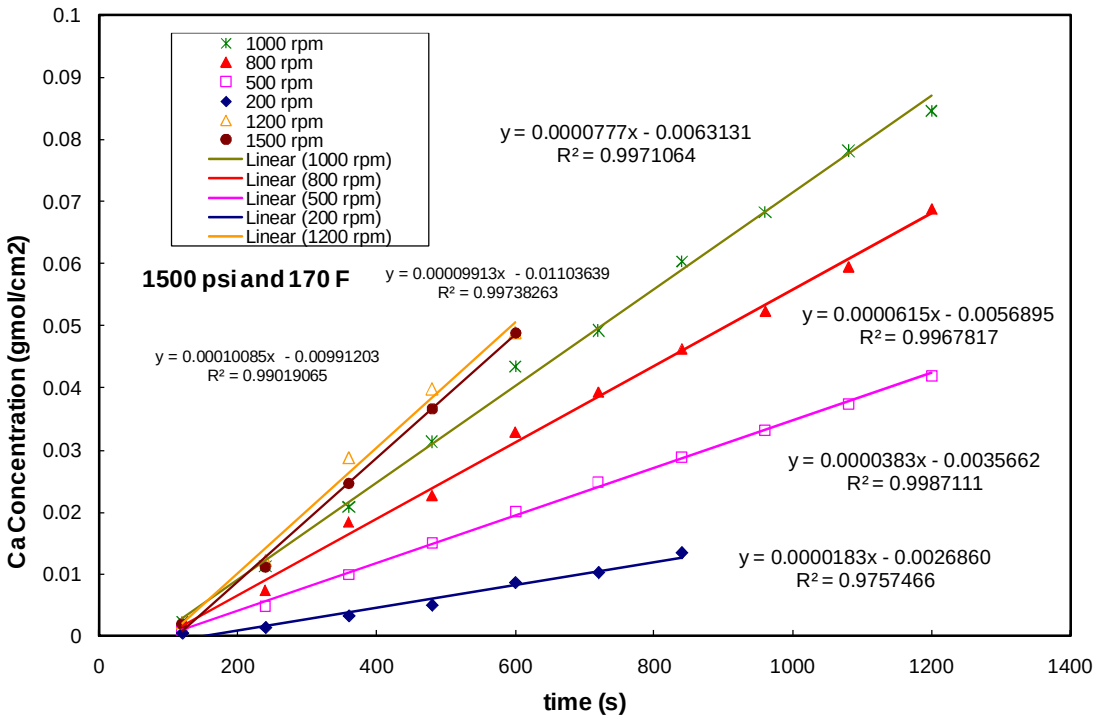


**Fig. 5.8—Linear performance of Ca concentration at various disk rotating speed with time.**

As mentioned above, for Newtonian fluid, the rock dissolution rate should be linear with the square root of rotating speed if the reaction is mass transfer limited. **Fig. 5.9** shows the straight fitting line and indicates that the reaction between the limestone and the surfactant-based acid was controlled by mass transfer up to 1200 rpm, 170$^{o}$F.

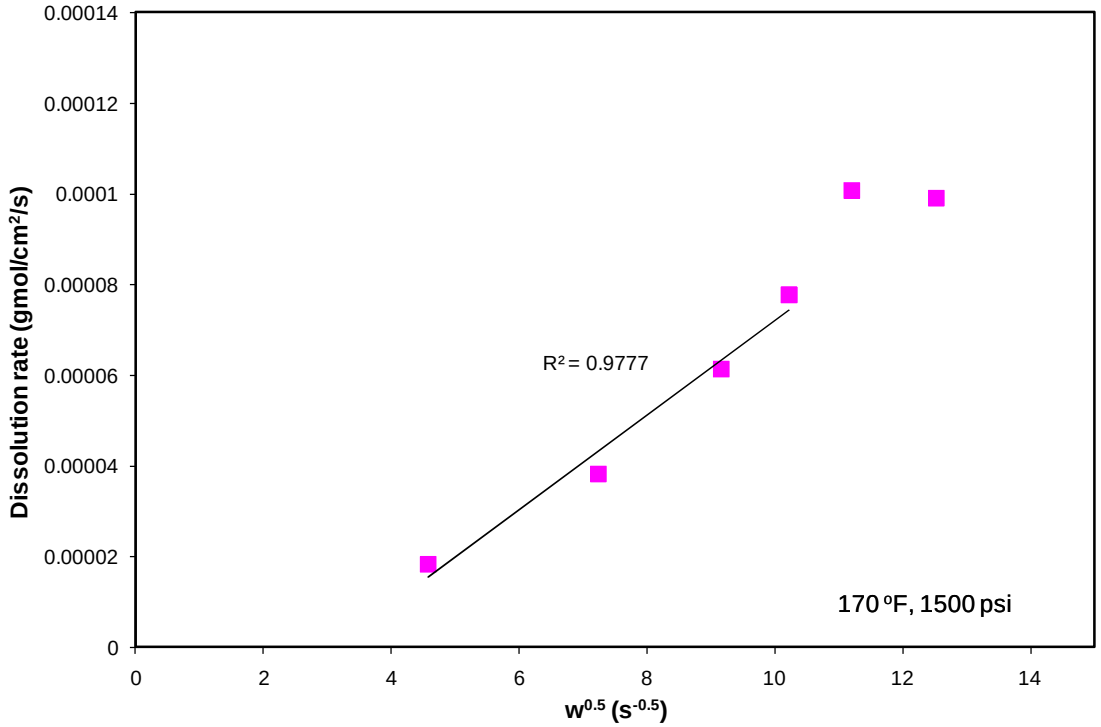


**Fig. 5.9—Linear performance of rock dissolution rate with the square root of rotating speed.**

***Diffusion Coefficient***

Based on **Eq. 5.10**,

$$CaCO_3 + 2HCl \rightarrow Ca^{2+} + 2Cl^- + CO_2 + H_2O \quad \text{.....Eq. 5.10}$$

it can be noted that the flux of $H^+$ to the surface of the disk is twice that of $Ca^{2+}$ ions away from the surface. Therefore,

$$J_{H^+} = 2J_{Ca^{2+}} = \frac{(0.62048)(Sc^{2/3})\sqrt{\omega\nu}}{1+(0.2980)Sc^{-1/3}+(0.14514)Sc^{-2/3}}(C_B - C_S)$$

$$\approx 0.62 C_0 D^{2/3}\left(\frac{\mu}{\rho}\right)^{-1/6}\omega^{1/2} \quad \text{.....Eq. 5.11}$$

The diffusion coefficient of $H^+$ can be obtained by

$$D = \left( \frac{J_{H^+}}{0.62 C_0 \left( \frac{\mu}{\rho} \right)^{-1/6}} \right)^{3/2} = \left( \frac{2 \times reaction \quad rate}{0.62 C_0 \left( \frac{\mu}{\rho} \right)^{-1/6}} \right)^{3/2} \quad \text{.....Eq. 5.12}$$

After the calculation, the diffusion coefficient of $H^+$ in the surfactant-based acid at 170 $^oF$ was 0.0001189 $cm^2/s$.

**Fig. 5.10** shows the temperature effect on the concentration of calcium. The experiments were done at 1500 psi and 500 rpm. The result indicates that Ca concentration linearly increased with the time. Also, the concentration of calcium at a given time increased as the temperature increased.

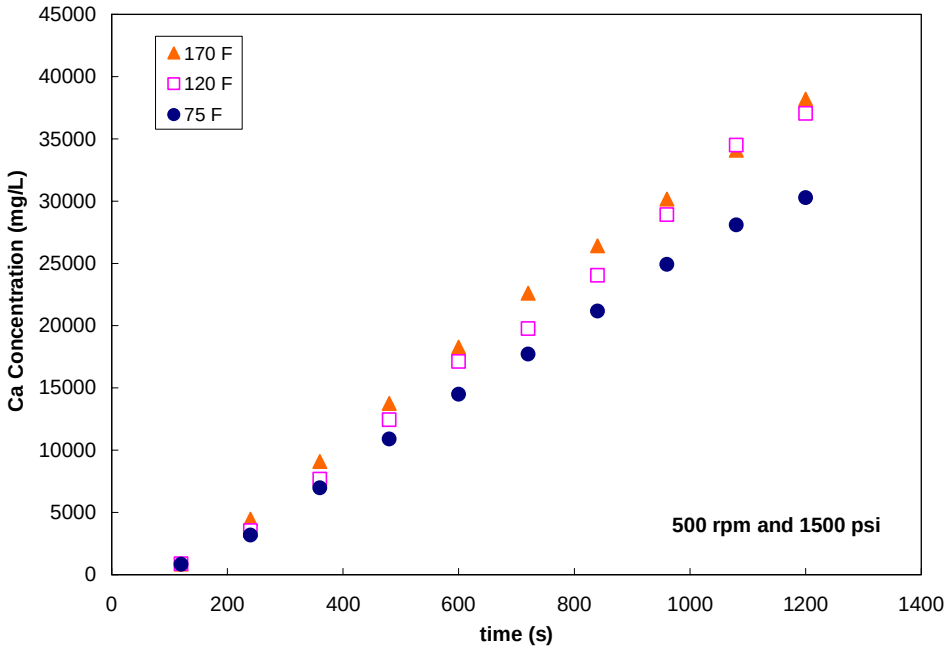


**Fig. 5.10—Ca concentration at various temperatures for 20 wt% HCl, 6 vol% surfactant-AW and 1 vol% corrosion inhibitor-5 at 1500 psi and 500 rpm.**

**Fig. 5.11** shows the linear relationship between Ca concentration and time. The slopes of the straight lines were Ca dissolution rates at 75, 120 and 170°F.

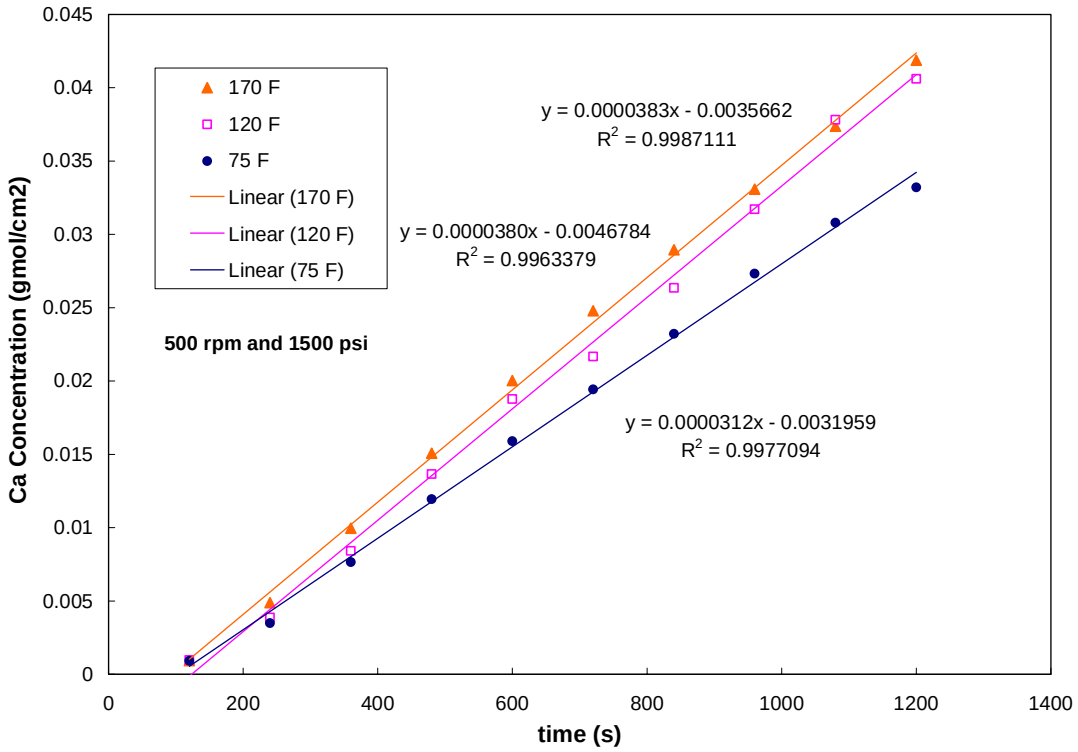


**Fig. 5.11—Linear performance of Ca concentration at various temperatures with time.**

### *Surfactant-based 7 wt% HCl Live Acids*

*Effect of Temperatures*

**Fig. 5.12** shows the Ca concentration in live acid with 7 wt% HCl, 6 vol% surfactant-AW, and 1 vol% corrosion inhibitor-5. The experiments were done at 500 rpm and 1500 psi. The results indicate that more Ca was obtained if the temperature was increased from 120°F to 170°F. It should be noted that according to Fig. 5.5, the viscosity of this acid at 500 rpm (52 $s^{-1}$) was about 200 cp.

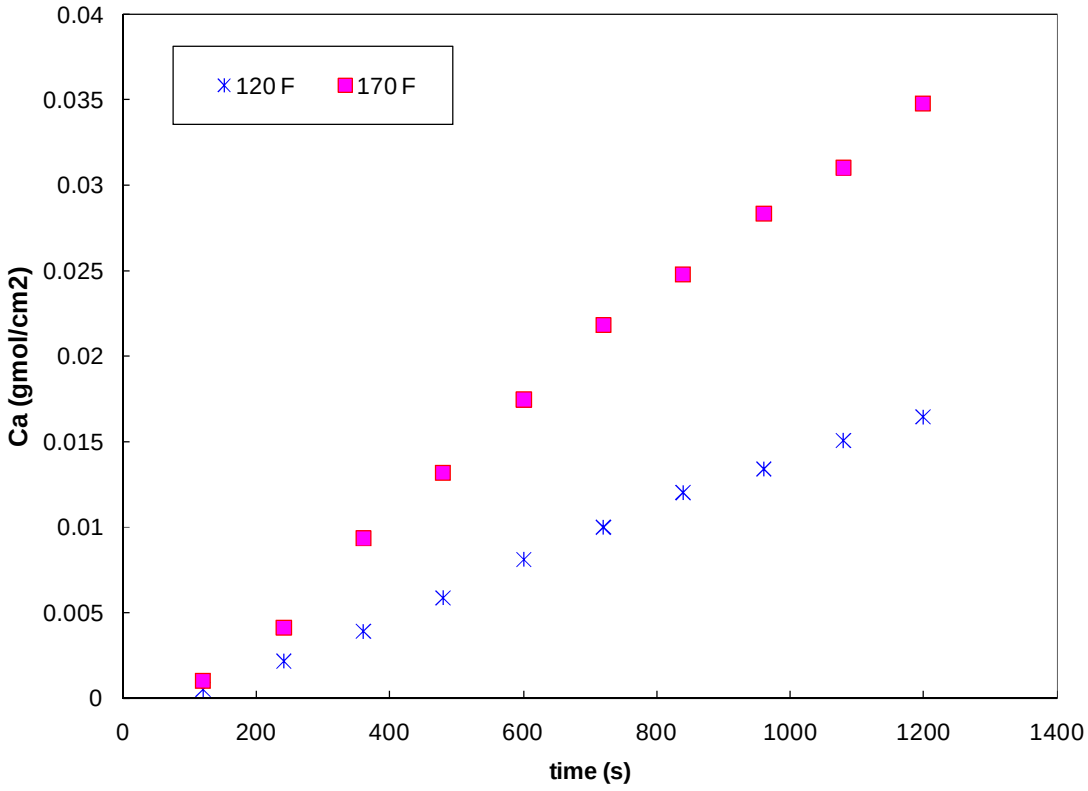


**Fig. 5.12—Ca concentration at various temperatures for 7wt% HCl, 6vol% surfactant-AW and 1vol% CI-5 at 1500 psi and 500 rpm.**

*Effect of Acid Additives*

**Fig. 5.13** shows the Ca concentration with time in surfactant-based 7 wt% HCl acid at 500 rpm, and 170 $^{o}$F. More Ca was generated with the addition of mutual solvent due to the break-up of rod like micelles. The obtained Ca concentration decreased if 1 wt% citric acid was added probably because of the deposition of calcium citrate salt on the surface of the disk. The addition of 0.03 wt% $FeCl_3$ caused the reduced reaction rate.

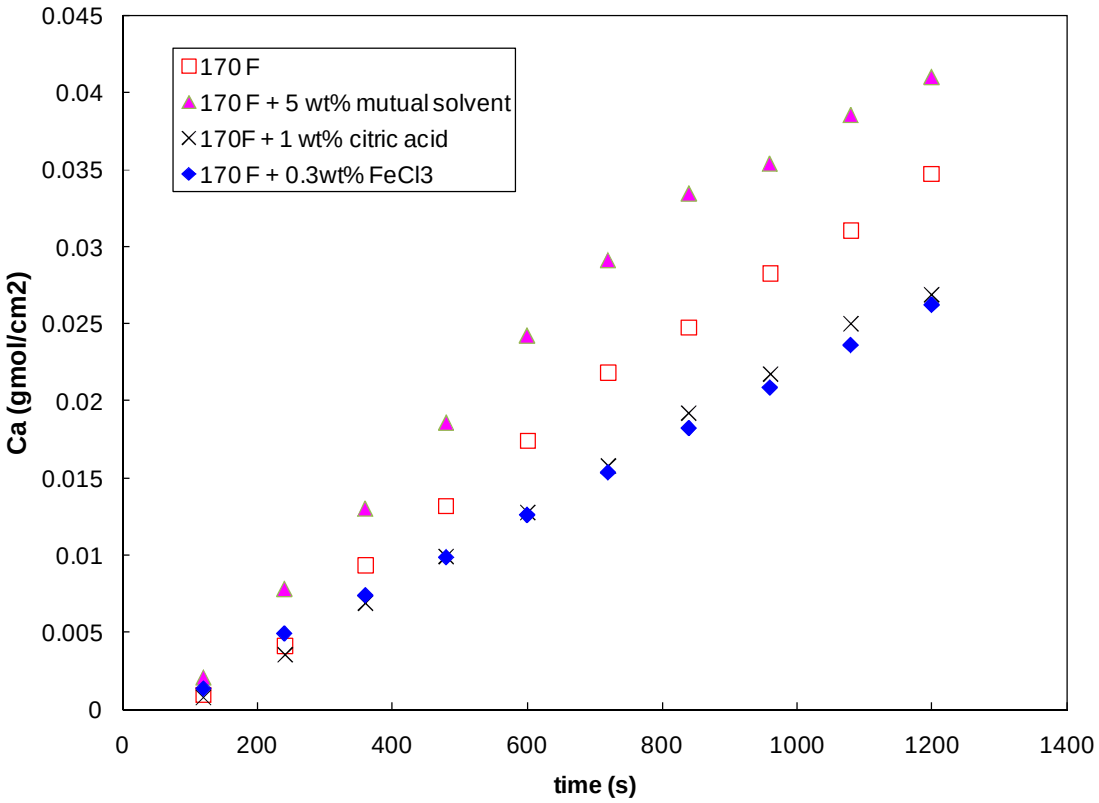


**Fig. 5.13—Effect of acid additives on Ca concentration for 7wt% HCl, 6vol% surfactant-AW and 1vol% CI-5 at 170 °F and 500 rpm.**

## Conclusions

Kinetic studies between amidoamine oxide-based acid and limestone were examined by using rotating disk apparatus at different temperatures and rotating speeds. The following conclusions can be made based on the results:

1. The amidoamine-oxide surfactant based 20 wt% HCl acids are Newtonian fluid at 75, 120 and 170 °F.
2. The amidoamine-oxide surfactant based 7 wt% HCl acids are shear thinning fluid at 75, 120 °F, and Newtonian fluid at 170 °F.

3. Ca concentration was found to increase linearly with time at various rotating speed at 170$^{o}$F.
4. Ca concentration was found to increase linearly with time at 500rpm and various temperatures (75, 120 and 170$^{o}$F).
5. The reaction between limestone and surfactant-based 20 wt% HCl acid was mass transfer limited up to 1200 rpm at 170$^{o}$F.
6. The diffusion coefficient of $H^{+}$ in the surfactant-based 20 wt% HCl acid at 170$^{o}$F was 0.0001189 $cm^{2}/s$.
7. The addition of mutual solvent increased the reaction rate of surfactant-based 7 wt% HCl with limestone, while as, the addition of citric acid and $FeCl_3$ reduced its reaction rate.

# CHAPTER VI

# CONCLUSIONS

In this study, the amphoteric surfactants "amidoamine oxides" were examined as a diverting agent. A HPHT rheometer was used to measure the rheological properties: apparent viscosity, elastic modulus (G'), and viscous modulus (G''). Rotating disk apparatus was used to investigate the kinetic studies of surfactant-based acid and limestone. Cryo-TEM was conducted to evaluate the effect of acid additives on the micelle structure. Two amidoamine oxides were compared and their stability and compatibility were examined at high temperature high pressure. Through this research, it was determined that:

1. The apparent viscosity of surfactant-based water system, live acid and spent acid was found to be a function of temperature.
2. The apparent viscosity of live acids was a function of HCl concentrations. The live acids made with surfactant-A and CI-A showed two phase separation if HCl concentration was 4 ~ 7 wt%. On the other hand, live acids containing surfactant-AW and CI-28/CI-5 always showed homogeneous solutions, no matter what HCl concentration was used.
3. Ferric ion had a significant effect on the apparent viscosity of surfactant-based live acids. It could cause enhanced viscosity, phase separation and surfactant precipitation. Therefore, the well tubulars should be pickled before the acid injection and the clean mixing tank is required.

4. The addition of acid additives, such as mutual solvent, methanol, demulsifier, $H_2S$ scavenger, and organic acids/chelating agents, to the surfactant-based acid was noted to reduce its apparent viscosity. One exception was citric acid. The addition of citric acid to the spent acid not only increased the apparent viscosity, but it also broadened the temperature range that surfactant can be used, due to the generation of suspended solids of calcium citrate.
5. The addition of organic acids to spent acids (pH 4-5) did form a precipitate. Therefore, laboratory testing of using organic acids/chelating agents should be done prior to field use, to avoid any formation damage.
6. Cryo-TEM photomicrographs confirmed that
    - The addition of corrosion inhibitor to the spent acid was able to prevent the rod like micelle formation.
    - The addition of organic acid to the spent acid generated fewer elongated micelle structures and resulted in less apparent viscosity.
7. The addition of corrosion inhibitor to the spent acids significantly affected G' and G''. For spent acids without any corrosion inhibitors, the elasticity was predominate at temperatures of 130-190$^{o}$F. However, for spent acids made with corrosion inhibitors, the viscous modulus (G'') was higher than the elastic modulus (G') at almost all the examined temperatures.
8. If corrosion inhibitor CI-5 was used to prepare surfactant-based acids, the system with surfactant-AW can be effectively used at higher temperatures (>150$^{o}$F);

whereas acids prepared with surfactant-A can be efficiently applied at lower temperatures (<150$^{o}$F).

9. The spent acid with 5 vol% surfactant-AW and 1 vol% CI-5 showed good thermal stability at high temperatures. The apparent viscosity can be stabilized for 100 min at 150 and 190$^{o}$F.
10. The amidoamine-oxide surfactant based 20 wt% HCl acids are Newtonian fluid at 75, 120 and 170$^{o}$F.
11. The reaction between limestone and surfactant-based acid was mass transfer limited up to 1000 rpm at 170$^{o}$F.
12. The diffusion coefficient of $H^{+}$ in the surfactant-based 20 wt% HCl acid at 170$^{o}$F was 0.0001189 $cm^2/s$.
13. The addition of mutual solvent increased the reaction rate of surfactant-based 7 wt% HCl with limestone, while as, the addition of citric acid and $FeCl_3$ reduced its reaction rate.

# REFERENCES

Al-Anazi, H.A., Nasr-El-Din, H.A., and Mohamed, S.K. 1998. Stimulation of Tight Carbonate Reservoirs Using Acid-in-Diesel Emulsions: Field Application. Paper SPE 39418 presented at the SPE International Symposium on Formation Damage Control, Lafayette, Louisiana, 18-19 February. doi: 10.2118/39418-MS.

Alkattan, M., Oelkers, E., Dandurand, J.-L., and Schott, J. 1998. An Experimental Study of Calcite and Limestone Dissolution Rates as a Function of pH from –1 to 3 and Temperature from 25 to 80°C. *Chemical Geology* **151** (1–4): 199–214.

Alkattan, M., Oelkers, E., Dandurand, J.-L., and Schott, J. 2002. An Experimental Study of Calcite Dissolution Rates at Acidic Conditions and 25°C in the Presence of $NaPO_3$ and $MgCl_2$. *Chemical Geology* **190** (1–4): 291–302.

Al-Khaldi, M.H., Nasr-El-Din, H.A., Mehta, S., and Al-Aamri, A.D. 2007. Reaction of Citric Acid with Calcite. *Chem. Eng. Sci.* **62** (21): 5880-5896

Al-Mohammad, A.M., Nasr-El-Din, H.A., Al-Aamri, A.M., and Al-Fuwaires, O. 2006. Reaction of Calcite with Surfactant-Based Acids. Paper SPE 102838 presented at the SPE Annual Technical Conference and Exhibition, San Antonio, Texas, USA, 24–27 September. doi: 10.2118/102838-MS.

Al-Muhareb, M.A., Nasr-El-Din, H.A., Samuel, E., Marcinew, R.P., and Samuel, M. 2003. Acid Fracturing of Power Water Injectors: A New Field Application Using Polymer-Free Fluids. Paper SPE 82210 presented at the SPE European Formation Damage Conference, The Hague, The Netherlands13-14 May. doi: 10.2118/82210-MS.

Al-Mutawa, M., Al-Anzi, E., Jemmali, M., Chang, F., Samuel, E., and Samuel, M. 2005. Zero-Damaging Stimulation and Diversion Fluid: Field Cases from the Carbonate Formations in North Kuwait. *SPE Prod & Fac* **20** (2): 94-105. SPE-80225-PA. doi: 10.2118/80225-PA.

Al-Nakhli, A., Nasr-El-Din, H.A., and Al-Baiyat A.A. 2008. Interactions of Iron and Viscoelastic Surfactants: A New Formation Damage Mechanism. Paper SPE 112465 presented at the SPE International Symposium and Exhibition on Formation Damage Control held in Lafayette, Louisiana, 13-15 February. doi: 10.2118/112465-MS.

Anderson, M.S. 1991. Reactivity of San Andres Dolomite. *SPE Prod & Eng* **6** (2): 227-232. SPE-20115-PA. doi: 10.2118/20115-PA.

Bakken, V., and Schöffel, K. 1996. Semi-Quantitative Study of Chelating Agents Suitable for Removal of Scales. *Oil & Gas Science and Technology--Rev. IFP* **51** (1): 151-160. doi: 10.2516/ogst:1996014.

Bennion, D.B., Thomas, F.B., and Bietz, R.F. 1996. Low permeability Gas Reservoirs: Problem, Opportunities and Solution for Drilling, Completion, Stimulation and Production. Paper SPE 35577 presented at the Gas Technology Conference held in Calgary, Alberta, Canada, 28 April-1 May. doi: 10.2118/35577-MS.

Bergstrom, J.M., and Miller, B.D. 1975. Results of Acid-in-oil Emulsion Stimulations of Carbonate Formations. Paper SPE 5648 presented at the 50th Annual Fall Meeting of the Society of Petroleum Engineers of AIME, Dallas, Texas, 28 September-1 October. doi: 10.2118/5648-MS.

Buijse, M., Boer, P., Breukel, B., Klos, M., and Burgos, G. 2004. Organic Acids in Carbonate Acidizing. *SPE Prod & Fac* **19** (3): 128-134. SPE-82211-PA. doi: 10.2118/82211-PA.

Burns, K.L. 2002. A Rotating Disk Study of the Mechanisms of Calcite Dissolution in the Presence of Environmentally Benign Polyaspartic Acid. Masters Thesis, North Carolina State University.

Cawiezel, K.E. and Dawson, J.C. Dec. 4, 2007. Method of Acidizing a Subterranean Formation with Diverting Foam or Fluid. US Patent No. 7,303,018 B2.

Chang, F., Qu, Q., and Frenier, W. 2001. A Novel Self-Diverting-Acid Developed for Matrix Stimulation of Carbonate Reservoirs. Paper SPE 65033 presented at the SPE International Symposium on Oilfield Chemistry, Houston, Texas, 13-16 February. doi: 10.2118/65033-MS.

Chang, F.F., Qu, Q., and Miller, M.J. June 4, 2002. Fluid System Having Controllable Reversible Viscosity. US Patent No. 6,399,546.

Chatriwala, S.A., Al-Rufaie, Y., Nasr-El-Din, H.A., Altameimi, Y., and Cawiezel, K. 2005. A Case Study of a Successful Matrix Acid Stimulation Treatment in Horizontal Wells Using a New Diversion Surfactant in Saudi Arabia. Paper SPE 93536 presented at the SPE Middle East Oil and Gas Show and Conference, Bahrain, 12-15 March. doi: 10.2118/93536-MS.

Conway, M.W., Asadi, M., Penny, G., and Chang, F. 1999. A Comparative Study of Straight/Gelled/Emulsified Hydrochloric Acid Diffusivity Coefficient Using Diaphragm Cell and Rotating Disk. Paper SPE 56532 presented at the SPE Annual Technical Conference and Exhibition, Huston, 3–6 October. doi: 10.2118/56532-MS.

Crews, J.B. 2005. Internal Phase Breaker Technology for Viscoelastic Surfactant Gelled Fluids. Paper 93449 presented at SPE International Symposium on Oilfield Chemistry, Houston, Texas, 2-4 February. doi: 10.2118/93449-MS.

Crews, J.B. and Huang, T. 2007. Internal Breakers for Viscoelastic-Surfactant Fracturing Fluids. Paper SPE 106216 presented at the SPE International Symposium on Oilfield Chemistry Conference, Houston, Texas, 28 February-2 March. doi: 10.2118/106216-MS.

Crowe, C.W. 1985. Evaluation of Agents for Preventing Precipitation of Ferric Hydroxide from Spent Treating Acid. *J. Pet. Technol*. **37** (4): 691-695. SPE-12497-PA. doi: 10.2118/12497-PA.

Crowe, C.W. 1986. Prevention of Undesirable Precipitates from Acid Treating Fluids. Paper SPE 14090 presented at the SPE International Meeting on Petroleum Engineering, Beijing, China, 17-20 March. doi: 10.2118/14090-MS.

Crowe, C.W., and Miller, B.D. 1974. New, Low-Viscosity Acid-in-Oil Emulsions Provide High Degree of Retardation at High Temperature. Paper SPE 4937 presented at the Rocky Mountain Regional Meeting of the Society of Petroleum Engineers of AIME, Billings, Montana, 15-17 May. doi: 10.2118/4937-MS.

Dabbousi, B.O., Nasr-El-Din, H.A., and Al-Muhalsh, A.S. 1999. Influence of Oilfield Chemicals on the Surface Tension of Stimulating Fluids. Paper SPE 50732 presented at the SPE International Symposium on Oilfield Chemistry, Houston, Texas, 16-19 February. doi: 10.2118/50732-MS.

Daccord, G., Touboul, E., and Lenormand, R. 1989. Carbonate Acidizing: Toward a Quantitative Model of the Wormholing Phenomenon. *SPE Prod & Eng* **4** (1): 63-68. SPE-16887-PA. doi: 10.2118/16887-PA.

Dunlap, D.D., and Houchin, L.R., 1990. Evaluation of Acid System Design and Formation Damage Using Polarized Microscopy. Paper SPE 19425 presented at SPE Formation Damage Control Symposium, Lafayette, Louisiana, 22-23 February. doi: 10.2118/19425-MS.

Dill, W., and Smolarchuk, P. 1988. Iron Control in Fracturing and Acidizing Operations. *J. Can. Pet. Tech*. **27** (3): 75-78. JCPT 88-03-08. doi: 10.2118/88-03-08.

Figueroa-Ortiz, V., and Cazares-Robles, F. 1996. Controlling Organic Deposits and Sludge in a Severe Hostile Environment. Paper SPE 31124 presented at the Formation Damage Control Symposium, Lafayette, Louisiana, 14-15 February. doi: 10.2118/31124-MS.

Fredd, C.N., and Fogler, H.S. 1998a. The Kinetics of Calcite Dissolution in Acetic Acid Solutions. *Chem. Eng. Sci.* **53** (22): 3863–3874.

Fredd, C.N., and Fogler, H.S. 1998b. Alternative Stimulation Fluids and Their Impact on Carbonate Acidizing. *SPE J* **3** (1): 34–41. SPE-31074-PA. doi: 10.2118/31074-PA.

Fredd, C.N., and Fogler, H.S. 1998c. The Influence of Chelating Agents on the Kinetics of Calcite Dissolution. *J. Colloid Interf. Sci.* **204** (1):187–197.

Frenier, W., Brady, M., Al-Harthy, S., Arangath, R., Chan, K.S., Flamant, N., and Samuel, M. 2004. Hot Oil and Gas Wells Can Be Stimulated Without Acids. Paper SPE 86522 presented at the SPE International Symposium and Exhibition on Formation Damage Control, Lafayette, Louisiana, 18-20 February. doi: 10.2118/86522-MS.

Fu, D., and Chang, F. August 16, 2005. Composition and Methods for Treating a Subterranean Formation. US Patent No. 6,929,070.

Gautelier, M., Oelkers, E., and Schott, J. 1999. An Experimental Study of Dolomite Dissolution Rates as a Function of pH from –0.5 And Temperature from 25 to 80 $^{o}$C. *Chemical Geology* **157** (1–2) 13–26.

Hall, B.E., and Dill, W.R. 1988. Iron Control Additives for Limestone and Sandstone Acidizing of Sweet and Sour Wells. Paper SPE 17157 presented at the SPE Formation Damage Control Symposium, Bakersfield, 8-9 February. doi: 10.2118/17157-MS.

Hansford, G.S., and Litt, M. 1968. Mass Transfer from a Rotating Disk into Power-Law Liquids. *Chem. Eng. Sci.* **23** (8): 849-864.

Hoefner, M.L., Fogler, H.S., Stenius, P., and Sjöblom, J. 1987. Role of Acid Diffusion in Matrix Acidizing of Carbonates. *J. Pet. Technol.*, **39** (2): 203-208. SPE-13564-PA. doi: 10.2118/13564-PA.

Houchin, L.R., and Hudson, L.M. 1986. The Prediction, Evaluation, and Treatment of Formation Damage Caused by Organic Deposition. Paper SPE 14818 presented at the Seventh SPE Symposium on Formation Damage Control of the Society of Petroleum Engineers, Lafayette, Louisiana, 26-27 February. doi: 10.2118/14818-MS.

Huang, T., and Crews, J.B. 2008. Do Viscoelastic-Surfactant Diverting Fluids for Acid Treatments Need Internal Breakers? Paper SPE 112484 presented at the 2008 SPE International Symposium and Exhibition on Formation Damage, Lafayette, Louisiana, 13-15 February. doi: 10.2118/112484-MS.

Jacobs. I.C., and Thorne, M.A. 1986. Asphaltene Precipitation during Acid Stimulation Treatments. Paper SPE 14823 presented at the Seventh SPE Symposium on Formation Damage Control, Lafayette, Louisiana, 26-27 February. doi: 10.2118/14823-MS.

Johnson, D.E., Fox, K.B., Burns, L.D., and O'Mara, E.M. 1988. Carbonate Production Decline Rates Are Reduced Through Improvements in Gelled Acid Technology. Paper SPE 17297 presented at the Permian Basin Oil and Gas Recovery Conference, Midland, Texas, 10-11 March. doi: 10.2118/17297-MS.

Kim, Y.H., Calabrese, J. and McEwen, C. 1996. $CaCl_3^-$ and $Ca_2Cl_4$ Complexing Cyclic Aromatic Amide. Template Effect on Cyclization. *J. Am. Chem. Soc.* **118** (6): 1545-1546. doi: 10.1021/JA953268c.

Kim, C., and Hsieh, Y-L. 2001. Wetting and Absorbency of Nonionics Surfactants Solutions on Cotton Fabrics. *Colloids and Surfaces A: Physicochemical and Engineering Aspects* **187-188**: 385-397

Laulhere, J.P. and Briat, J.F. 1993. Iron Release and Uptake by Plant Ferritin: Effects of pH, Reduction and Chelation. *Biochem. J.* **290**: 693-699.

Levich, V.G. 1962. Physicochemical Hydrodynamics, Englewood Cliffs, New Jersey: Prentice-Hall, Inc.

Li, L., Nasr-El-Din, H.A., and Cawiezel, K.E. 2010. Rheological Properties of a New Class of Viscoelastic Surfactant. *SPE Prod & Oper* **25** (3): 355-366. SPE-121716-PA. doi: 10.2118/121716-PA.

Li, L., Nasr-El-Din, H.A., Crews, J.B., and Cawiezel, K.E. 2011. Impact of Organic Acid/Chelating Agents on the Rheological Properties of an Amidoamine Oxide Surfactant. *SPE Prod & Oper* **26** (1): 30-40. SPE-128091-PA. doi: 10.2118/128091-PA.

Lichaa, P.M., and Herrera, L. 1975. Electrical and Other Effects Related to the Formation and Prevention of Asphaltene Deposition Problem in Venezuelan Crudes. Paper SPE 5304 presented at the International Symposium on Oilfield Chemistry of the Society of Petroleum Engineers of AIME, Dallas, Texas, 16-17 January. doi: 10.2118/5304-MS.

Lomax, E.G. 1996. Amphoteric Surfactants. Second Edition. New York: Marcel Dekker, Inc.

Lund, K., Fogler, H.S., McCune, C.C., and Ault, J.W. 1975. Acidizing-II. The Dissolution of Calcite in Hydrochloric Acid. *Chem. Eng. Sci.* **30** (8): 825-835.

Lungwitz, B., Fredd, C., Brady, M., Miller, M., Ali, S., and Hughes, K. 2007. Diversion and Cleanup Studies of Viscoelastic Surfactant-Cased Self-Diverting Acid. *SPE Prod & Oper* **22** (1): 121-127. SPE-86504-PA. doi: 10.2118/86504-PA.

Lynn, J.D. and Nasr-El-Din, H.A. 2001. A Core Based Comparison of the Reaction Characteristics of Emulsified and In-Situ Gelled Acids in Low Permeability, High Temperature, Gas Bearing Carbonates. Paper SPE 65386 presented at the SPE International Symposium on Oilfield Chemistry, Houston, Texas, 13-16 February. doi: 10.2118/65386-MS.

McLeod, H.O. 1984. Matrix Acidizing. . *J. Pet. Technol*. **36** (12): 2055-2069. SPE-13752-PA. doi: 10.2118/13752-PA.

Mohamed, S.K., Nasr-El-Din, H.A. and Al-Furaidan, Y.A., 1999. Acid Stimulation of Power Water Injectors and Saltwater Disposal Wells in a Carbonate Reservoir in Saudi Arabia: Laboratory Testing and Field Results. Paper SPE 56533 presented at the SPE Annual Technical Meeting, Houston, Texas, 3-6 October. doi: 10.2118/56533-MS.

Moore, E.W., Crowe, C.W., and Hendrickson, A.R. 1965. Formation, Effect and Prevention of Asphaltene Sludges during Stimulation Treatments. *J. Pet. Technol*., **17** (9): 1023-1028. SPE-1163-PA. doi: 10.2118/1163-PA.

Nasr-El-Din, H.A., Al-Anazi, H.A., and Mohamed, S.K. 1999. Stimulation of Water Disposal Wells Using Acid-In-Diesel Emulsion: Case Histories. Paper SPE 50739 presented at the SPE International Symposium on Oilfield Chemistry, Houston, Texas, 16-19 February. doi: 10.2118/50739-MS.

Nasr-El-Din, H.A., Al-Driweesh, S.M., Al-Muntasheri, G.A., Marcinew, R., Daniels, J., and Samuel, M. 2003a. Acid Fracturing HT/HP Gas Wells Using a Novel Surfactant Based Fluid System. Paper SPE 84516 presented at the SPE Annual Technical Conference and Exhibition. Denver, 5-8 October. doi: 10.2118/84516-MS.

Nasr-El-Din, H.A, Al-Ghamdi, A.H., Al-Qahtani, A.A., and Samuel, M.M. 2008a. Impact of Acid Additives on the Rheological Properties of a Viscoelastic Surfactant and Their Influence on Field Application. *SPE J* **13** (1): 35-47. SPE-89418-PA. doi: 10.2118/89418-PA.

Nasr-El-Din, H.A., Al-Habib, N.S., Al-Mumen, A.A., Jemmali, M., and Samuel, M. 2006a. A New Effective Stimulation Treatment for Long Horizontal Wells Drilled in Carbonate Reservoirs. *SPE Prod & Oper* **21** (3): 330-338. SPE-86516-PA. doi: 10.2118/56516-PA.

Nasr-El-Din, H.A., Al-Mohammed, A.M., Al-Aamri, A.D., Al-Fahed, M.A., and Chang, F.F., 2009. Quantitative Analysis of Reaction Rate Retardation in Surfactant-based Acids. *SPE Prod & Oper* **24** (1): 107-116. SPE-107451-PA. doi: 10.2118/107451-PA.

Nasr-El-Din, H.A., Al-Mohammed, A., Al-Aamri, A.D., and Al-Fuwaires, O. 2008b. Reaction of Gelled Acids with Calcite. *SPE Prod & Oper* **23** (3): 353-361. SPE-103979-PA. doi: 10.2118/103979-PA.

Nasr-El-Din, H.A., Al-Yami, A., and Al-Aamri, A. 2007. A Study of Acid Cement Reactions Using the Rotating Disk Apparatus. Paper SPE 106443 presented at the SPE International Symposium on Oilfield Chemistry, Houston, Texas, 28 February-2 March. doi: 10.2118/106443-MS.

Nasr-El-Din, H.A., Chesson, J.B., Cawiezel, K., and Devine C.S. 2006b. Investigation and Field Evaluation of a Foamed Viscoelastic Surfactant Diversion Fluid Applied During Coiled-Tubing Matrix-Acid Treatment. Paper SPE 99651 presented at the 2006 SPE/CoTA Coiled Tubing and Well Intervention Conference and Exhibition, The Woodlands, Texas, 4-5 April. doi: 10.2118/99651-MS.

Nasr-El-Din, H.A., Chesson, J.B., Cawiezel, K., and Devine C.S. 2006c. Lessons Learned and Guidelines for Matrix Acidizing with Viscoelastic Surfactant Diversion in Carbonate Formations. Paper SPE 102468 presented at the 2006 SPE Annual Technical Conference and Exhibition, San Antonio, Texas, 24-27 September. doi: 10.2118/102468-MS.

Nasr-El-Din, H.A., Chesson, J.B., Cawiezel, K., and Devine C.S. 2006d. Field Success in Carbonate Acid Diversion, Utilizing Laboratory Data Generated by Parallel Flow Testing. Paper SPE 102828 presented at the 2006 SPE Annual Technical Conference and Exhibition, San Antonio, Texas, 24-27 September. doi: 10.2118/102828-MS.

Nasr-El-Din, H.A., Samuel, E., and Samuel, M. 2003b, Application of New Class of Surfactants in Stimulation Treatments. Paper SPE 84898 presented at the SPE International Improved Oil Recovery Conference in Asia Pacific, Kuala Lumpur, 20-21 October. doi: 10.2118/84898-MS.

Nasr-El-Din, H.A., and Samuel, M. 2007. Lessons Learned from Using Viscoelastic Surfactants in Well Stimulation. *SPE Prod & Oper* **22** (1): 112-120. SPE-90383-PA. doi: 10.2118/90383-PA.

Nasr-El-Din, H.A., and Taylor, K.C., and Al-Hajji, H.H. 2002. Propagation of Cross-Linkers Used in In-Situ Gelled Acids in Carbonate Reservoirs. Paper SPE 75257 presented at the SPE/DOE Improved Oil Recovery Symposium, Tulsa, 13-17 April. doi: 10.2118/75257-MS.

Nelson, E.B., Lungwitz, B., Dismuke, K., Samuel, M., Salamat, G., Hughes, T., Lee, J., Fletcher, P., Fu, D., Hutchins, R., Parris, M., and Tustin, G.J. April 19, 2005. Viscosity Reduction of Viscoelastic Based Fluids. US Patent No. 6,881,709.

Nierode, D.E., and Williams, B.B. 1971. Characteristics of Acid Reaction in Limestone Formations. *SPE J.* **11** (4): 406-418. SPE-3101-PA. doi: 10.2118/3101-PA.

Qu, Q., Nelson, E.B., Willberg, D.M., Samuel, E.E., Lee, Jr., J.C., Chang, F.F., Card, R.J., Vinod, P.S., Brown, J.E., and Thomas, R.L. August 20, 2002. Compositions Containing Aqueous Viscosifying Surfactants and Methods for Applying Such Compositions in Subterranean Formations. US Patent No. 6,435,277.

Peters, F.W., and Saxon, A. 1989. Nitrified Emulsion Provides Dramatic Improvements in Live Acid Penetration. Paper SPE 19496 presented at the SPE Asia-Pacific Conference, Sydney, Australia, 13-15 September. doi: 10.2118/19496-MS.

Porter, M.R. 1994. Handbook of Surfactants. Second Edition. Glasgow: Blankie; New York: Chapman & Hall.

Rabie, A.I., Gomaa, A.M., and Nast-El-Din, H.A. 2010. Determination of Reaction Rate of In-Situ Gelled Acids with Calcite Using the Rotating Disk Apparatus. Accepted by *SPE J.* In Press. Paper SPE 133501-PA doi: 10.2118/133501-PA.

Salager, J-L. 2002. Surfactants Types and Uses. Version #2. FiRP Booklet # E300-A. Merida Venezuela:Universidad de Los Andes.

Samuel, M., Marcinew, R., Al-Harbi, M., Samuel, E., Xiao, Z., Ezzat, A.M., Khamees, S.A., Jarrett, C., Ginest, N.H., Bartko, K., Hembling, D., and Nasr-El-Din, H.A. 2003. A New Solids-Free Non-Damaging High Temperature Lost-Circulation Pill: Development and First Field Applications. Paper SPE 81494 presented at the SPE Middle East Oil Show, Bahrain, 9-12 June. doi: 10.2118/81494-MS.

Saxon, A., Chariag, B., and Abdel Rahman, M.R. 2000. An Effective Matrix Diversion Technique for Carbonate Reservoirs. *SPE Drill & Compl* **15** (1): 57-62. SPE-62173-PA. doi: 10.2118/62173-PA.

Schramm, L.L. 2000. Surfactants, Fundamentals and Applications in the Petroleum Industry. Cambridge, U.K.; New York: Cambridge University Press.

Smith, C.F., Crowe, C.W., and Nolan, T.J. III. 1969. Secondary Deposition of Iron Compounds Following Acidizing Treatments. . *J. Pet. Technol*. **21** (9): 1121-1129. SPE-2358-PA. doi: 10.2118/2358-PA.

Taylor, K.C., Al-Ghamdi, A.H., and Nasr-El-Din, H.A. 2004a. Effect of Additives on the Acid Dissolution Rates of Calcium and Magnesium Carbonates. *SPE Prod & Fac* **19** (3): 122–127. SPE-80256-PA. doi: 10.2118/80256-PA.

Taylor, K.C., Al-Ghamdi, A.H., and Nasr-El-Din, H.A. 2004b. Measurement of Acid Reaction Rates of a Deep Dolomitic Gas Reservoir. *J. Cad. Pet. Tech*. **43** (10): 49–56. JCPT 04-10-05. doi: 10.2118/04-10-05.

Taylor, D., Kumar, P.S., Fu, D., Jemmali, M., Helou, H., Chang, F., Davies, S., and Al-Mutawa, M. 2003. Viscoelastic Surfactant Based Self-Diverting Acid for Enhanced Stimulation in Carbonate Reservoirs. 2003. Paper SPE 82263 presented at the SPE European Formation Damage Conference, The Hague, The Netherlands, 13-14 May. doi: 10.2118/582263-MS.

Taylor, K.C. and Nasr-El-Din, H.A. 2002. Coreflood Evaluation of In-Situ Gelled Acid. Paper SPE 73707 presented at the SPE International Symposium and Exhibition on Formation Damage Control, Lafayette, Louisiana, 20-21 February. doi: 10.2118/73707-MS.

Taylor, K.C. and Nasr-El-Din, H.A. 2003. Laboratory Evaluation of In-Situ Gelled Acid for Carbonate Reservoirs. *SPE J* **8** (4): 426-434. SPE-87331-PA. doi: 10.2118/87331-PA.

Taylor, K.C., Nasr-El-Din, H.A., and Al-Alawi, M. 1999. Systematic Study of Iron Control Chemicals Used During Well Stimulation. *SPE J* **4** (1): 19-24. SPE-54602-PA. doi: 10.2118/54602-PA.

Thomas, R.L., Ali, S.A., Robert, J.A., and Acock, A.M. 1998. Field Validation of a Foam Diversion Model: A Matrix Stimulation Case Study. Paper SPE 39422 presented at the SPE Formation Damage Control Symposium, Lafayette, Louisiana, 18-19 February. doi: 10.2118/39422-MS.

Vinson, E.F. 1996. A Novel Reducing Agent for Combatting Iron-Induced Crude Oil Sludging: Development and Case Histories. Paper SPE 31127 presented at the SPE Formation Damage Control Symposium, Lafayette, Louisiana, 14-15 February. doi: 10.2118/31127-MS.

Williams, B.B., and Nierode, D.E. 1972. Design of Acid Fracturing Treatments. *J. Pet. Technol*. **24** (7) 849-859. SPE-3720-PA. doi: 10.2118/3720-PA.

Yeager, V. and Shuchart, C. 1997. In Situ Gels Improve Formation Acidizing, *Oil & Gas J.* **95** (3): 70-72.

Yu, M., Mahmoud, M.A., and Nasr-El-Din, H.A. 2009. Quantitative Analysis of An Amphoteric Surfactant in Acidizing Fluids and Coreflood Effluent. Accepted by *SPE J*. In Press. SPE-121715-PA. doi: 10.2118/121715-PA.

# APPENDIX A

# RELATED STUDIES

# MIXED HCl/ORGANIC ACID SYSTEMS:

# DO THEY CAUSE FORMATION DAMAGE?

## Introduction

The white calcium precipitation was observed at the bottom of tubes for spent acids containing organic acid/chelating agents, as mentioned in Chapters II and III. Therefore, people should be very careful when they deal with organic acids.

Hydrochloric acid is commonly used in matrix and acid fracturing treatments in carbonate reservoirs. However, application of HCl in deep wells is a concern because of its high reactivity and sludging tendencies when the acid contacts asphaltic crude oils. Retarded HCl systems, such as in-situ gelled acid, emulsified acid and surfactant based acid were introduced to lower down the reaction of HCl with rock, divert the acid system further into the formation and decrease the leak-off rate. In addition, concentrated HCl-based acids are very corrosive to well tubulars, especially at high temperatures. Instead of using large amount of expensive corrosion inhibitor and its intensifier, people started focusing on organic acids, such as acetic acid and formic acid 40 years ago (Harris, 1961). These acids are weakly ionized and slow reacting. Acetic and formic acids are less corrosive than mineral acids and can be inhibited. However, they still have some limitations. The optimal concentrations for acetic and formic acids are 13 and 9 wt%, respectively (Robert and Crowe, 2000) to avoid precipitations of calcium acetate and

calcium formate. Organic acids have less dissolving power than HCl since the reaction is reversible and organic acids can not be consumed completely (Buijse et al., 2004).

Based on those limitations of HCl and organic acids, mixing HCl and organic acids is considered as a good alternative to either acid and has been successfully used for high-temperature stimulation. These blends are less corrosive than equivalent strength HCl acids (Dill and Keeney, 1978; Van Domelen and Jennings, 1995) and can be viscosified by surfactant or polymer (Nasr-El-Din et al., 2003c, 2006e; Welton and van Domelen, 2006).

Various concentrations of HCl and organic acid blends were applied to the field and tested in the lab. Nasr-El-din et al (1997) and Hashem (1998) used 5 wt% HCl and 5 wt% acetic acid to stimulate water supply and injection wells in a sandstone field in central Saudi Arabia. Burgos et al. (2005) applied 11 wt% formic acid and 7 wt% HCl in Lake Maracaibo. Nasr-El-Din et al. (2003) and Bartko et al. (2003) used 15 wt% HCl and 9 wt% formic acid to acid fracture deep gas wells. Recently, Welton and van Domelen (2006) examined gelled and in-situ crosslinked 20 wt% HCl / 10 wt% formic acid and gave the positive results. Chang et al. (2008) utilized a chemical analysis model to simulate how 15 wt% HCl / 10 wt% acetic acid and 15 wt% HCl / 9 wt% formic acid reacted with calcite at 150$^{o}$F. Results showed no precipitation was observed when pH was in the range of 4-5 and the conversion of organic acid was increased with the help of HCl.

The following equations describe the reactions of HCl/organic acids with calcite. Eq. (A.1) shows irreversible and complete reaction between HCl and calcite. Organic acids

do not start reacting with the rock until HCl is consumed completely. Once the organic acid HA dissociates to $H^+$ and $A^-$, $H^+$ will dissolve calcite and generate $Ca^{2+}$. The ion $A^-$ can associate with Ca cation and form $CaA^+$ and $CaA_2$. It must be noted that Eqs. (A.2)(A.4)(A.5) are all reversible and incomplete.

For the reaction of HCl and calcite:

$$2HCl + CaCO_3 \rightarrow CaCl_2 + H_2O + CO_2 \quad (A.1)$$

For the reaction of organic acid and calcite:

$$HA \leftrightarrow H^+ + A^- \quad (A.2)$$
$$2H^+ + CaCO_3 \rightarrow Ca^{2+} + H_2O + CO_2 \quad (A.3)$$
$$Ca^{2+} + A^- \leftrightarrow CaA^+ \quad (A.4)$$
$$Ca^{2+} + 2A^- \leftrightarrow CaA_2 \quad (A.5)$$

Formic acid (9 wt%) can be used in the field without generating any precipitate. Does it mean addition of 15 or 20 wt% HCl to 9 wt% formic acid can dissolve calcite and without forming any precipitate as well? As we know, if concentration of HCl is high, a large amount of $Ca^{2+}$ can be generated. In this case, there is a potential precipitation of $CaA_2$. The objective of this study is to determine what concentrations of HCl and organic acid can be used to mix together without causing any formation damage.

**HCl/Formic Acid**

***Calculations***

Solubility values in the calcium formate-calcium chloride-water system at 25°C were reported by IUPAC-NIST solubility database (**Table A.1**). The solubility of calcium

formate decreases if the mass fraction of calcium chloride is increased. Therefore, calculations can be done based on this table. The amount of calcium chloride can be obtained if concentration of HCl is known. The maximum amount of calcium formate that can co-exist with calcium chloride in the solution can be read from Table A.1, so the maximum mass fraction of formic acid that can be mixed with HCl without causing any precipitation can be derived.

**TABLE A.1--SOLUBILITY VALUES OF CALCIUM FORMATE-CALIUM CHLORIDE-WATER SYSTEM.**

| Mass Fraction | |
|---|---|
| **Ca Formate** | **$CaCl_2$** |
| 14.62 | … |
| 11.51 | 4.31 |
| 8.94 | 10.68 |
| 6.99 | 15.9 |
| 4.65 | 22.27 |
| 4.03 | 27.42 |
| 3.74 | 34.55 |

The results are: 1) for mixing with 15 wt% HCl acid solution, only < 4.4 wt% formic acid can be used. 2) for mixing with 20 wt% HCl, only < 3.5 wt% formic acid can be used. 3) for mixing with 9 wt% formic acid, the concentration of HCl can not be bigger than 3.3 wt%.

It must be noted that Table A.1 shows the system at neutral conditions, however, the final pH is between 4 and 5 after acid stimulation in carbonate reservoir because of $CO_2$.

***Experiments and Results***

ACS grade HCl and formic acid were mixed together and diluted with deionized water. Different concentrations of HCl/formic acid system can be obtained based on various amounts of acids. Calcium carbonate was added slowly to the acid solution until pH reaches 4. The final result was shown in **Table A.2**: 1) at room temperature, for 20 wt% HCl system, the concentration of formic acid can not be used at more than 2 wt%. 2) for 9 wt% formic acid, no more than 3 wt% HCl can be used.

**TABLE A.2--RESULTS OF USING CALCIUM CARBONATE TO NEUTRALIZE VARIUOS HCl/FORMIC ACID BLENDS.**

| HCl (wt%)/Formic acid (wt%) | Observation |
|---|---|
| 20/12 | lots of white precipitation |
| 20/9 | lots of white precipitation |
| 20/3 | some white precipitation |
| 20/2 | some white precipitation |
| 20/1 | slight white precipitation |
| 3/9 | slight white precipitation |
| 2/9 | no white precipitation |
| 1/9 | no white precipitation |

Experimental results always show less concentration than that from calculations, because of different pHs. Although calculations are not 100% accurate, at least we can estimate the upper concentrations of HCl and formic acid that can be mixed together without causing serious formation damage.

***pH Effect***

As mentioned before, hydrochloric acid reacts with calcite first and formic acid can not start the reaction until all of HCl is consumed. The pH value of the solution only containing 9 wt% formic acid is 1.6-1.7. However, the pH value of the solution containing 9 wt% formic acid and calcium chloride that 20 wt% HCl produced was < -1.2, because $Ca^{2+}$ can associate with $HCOO^-$ (reaction A.4), and force the reaction (A.2) to generate more $H^+$. When calcium carbonate was added slowly to neutralize this solution, the result showed that the solution became cloudy (the sign of precipitation) when pH increased to 1.8. Finally, lots of white precipitate of calcium formate was formed when pH reached 4.

**HCl/Acetic Acid**

ACS grade HCl and formic acid were mixed together and diluted with deionized water. Different concentrations of HCl/acetic acid system can be obtained based on various amounts of acids. At room temperature, calcium carbonate was added slowly to the acid solution until pH reaches 4. The final result was shown in **Table A.3**: 1) for 20 wt% HCl system, the concentration of formic acid can not be used at more than 3 wt%. 2) for 13 wt% acetic acid, no more than 5 wt% HCl can be used.

| TABLE A.3--RESULTS OF USING CALCIUM CARBONATE TO NEUTRALIZE VARIUOS HCl/ACETIC ACID BLENDS. | |
|---|---|
| **HCl (wt%)/Acetic acid (wt%)** | **Observation** |
| 20/3 | some white precipitation |
| 15/2 | some white precipitation |
| 15/13 | lots of white precipitation |
| 5/13 | slight white precipitation |
| 3/13 | no white precipitation |

**Solubility at High Temperatures**

**Table A.4** shows the solubility of calcium chloride, calcium formate and dihydrate calcium acetate in water at different temperatures (IUPAC-NIST solubility database). It can be seen that the solubility of calcium formate slightly increases when the temperature increases. Oppositely, the amount of solubilized calcium acetate decreases at higher temperatures.

Therefore, in the HTHP carbonate reservoirs, white calcium acetate precipitation will be generated if more than 2 wt% acetic acid is mixed with 15 wt% HCl, because of its lower solubility at high temperatures. In addition, more acetic acid used, more severe damage obtained.

| TABLE A.4--SOLUBILITY TABLE | | | |
|---|---|---|---|
| **Temperature ($^oC$)** | **Solubility of $CaCl_2$ (g/100 g $H_2O$)** | **Solubility of Ca formate (g/100 g $H_2O$)** | **Solubility of Ca acetate.$2H_2O$ (g/100 g $H_2O$)** |
| 0 | 59.5 | 16.15 | 37.4 |
| 10 | 64.7 | 16.37 | 36 |
| 20 | 74.5 | 16.6 | 34.7 |
| 30 | 100 | 16.82 | 33.8 |
| 40 | 128 | 17.05 | 33.2 |
| 60 | 137 | 17.5 | 32.7 |
| 80 | 147 | 17.95 | 33.5 |
| 90 | 154 | 18.17 | 31.1 |
| 100 | 159 | 18.4 | 29.7 |

**Conclusions**

More and more people are interested in mixing organic acids (formic acid/acetic acid) with HCl to get the further acid penetration, less corrosion and decreased interfacial tension. Some commercial available analytical software is commonly used to optimize the stimulation treatment and the results have never been found to cause the formation damage. However, the laboratory work was done in this study and proved that there is a risk to use the acid blend because of the organic salt precipitation, especially, the solubility of calcium acetate decreases with the temperature, causing more severe formation damage at high temperatures than it does at room temperatures.

More additional work should be worked on and confirm what was observed. Core flood tests are one of the most useful methods, but it should be operated with a long core so that pH can reach that high and make sure if there is a precipitation.

**References**

Bartko, K.M., Nasr-El-Din, H.A., Rahim, Z., and Al-Muntasheri, G.A. 2003. Acid Fracturing of a Gas Carbonate Reservoir: The Impact of Acid Type and Lithology on Fracture Half Length and Width. Paper SPE 84130 was presented at the SPE Annual Technical Conference and Exhibition, Denver, 5-8 October. doi: 10.2118/84130-MS.

Burgos, G., Buijse, M., Fonseca, E., Milne, A., Brady, M., and Olvera, R. 2005. Acid Fracturing in Lake Maracaibo: How Continuous Improvements Kept on Raising the Expectation Bar. Paper SPE 96531 presented at the SPE Annual Technical Conference and Exhibition, Dallas, 9-12 October. doi: 10.2118/96531-MS.

Chang, F.F., Nasr-El-Din, H.A., Lindvig, T., and Qiu, X.W. 2008. Matrix Acidizing of Carbonate Reservoirs Using Organic Acids and Mixture of HCl and Organic Acids. Paper SPE 116601 presented at the SPE Annual Technical Conference and Exhibition, Denver, Colorado, 21-24 September. doi: 10.2118/116601-MS.

Dill, W.R., and Keeney, B.R. 1978. Optimizing HCl-Formic Acid Mixtures for High Temperature Stimulation. Paper PSE 7567 presented at the 53rd SPE Annual Fall Technical Conference and Exhibition of the Society of Petroleum Engineers of AIME, Houston, 1-3 October. doi: 10.2118/7567-PA.

Harris, F.N., 1961. Application of Acetic Acid to Well Completion, Stimulation and Reconditioning. *J Pet Technol* **13** (7): 637–639. SPE-63-PA. doi: 10.2118/63-PA.

Hashem, M.K., Nasr-El-Din, H.A., and Hopkins, J.A. 1999. An Experience in Acidizing Sandstone Reservoirs: A Scientific Approach. Paper SPE 56528 presented at the SPE Annual Technical Conference and Exhibition, Houston, 3-6 October. doi: 10.2118/56528-MS.

Nasr-El-Din, H.A., Al-Anazi, H.A., and Hopkins, J.A. 1997. Acid/Rock Interactions During Stimulation of Sour Water Injectors in a Sandstone Reservoir. Paper SPE 37215 presented at the 1997 SPE International Symposium on Oilfield Chemistry, Houston, 18-21 February. doi: 10.2118/37215-MS.

Nasr-El-Din, H.A., Driweesh, S.M., and Muntasheri, G.A. 2003c. Field Application of HCl-Formic Acid System to Acid Fracture Deep Gas Wells Completed with Super Cr-13 Tubing in Saudi Arabia. Paper SPE 84925 presented at the SPE International Improved Oil Recovery Conference in Asia Pacific, Kuala Lumpur, Malaysia, 20-21 October. doi: 10.2118/84925-MS.

Nasr-El-Din, H.A., Al-Driweesh, S.M., Sierra, L., van Domelen, M., and Welton, T. 2006e. Long-Term Comparative Evaluation of HCl/Formic Acid System Used to Stimulate Carbonate Formations at Severe Conditions in Saudi Arabia. Paper SPE

103978 presented at the First International Oil Conference and Exhibition in Mexico, Cancun, Mexico, 31 August-2 September. doi: 10.2118/103978-MS.

Robert, J.A., and Crowe, C.W. 2000. Carbonate Acidizing Design. Reservoir Stimulation, Economides, M.J. and Nolte, K.G. 3rd Edition, John Wiley & Sons Inc. 17-11.

Van Domelen, M., and Jennings, A.R. 1995. Alternate Acid Blends for HPHT Applications. Paper SPE 30419 presented at the Offshore Europe Conference, Aberdeen, Scotland, 5-8 September. doi: 10.2118/30419-MS.

Welton, T.D., and van Domelen, M.S. 2006. High-Viscosity-Yield Acid Systems for High-Temperature Stimulation. Paper SPE 98237 presented at the SPE International Symposium and Exhibition on Formation Damage Control, Lafayette, 15-17 February. doi: 10.2118/98237-MS.

http://srdata.nist.gov/solubility/sol_detail.aspx?goBack=Y&sysID=73_167

http://srdata.nist.gov/solubility/sol_detail.aspx?sysID=73_17

# APPENDIX B

# DETAILS OF EXPERIMENTAL METHOD

## HPHT Viscometer M5600

### *Instrument Calibration*

The viscometer (shown in **Fig. B.1**) can be used to measure the viscosity and dynamic studies of non-Newtonian fluid at high temperature and high pressure. The measurement range is shown below:

Speed range: 0.0001 ~ 1100 rpm continuous

Shear rate: 0.00004 ~ 1870 $s^{-1}$

Frequency range: 0.01 ~ 5 Hz (with dynamic option)

Amplitude range: 0.1% ~ 500% (with dynamic option)

Temperature range: ambient (20 $^{o}$F with chiller) ~ 500 $^{o}$F

Pressure range: atm ~ 1000 psi

Viscosity range: 0.5 ~ 5,000,000 cp

Sample size: 32~ 78 ml

Torque: 14 μN.m ~ 100 mN.m

Shear stress: 1 ~ 15,000 dyne/$cm^2$

Resolution: 0.01% of full scale range or better

Repeatability: ±0.5% of full scale range or better


**Fig. B.1—The photo of HPHT viscometer M5600.**

*Torque Calibration*

1) Display the Calibration screen (**Fig. B.2.**). 2) Select the rheometer and bob size. 3) Enter the viscosity rating for the calibration fluid by matching the viscosity value with the sample temperature displayed on the M5600 LCD screen. (Refer to the chart included with the calibration fluid). The calibration fluid must be loaded into the sample cup before the reading can be taken. 4) Enter the parameter for how much the viscosity

of calibration fluid is affected by an increase in temperature of 1 $^{o}$C. 5) Begin the torque calibration. 6) After the torque calibration, wait for a few minutes, then check the shear stress reading on the M5600 LCD screen. It should be in the range of -10 ~ 10 dyne/cm$^2$. If the reading is outside of this range, the head assembly may need to be cleaned.

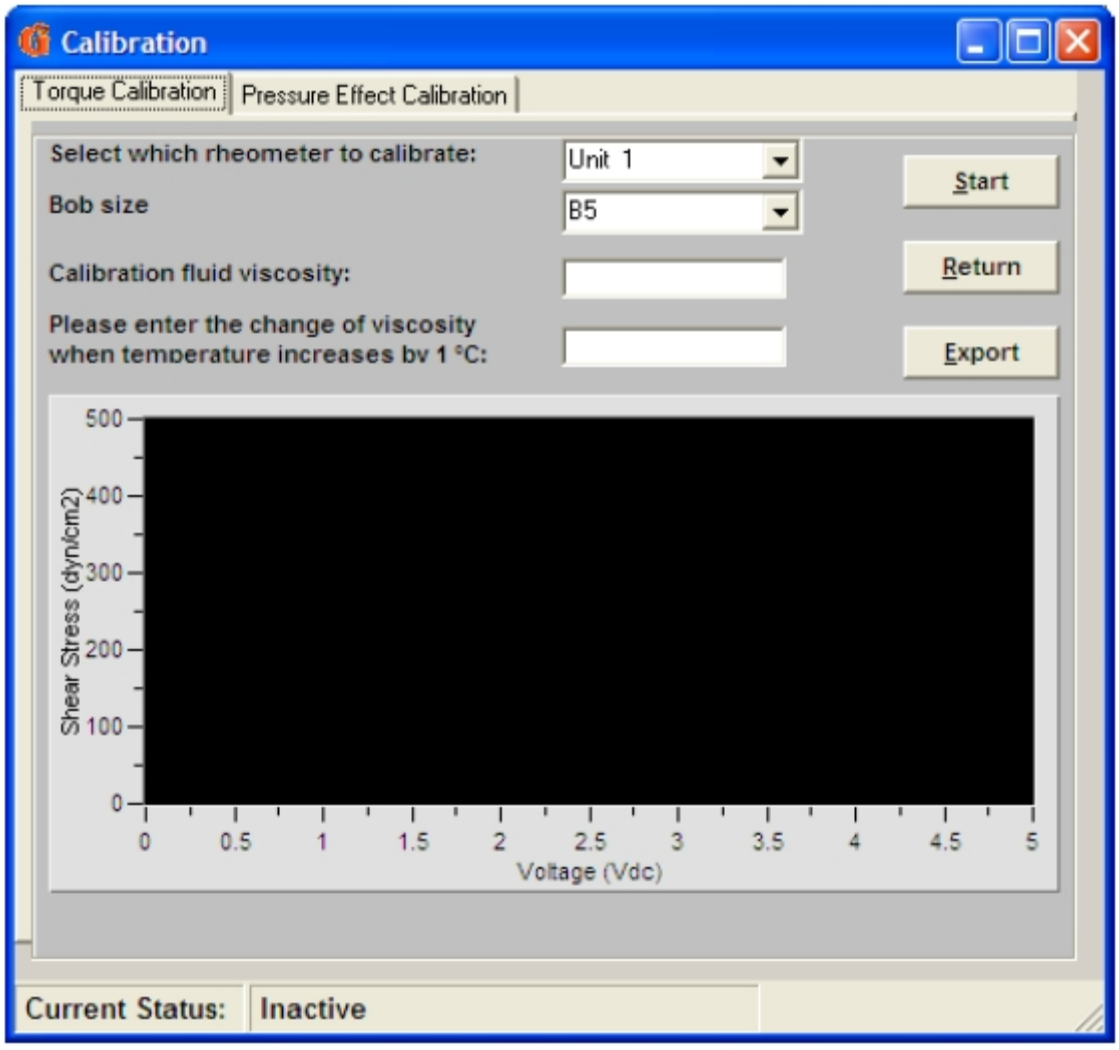


**Fig. B.2—The torque calibration screen.**

*Pressure Calibration*

1) Click on the "Pressure Effect Calibration" tab (shown in **Fig. B.3**) and then click "Start Automatic Pressure Effect Calibration". 2) Follow the directions on the lower part of the screen. 3) Once the pressure calibration is complete, the shear stress reading on M5600 LCD screen should be ±5 dyne/cm$^2$ based on the value from the torque calibration.

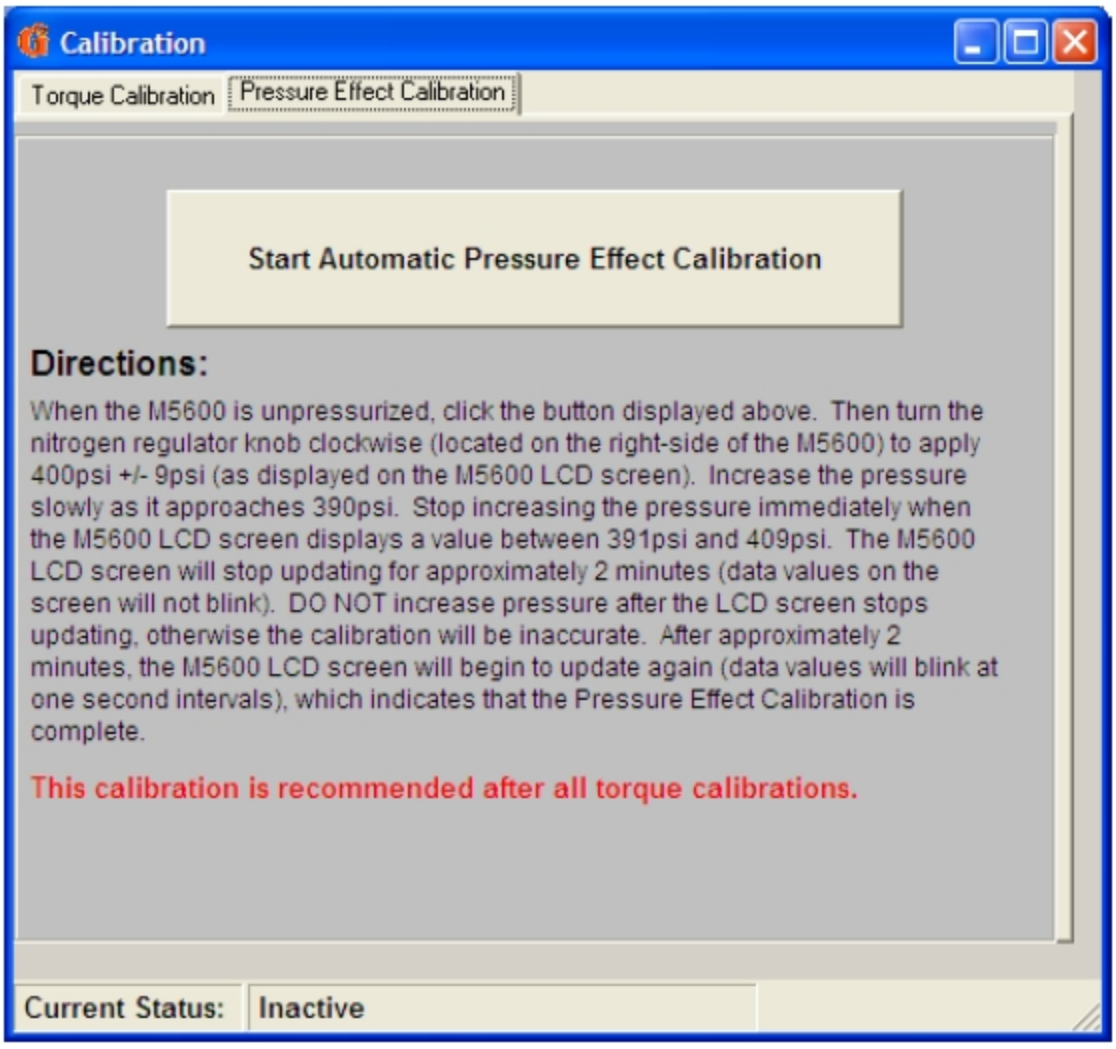


**Fig. B.3—The pressure effect calibration screen.**

***Perform Viscometry Test***

1) Click “Setup” tap on the main screen and test sequence setup will appear (**Fig. B.4**).
2) Choose “Viscometry, API 39” test type.
3) Create the sequence steps. Choose “temperature”, “shear rate” and “ramp”.
4) Save the sequence and click “return” button.
5) Click the “Real Time Test” button on the main screen. And then click “Regular Test” in the menu bar and choose “Add M5600 Unit 1”. The screen is shown in **Fig. B.5**.
6) Load the sample cup with a homogenous sample.
7) Click the “Zero” button to establish a zero value for the torque sensor.
8) Install the sample cup, loaded with the sample and turn the nitrogen pressure regulator knob clockwise to set the desired pressure.
9) Raise and secure the bath.
10) Click on the “Select Sequence” button to display pre-saved test files. Then click on the desired sequence.
11) Click “Start”. The test information will show up and “Test Name” is the only mandatory field.
12) Click “OK” to start the test.

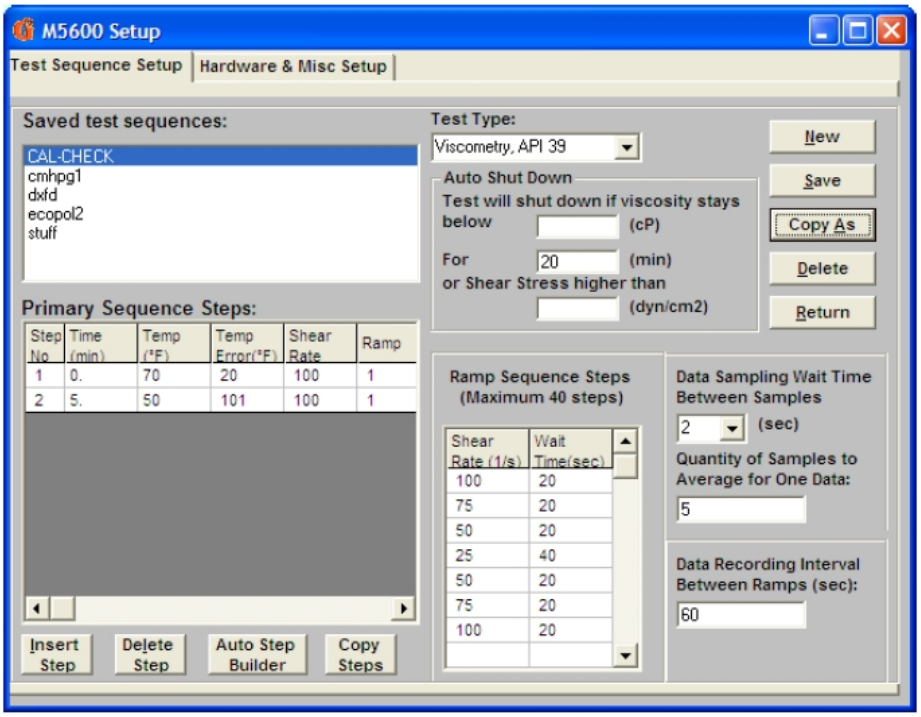


**Fig. B.4—Test sequence setup screen.**

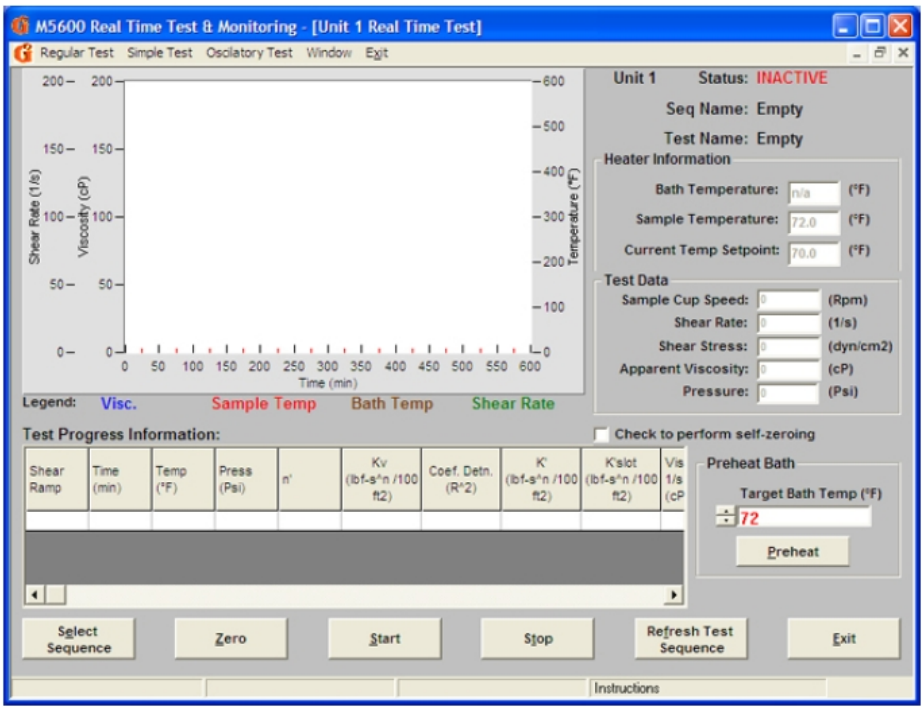


**Fig. B.5—Real time test screen.**

***Perform Oscillatory Test***

Real time oscillatory tests are divided into two types: single step and presaved sequence.

*A Single Step Real Time Oscillatory Test*

1) Click "Oscillatory Test" in the menu bar and choose "Add M5600 Unit 1". The screen is shown in **Fig. B.6**.
2) Install the proper bob, click "Zero" button, then install the sample cup, loaded with fluid.
3) Enter the appropriate values for the test, including chart type, bob size, frequency/Hz, strain (%), delay cycles and number of cycles to average.
4) Click the "Start" button.

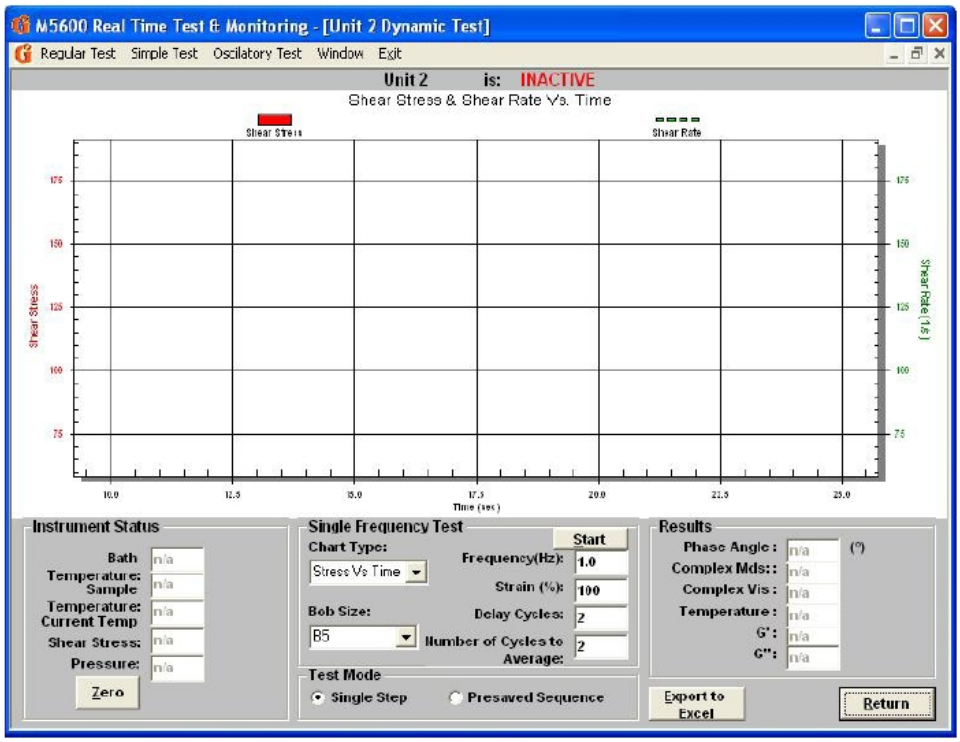


**Fig. B.6—A single step real time oscillatory test screen.**

*A Presaved Sequence Real Time Oscillatory Test*

1) Click "Oscillatory Test" in the menu bar and choose "Add M5600 Unit 1". Click "Presaved Sequence". The screen is shown in **Fig. B.7**.
2) Click "Select Sequence" to choose a pre-saved test sequence.
3) Install the proper bob, click "Zero" button, then install the sample cup, loaded with fluid.
4) Click "Start" to bring up the test window. Enter a unique name for the test file, and click "OK" to start the test.

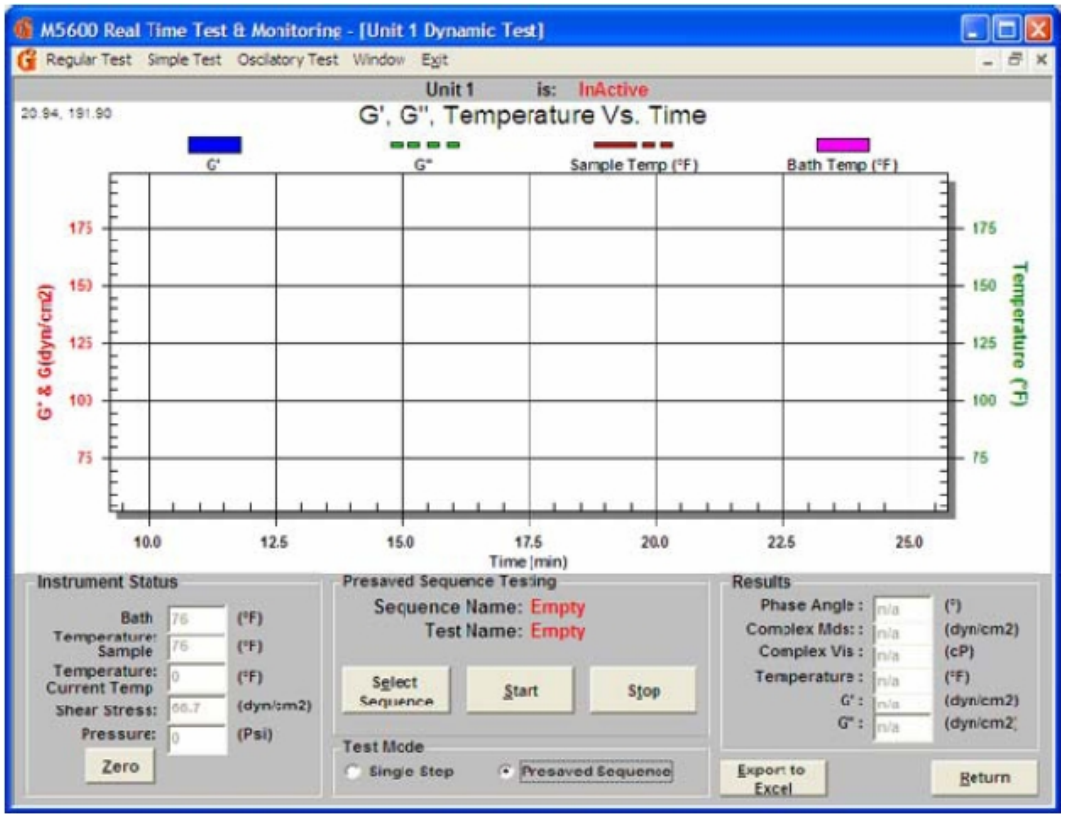


**Fig. B.7—A presaved sequence real time oscillatory test screen.**

**Rotating-Disk Corrosion Reactor System (RDA 100 MNT)**

***System Description***

The CORE LAB CRS Series Rotating-Disk Corrosion Reactor System is used to conduct corrosion tests of small metal samples (corrosion coupons) or rock core samples at high temperatures and pressures. The rotating (stirring) speed is adjusted through control pad on the instrument front panel. The system is constructed of materials that resist corrosion that can occur due to exposure to the test liquids. The reactor, reservoir, and other parts in contact with the test fluids are made of Hastelloy B alloy. A separate high-pressure, high-temperature fluid reservoir vessel allows introduction of pre-heated test liquid into the reactor at high pressures. The reactor vessel and reservoir are each heated with external band heaters. The temperature of each of the two vessels (reactor and reservoir) is set and read independently by separate auto-tuned temperature controllers with built-in digital-displays.

The photo of RDA 100 is shown in **Fig. B.8**. The capacity of reactor vessel is 500 ml. The maximum operation pressure and temperature are 35 MPa (5000) psig and 200$^{o}$C (392$^{o}$F), respectively. The motor is controlled by an internal drive, which can be controlled from the front panel. The maximum stirring speed is 1800 rpm and the maximum stirring torque is 3 N-m (2.2 lbf-ft).


**Fig. B.8—Rotating Disk Apparatus RDA 100.**

### *Operating Procedures*

1. The core with 1.5'' diameter and 1'' thickness is attached to the sample holder by using heat shrinkage Teflon tubing. Then the sample holder is put on the rotating shaft.

2. Control the temperature of experiment using the “Reactor Temperature” and “Reservoir temperature” controller. Their temperatures can be set using the up/down arrow keys on the panel.
3. To control the stirring manually, press the “LOCAL” key on the “STIRRING” motor controller to set it to Local mode. The controller will display “LOC”. Then, press its “FWD” key to start rotation in the Forward direction. Adjust the rotation speed using the up/down arrow keys.
4. Pour the liquid in the reservoir and open the “Gas Pressure 1 Valve” to pressurize the reservoir with $N_2$, and then open the “Inject Valve” to inject this fluid from the reservoir into the reactor.
5. The reactor can be pressurized by using the “Gas Pressure to Reactor Valve”. Monitor the pressure carefully, and manually open valves, as necessary, to relieve excess pressure.
6. The samples of test liquid can be taken as follows:
    - Open the “Sample Inlet Valve” for at least 10 seconds to get enough time for liquid from the bottom of the reactor vessel to fill the 2 ml sample tube, then close “Sample Inlet Valve”.
    - Open the “Sample Outlet Valve” for 20 seconds.
    - Open the “Sample Air Inlet Valve”.
    - Close the Sample Outlet Valve” when no fluid is flowing from the sample tube.

- Allow enough time for air to purge all the test liquids, then close "Sample Air Inlet Valve".
- Should be careful when deal with surfactant-based fluid because large amount of foams is generated.

7. Once the experiment is done. Open the "Inject Valve" to transfer the fluid from reactor to reservoir vessel, so that the reaction between the fluid and the rock sample is stopped.
8. Turn off the heaters by changing the set point temperature to $0^{o}C$.
9. Slowly open the "Vent/Vacuum" valve on the front panel to release the reactor pressure. Make sure HCl vapor goes into a vent hood.
10. Open the reactor vessel and take away the rock core. Rinse the core with deionized water and dry it.
11. Open the "Inject Valve" again and the fluid is transferred back to the reactor. Slowly release the pressure by using "Vent/Vacuum" valve.
12. After releasing all pressure, the reactor vessel can be drained by opening the "Sample Inlet Valve" and 'Sample Dump Valve".
13. Flush the system lines with clean water and acetone to remove the remaining surfactant or corrosion inhibitor.
14. Turn off the main electrical power switch.

# VITA


Name: Lingling Li

Address: 27-3-401 Longxin District, Daqing, Heilongjiang, China, 163453

Email Address: nanometerling@mail.com


Education:

2004 B.E., Macromolecule Materials & Engineering
University of Science & Technology of China

2007 M.S., Chemistry, Texas A&M University

2011 Ph.D. Petroleum Engineering, Texas A&M University